P-05-246

Oskarshamn site investigation

Groundwater flow measurements and SWIW test in borehole KLX03

Erik Gustafsson, Rune Nordqvist, Pernilla Thur

Geosigma AB

November 2006

Svensk Kärnbränslehantering AB
Swedish Nuclear Fuel
and Waste Management Co
Box 5864
SE-102 40 Stockholm Sweden
Tel 08-459 84 00
+46 8 459 84 00
Fax 08-661 57 19
+46 8 661 57 19

Abstract

This report describes the performance, evaluation and interpretation of in situ groundwater flow measurements and a single well injection withdrawal tracer test (SWIW test) in Laxemar area at the Oskarshamn site. The objective of the activity was to determine the groundwater flow in selected fractures/fracture zones intersecting the cored borehole KLX03. The objective was also to determine transport properties in a fracture zone by means of a SWIW test in the borehole.

Groundwater flow measurements were carried out in three single fractures and five fracture zones breaching KLX03 at borehole lengths ranging from 123 to 969 m (elevation –100 to –920 m). Hydraulic transmissivity ranged within $T = 1.6 \cdot 10^{-7}–1.3 \cdot 10^{-5}$ m^2/s. The results of the dilution measurements show that the groundwater flow varies considerably in fractures and fracture zones during natural undisturbed conditions, nevertheless the general trend is that flow rates and Darcy velocities decreases with depth. Flow rate ranged from 0.018 to 4.2 ml/min and Darcy velocity from $1.4 \cdot 10^{-9}$ to $1.2 \cdot 10^{-7}$ m/s ($1.2 \cdot 10^{-4}–1.0 \cdot 10^{-2}$ m/d), which are in accordance with results from previously preformed dilution measurements in the Simpevarp and Laxemar areas. In KLX03 the highest single flow rate and Darcy velocity was measured in the upper part of deformation zone DZ1. This is also the only section were the rock type is fine-grained diorite-gabbro, all the other sections passes through Ävrö granite. Hydraulic gradients, calculated according to the Darcy concept, are within the expected range (0.001–0.05) in the majority of the measured sections. Groundwater flow rate is also proportional to hydraulic transmissivity.

The SWIW test was carried out in the upper part of deformation zone DZ1 at a borehole length of c 740 m with a hydraulic transmissivity of $T = 4.5 \cdot 10^{-6}$ m^2/s. The model evaluation was made using a radial flow model with advection, dispersion and linear equilibrium sorption as transport processes.

A result from the SWIW tests is that there is a very clear retardation/sorption effect of both cesium and rubidium. The value of the retardation factor R for cesium (about 235) agrees approximately with values from cross-hole tests, obtained using similar transport models. Estimated values of R for rubidium (about 390) are larger than expected. Estimated tracer recovery at the last sampling time yields approximately 90%, 52% and 44% for Uranine, cesium and rubidium, respectively. The model simulations were carried out for four different values of porosity; 0.005, 0.01, 0.02 and 0.05, resulting in estimates of longitudinal dispersivity within 0.51–1.75 m.

Sammanfattning

Denna rapport beskriver genomförandet, utvärderingen samt tolkningen av in situ grundvattenflödesmätningar och enhåls spårförsök (SWIW test) i Laxemar, Oskarshamn. Syftet med aktiviteten var dels att bestämma grundvattenflödet i enskilda sprickor och sprickzoner som skär borrhålet KLX03 samt att bestämma transportegenskaper i potentiella flödesvägar genom att utföra och utvärdera SWIW test i en sprickzon i borrhålet.

Grundvattenflödesmätningar genomfördes i tre enskilda sprickor och i fem sprickzoner på borrhålslängd på nivåer från 123 till 969 m borrhålslängd (100 till 920 m nivå under havsytan). Den hydrauliska transmissiviteten varierade inom intervallet $T = 1{,}6 \cdot 10^{-7}$–$1{,}3 \cdot 10^{-5}$ m^2/s. Resultaten från utspädningsmätningarna i borrhål KLX03 visar att grundvattenflödet varierar avsevärt i sprickor och sprickzoner under naturliga ostörda hydrauliska förhållanden, ändå är den generella trenden att flödet och Darcyhastigheten minskar mot djupet. Beräknade grundvattenflöden låg inom intervallet 0,018–4,2 ml/min och Darcyhastigheten varierade från $1{,}4 \cdot 10^{-9}$ till $1{,}2 \cdot 10^{-7}$ m/s ($1{,}2 \cdot 10^{-4}$–$1{,}0 \cdot 10^{-2}$ m/d), vilket överensstämmer med tidigare genomförda mätningar i Simpevarp och Laxemar. I KLX03 uppmättes det enskilt största grundvattenflödet och Darcyhastighet i övre delen av deformationszonen DZ1. Det är också den enda sektionen med finkornig diorit-gabbro, alla andra sektioner är mätta i Ävrö granit. Grundvattenflödet är proportionellt mot hydrauliska transmissiviteten och hydrauliska gradienter, beräknade enligt Darcy konceptet, ligger inom det förväntade området (0,001–0,05) i flertalet av de testade sprickorna/zonerna.

SWIW testet genomfördes i övre delen av deformationszon DZ1 på cirka 740 m borrhålslängd med $T = 4{,}5 \cdot 10^{-6}$ m^2/s. Utvärderingen gjordes med en radiell flödesmodell med advektion, dispersion och linjär jämviktssorption som transportprocesser.

Ett resultat från SWIW testet är en tydlig effekt av fördröjning/sorption av cesium och rubidium. Det av modellen bestämda värdet på retardationsfaktorn R för cesium (ca 235) överensstämmer relativt bra med värden från flerhålsspårförsök, erhållna med motsvarande transportmodeller. För rubidium är värdet på R (ca 390) större än väntat. Den beräknade återtagningen av spårämnena i återpumpningsfasen var cirka 90 %, 52 % och 44 % för respektive Uranin, cesium och rubidium. Modellpassningar till mätdata gjordes för fyra olika värden på porositet; 0,005, 0,01, 0,02 och 0,05, vilket resulterade i longitudinell dispersivitet inom 0,51–1,75 m.

Contents

1 Introduction

SKB is currently conducting a site investigation for a deep repository in Laxemar, according to general and site specific programmes /SKB 2001ab, 2002/. Two, among several methods for site characterisation are in situ groundwater flow measurements and single well injection withdrawal tests (SWIW tests).

This document reports the results gained by a SWIW test and groundwater flow measurements with the borehole dilution probe in borehole KLX03. The work was conducted by Geosigma AB and carried out in July, September and October 2005, according to activity plan AP PS 400-05-025. In Table 1-1 controlling documents for performing this activity are listed. Both activity plans and method descriptions are SKB's internal controlling documents. Data and results were delivered to the SKB site characterization database SICADA.

The borehole KLX03 is situated at the Laxemar site near Oskarshamn, Figure 1-1. KLX03 is a sub-vertical core borehole with an inclination of –74.9° from the horizontal plane. The borehole is in total 1,000 m deep and cased down to 101 m. From 101 m down to 1,000 m the diameter is 76 mm.

Detailed information about the borehole KLX03 are listed in Appendix A (excerpt from the SKB database SICADA).

Table 1-1. Controlling documents for the performance of the activity.

Activity plan	Number	Version
Grundvattenflödesmätningar och SWIW-tester med Utspädningssond i borrhål KLX03	AP PS 400-05-025	1.0
Method descriptions	**Number**	**Version**
Metodbeskrivning för grundvattenflödesmätning	SKB MD 350.001	1.0
Kalibrering av tryckgivare, temperaturgivare och flödesmätare	SKB MD 353.014	2.0
Kalibrering av fluorescensmätning	SKB MD 353.015	2.0
Kalibrering Elektrisk konduktivitet	SKB MD 353.017	2.0
Utspädningsmätning	SKB MD 353.025	2.0
Löpande och avhjälpande underhåll av Utspädningssond	SKB MD 353.065	1.0
Systemöversikt – SWIW-test utrustning	SKB MD 353.069	1.0
Löpande och avhjälpande underhåll av SWIW-test utrustning	SKB MD 353.070	1.0
Kalibrering av flödesmätare i SWIW-test utrustning	SKB MD 353.090	1.0
Instruktion för längdkalibrering vid undersökningar i kärnborrhål	SKB MD 620.010	1.0
Instruktion för rengöring av borrhålsutrustning och viss markbaserad utrustning	SKB MD 600.004	1.0

Figure 1-1. *Overview of the Oskarshamn site investigation area, with sub areas Laxemar and Simpevarp, showing core boreholes (purple) and percussion boreholes (blue). KLX03 is located at coordinates 6366112 north and 1547718 east.*

2 Objective and scope

The objective of the activity was to measure groundwater flow under a natural gradient in order to achieve information about natural flows and hydraulic gradients in the Laxemar area.

The objective of the SWIW test was to determine transport properties of groundwater flow paths in fractures/fracture zones in a depth range of 300–700 m and a hydraulic transmissivity of $1 \cdot 10^{-8}$–$1 \cdot 10^{-6}$ m^2/s in the test section.

The groundwater flow measurements were performed in fractures and fracture zones at a borehole length range of 123–969 m using the SKB borehole dilution probe. The hydraulic transmissivity in the test sections ranged from $1.6 \cdot 10^{-7}$–$1.3 \cdot 10^{-5}$ m^2/s. Groundwater flow measurements were performed in totally eight test sections. In one of these sections a SWIW test was also performed, simultaneously using both sorbing and non-sorbing tracers.

3 Equipment

3.1 Borehole dilution probe

The borehole dilution probe is a mobile system for groundwater flow measurements, Figure 3-1. Measurements can be made in boreholes with 56 mm or 76 mm diameter and the test section length can be arranged for 1, 2, 3, 4 or 5 m with an optimised special packer/dummy system and section length between 1 and 10 m with standard packers. The maximum measurement depth is at 1,030 m borehole length. The main part of the equipment is the probe which measures the tracer concentration in the test section down hole and in situ. The probe is equipped with two different measurement devices. One is the Optic device, which is a combined fluorometer and light-transmission meter. Several fluorescent and light absorbing tracers can be used with this device. The other device is the Electrical Conductivity device, which measures the electrical conductivity of the water and is used for detection/analysis of saline tracers. The probe and the packers that straddle the test section are lowered in the borehole with an umbilical hose. The hose contains a tube for hydraulic inflation/deflation of the packers and electrical wires for power supply and communication/data transfer. Besides tracer dilution, the absolute pressure

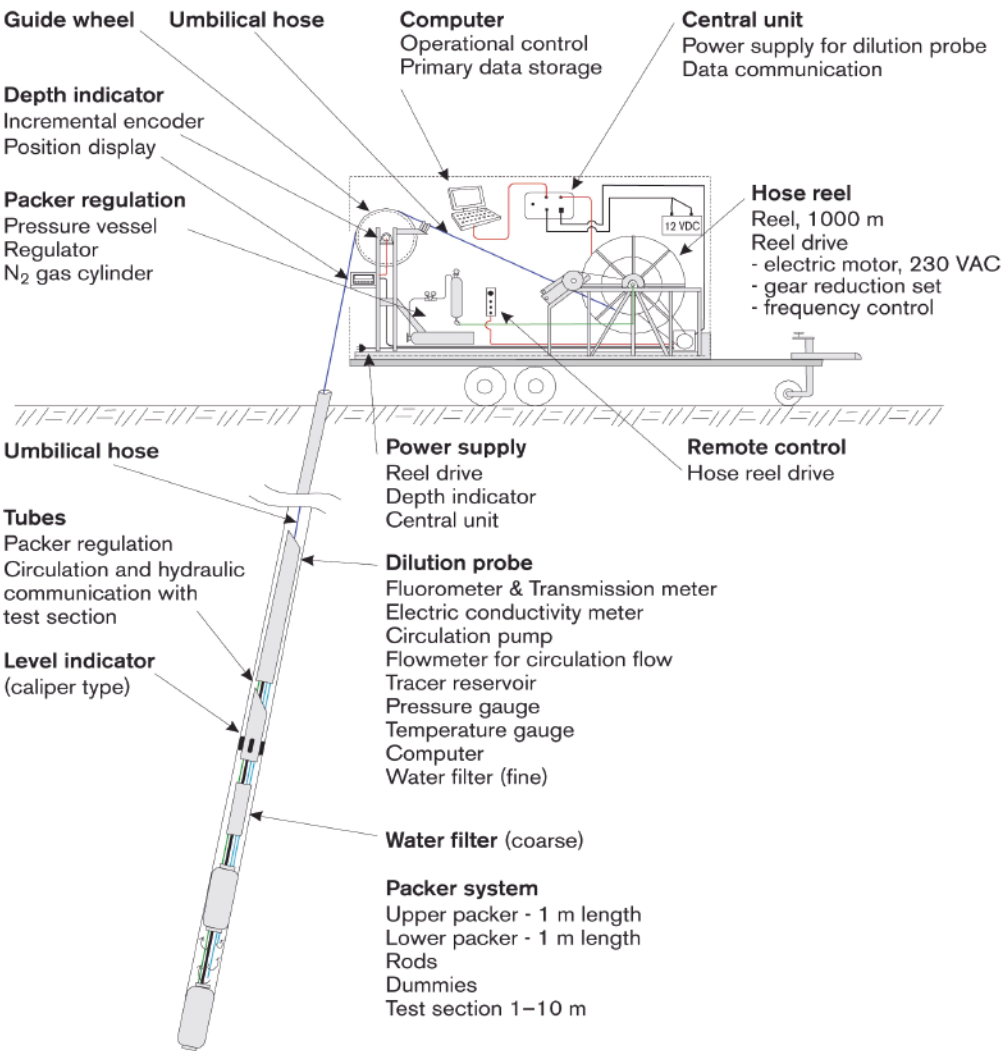

Figure 3-1. *The SKB borehole dilution probe.*

and temperature are also measured. The absolute pressure is measured during the process of dilution because a change in pressure indicates that the hydraulic gradient, and thus the groundwater flow, may have changed. The pressure gauge and the temperature gauge are both positioned in the dilution probe, about seven metres from top of test section. This bias is not corrected for as only changes and trends relative to the start value are of great importance for the dilution measurement. Since the dilution method requires homogenous distribution of the tracer in the test section also a circulation pump is installed and circulation flow rate measured.

A caliper log, attached to the dilution probe, is used to position the probe and test section at the pre-selected borehole length. The caliper detects reference marks previously made by a drill bit at exact length along the borehole, approximately every 50 m. This method makes it possible to position the test section with an accuracy of c ± 0.10 m.

3.1.1 Measurement range and accuracy

The lower limit of groundwater flow measurement is set by the dilution caused by molecular diffusion of the tracer into the fractured/porous aquifer, relative to the dilution of the tracer due to advective groundwater flow through the test section. In a normally fractured granite, the lower limit of a groundwater flow measurement is approximately at a hydraulic conductivity, K, between $6 \cdot 10^{-9}$ and $4 \cdot 10^{-8}$ m/s, if the hydraulic gradient, I, is 0.01. This corresponds to a groundwater flux (Darcy velocity), v, in the range of $6 \cdot 10^{-11}$ to $4 \cdot 10^{-10}$ m/s, which in turn may be transformed into groundwater flow rates, Q_w, corresponding to 0.03–0.2 ml/hour through a 1 m test section in a 76 mm diameter borehole. In a fracture zone with high porosity, and thus a higher rate of molecular diffusion from the test section into the fractures, the lower limit is about $K = 4 \cdot 10^{-7}$ m/s if $I = 0.01$. The corresponding flux value is in this case $v = 4 \cdot 10^{-9}$ m/s and flow rate $Q_w = 2.2$ ml/hour. The lower limit of flow measurements is, however, in most cases constrained by the time available for the dilution test. The required time frame for an accurate flow determination from a dilution test is within 7–60 hours at hydraulic conductivity values greater than about $1 \cdot 10^{-7}$ m/s. At conductivity values below $1 \cdot 10^{-8}$ m/s, measurement times should be at least 70 hours for natural undisturbed hydraulic gradient conditions.

The upper limit of groundwater flow measurements is determined by the capability of maintaining a homogeneous mix of tracer in the borehole test section. This limit is determined by several factors, such as length of the test section, volume, distribution of the water conducting fractures and how the circulation pump inlet and outlet are designed. The practical upper measurement limit is about 2,000 ml/hour for the equipment developed by SKB.

The accuracy of determined flow rates through the borehole test section is affected by various measurement errors related to, for example, the accuracy of the calculated test section volume and determination of tracer concentration. The overall accuracy when determining flow rates through the borehole test section is better than ± 30%, based on laboratory measurements in artificial borehole test sections.

The groundwater flow rates in the rock formation is determined from the calculated groundwater flow rates through the borehole test section and by using some assumption about the flow field around the borehole test section. This flow field depends on the hydraulic properties close to the borehole and is given by the correction factor α, as discussed below in Section 4.4.1. The value of α will, at least, vary within $\alpha = 2 \pm 1.5$ in fractured rock /Gustafsson 2002/. Hence, the groundwater flow in the rock formation is calculated with an accuracy of about ± 75%, depending on the flow-field distortion.

3.2 SWIW test equipment

The SWIW (Single Well Injection Withdrawal) test equipment constitutes a complement to the borehole dilution probe making it possible to carry out a SWIW test in the same test section as the dilution measurement, Figure 3-2. Measurements can be made in boreholes with 56 mm or 76 mm diameter and the test section length can be arranged for 1, 2, 3, 4 or 5 m with an optimised special packer/dummy system for 76 mm boreholes. The equipment is primarily designed for measurements in the depth interval 300–700 m. However, measurements can be carried out at shallower depths as well at depths larger than 700 m. The possibility to carry out a SWIW test much depends on the hydraulic transmissivity in the investigated test section and frictional loss in the tubing at tracer withdrawal pumping. Besides the dilution probe the main parts of the SWIW test equipment are:

- Polyamide tubing constituting the hydraulic connection between SWIW test equipment at ground surface and the dilution probe in the borehole.
- Air tight vessel for storage of groundwater under anoxic conditions, i.e. N_2-athmosphere.
- Control system for injection of tracer solution and groundwater (chaser fluid).
- Injection pumps for tracer solution and groundwater.

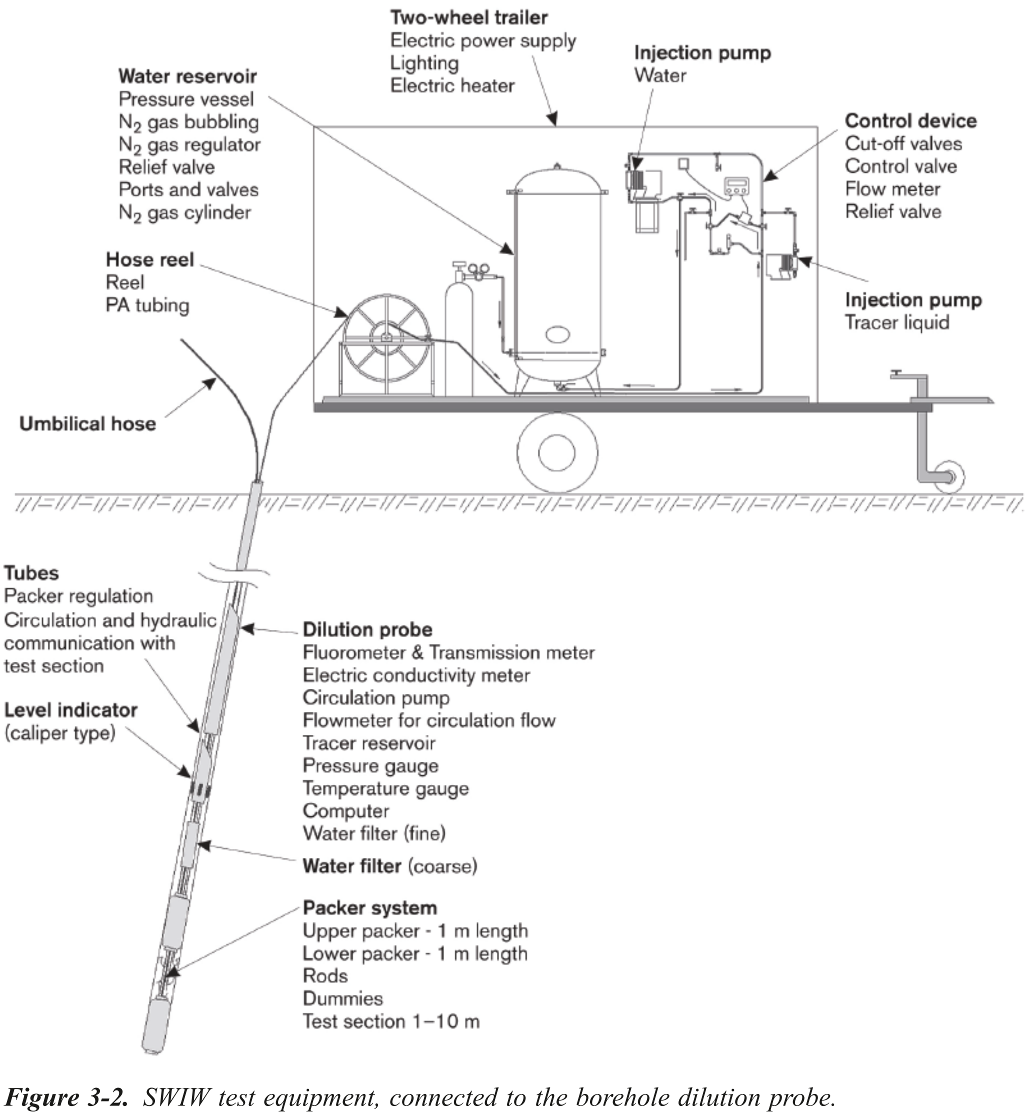

***Figure 3-2.** SWIW test equipment, connected to the borehole dilution probe.*

3.2.1 Measurement range and accuracy

The result of a SWIW test depends on the accuracy in the determination of the tracer concentration in injection solutions and withdrawn water. The result also depends on the accuracy in the volume of injection solution and volumes of injected and withdrawn water. For non-sorbing dye tracers (e.g. Uranine) the tracer concentration in collected water samples can be analysed with a resolution of 10 µg/l in the range 0.0–4.0 mg/l. The accuracy is within ± 5%. The volume injected tracer solution can be determined within ± 0.1% and the volume of injected and withdrawn water determined within ± 5%.

The evaluation of a SWIW test and determination of transport parameters is done with model simulations, fitting the model to the measured data (concentration as a function of time). The accuracy in determined transport parameters depends on selection of model concept and how well the model fits the measured data.

4 Execution

The measurements were performed according to AP PS 400-05-025 (SKB internal controlling document) in compliance with the methodology descriptions for the borehole dilution probe equipment – SKB MD 350.001 Metodbeskrivning för grundvattenflödesmätning –, and the measurement system description for SWIW test – SKB MD 353.069, MSB; Systemöversikt – SWIW-test utrustning – (SKB Internal controlling documents), Table 1-1.

4.1 Preparations

The preparations included calibration of the fluorometer and the electric conductivity meter before arriving at the site. Briefly, this was performed by adding certain amounts of the tracer to a known test volume while registering the measured A/D-levels. From this, calibration constants were calculated and saved for future use by using the measurement application. The other sensors had been calibrated previously and were hence only control calibrated.

Extensive functionality checks were performed prior to transport to the site and limited function checks were performed at the site The equipment was cleaned to comply with SKB cleaning level 1 before lowering it into the borehole.

All preparations were performed according to SKB Internal controlling documents, cf Table 1-1.

4.2 Procedure

4.2.1 Groundwater flow measurement

In total 8 groundwater flow measurements were carried out, Table 4-1. Each measurement was performed according to the following procedure. The equipment was lowered to the right borehole length where background values of tracer concentration and supporting parameters, pressure and temperature were measured and logged. Then, after inflating the packers and the pressure had stabilized, tracer was injected in the test section. The tracer concentration and supporting parameters were measured and logged continuously until the tracer had been diluted to such a degree that the groundwater flow rate could be calculated.

Table 4-1. Performed dilution measurements.

Test section (m)	Number of flowing fractures*	T (m^2/s)*	Tracer	Measurement period (yymmdd–yymmdd)
123.7–124.7	1	2.31E–07	Uranine	050707–050711
195.0–198.0	2–3	1.25E–05	Uranine	050908–050909
266.2–267.2	1	7.85E–07	Uranine	050711–050713
409.6–410.6	1	1.62E–07	Uranine	050713–050718
662.2–663.2	1–2	2.06E–07	Uranine	050919–050922
740.4–744.4	3–4	4.48E–06	Uranine	050926–050927
769.7–772.7	2–4	5.30E–07	Uranine	050909–050913
969.7–970.7	1–2	4.52E–07	Uranine	050914–050919

* /Rouhiainen et al. 2005/

4.2.2 SWIW test

One SWIW test was performed, Table 4-2. BIPS logging of the test section is shown in Appendix C. To conduct a SWIW test requires that the SWIW equipment is connected to the borehole dilution probe, Figures 3-1 and 3-2.

The SWIW test was performed according to the following procedure. The equipment was lowered to the right borehole length where background values of Uranine and supporting parameters, pressure and temperature were measured and logged. Then, after inflating the packers and the pressure had stabilized, the circulation pump in the dilution probe was used to pump groundwater from the test section to the air tight vessel at ground surface. Water samples were also taken for analysis of background concentration of Uranine, rubidium and cesium. When pressure had recovered after the pumping in the test section, the injection phases started with pre-injection of the native groundwater to reach steady state flow conditions. Thereafter injection of groundwater spiked with the tracers Uranine, rubidium and cesium and at last injection of native groundwater to push the tracers out into the fracture zone was performed. The withdrawal phase started by pumping water to the ground surface. An automatic sampler at ground surface was used to take water samples for analysis of Uranine, rubidium and cesium in the withdrawn water.

4.3 Data handling

During groundwater flow measurement with the dilution probe, data is automatically transferred from the measurement application to a SQL database. Data relevant for analysis and interpretation is then automatically transferred from SQL to Excel via an MSSQL (ODBC) data link, set up by the operator. After each measurement the Excel data file is copied to a CD or to USB memory.

The water samples from the SWIW tests were analysed for Uranine tracer content at the Geosigma Laboratory in Uppsala. Cesium and rubidium content were analysed at the Analytica laboratory in Luleå.

4.4 Analyses and interpretation

4.4.1 The dilution method – general principles

The dilution method is an excellent tool for in situ determination of flow rates in fractures and fracture zones.

In the dilution method a tracer is introduced and homogeneously distributed into a bore-hole test section. The tracer is subsequently diluted by the ambient groundwater, flowing through the borehole test section. The dilution of the tracer is proportional to the water flow through the borehole section, Figure 4-1.

Table 4-2. Performed SWIW test.

Borehole	Test section (m)	Number of flowing fractures*	T (m^2/s)*	Tracers	Measurement period (yymmdd–yymmdd)
KLX03	740.4–744.4	3–4	4.48E–06	Uranine/cesium/rubidium	050928–051010

* /Rouhiainen et al. 2005/.

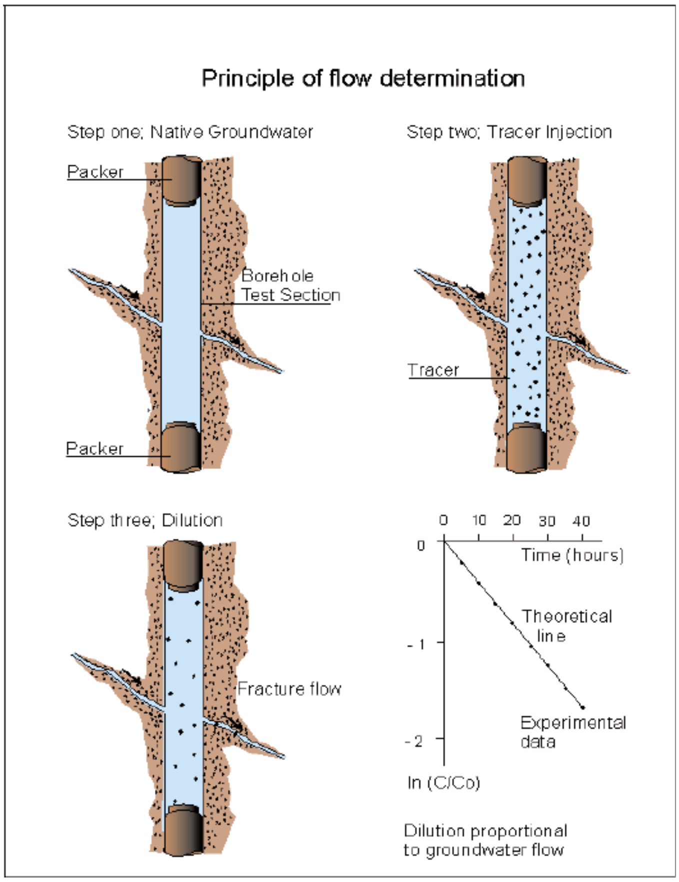

***Figure 4-1.** General principles of dilution and flow determination.*

The dilution in a well-mixed borehole section, starting at time t = 0, is given by:

$$\ln(C/C_0) = -\frac{Q_w}{V}\cdot t \qquad \text{(Equation 4-1)}$$

where C is the concentration at time t (s), C_0 is the initial concentration, V is the water volume (m^3) in the test section and Q_w is the volumetric flow rate (m^3s^{-1}). Since V is known, the flow rate may then be determined from the slope of the line in a plot of ln (C/C_0), or ln C, versus t.

An important interpretation issue is to relate the measured groundwater flow rate through the borehole test section to the rate of groundwater flow in the fracture/fracture zone straddled by the packers. The flow-field distortion must be taken into consideration, i.e. the degree to which the groundwater flow converges and diverges in the vicinity of the borehole test section. With a correction factor, α, which accounts for the distortion of the flow lines due to the presence of the borehole, it is possible to determine the cross-sectional area perpendicular to groundwater flow by:

$$A = 2\cdot r\cdot L\cdot \alpha \qquad \text{(Equation 4-2)}$$

where A is the cross-sectional area (m^2) perpendicular to groundwater flow, r is borehole radius (m), L is the length (m) of the borehole test section and α is the correction factor. Figure 4-2 schematically shows the cross-sectional area, A, and how flow lines converge and diverge in the vicinity of the borehole test section.

Assuming laminar flow in a plane parallel fissure or a homogeneous porous medium, the correction factor α is calculated according to Equation (4-3), which often is called the formula of Ogilvi /Halevy et al. 1967/. Here it is assumed that the disturbed zone, created by the presence of the borehole, has an axis-symmetrical and circular form.

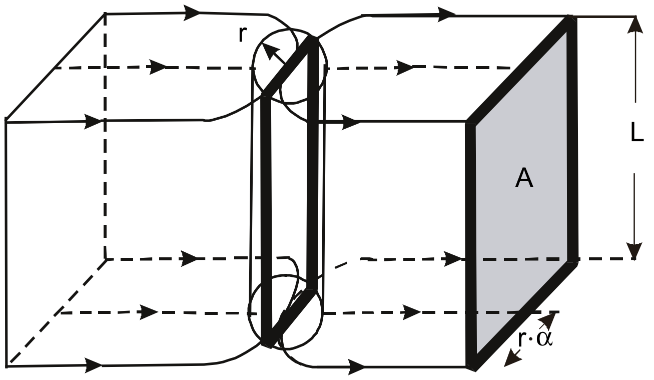

Figure 4-2. Diversion and conversion of flow lines in the vicinity of a borehole test section.

$$\alpha = \frac{4}{1 + (r/r_d) + (K_2/K_1)(1 - (r/r_d)^2)} \qquad \text{(Equation 4-3)}$$

where r_d is the outer radius (m) of the disturbed zone, K_1 is the hydraulic conductivity (m/s) of the disturbed zone, and K_2 is the hydraulic conductivity of the aquifer. If the drilling has not caused any disturbances outside the borehole radius, then $K_1 = K_2$ and $r_d = r$ which will result in $\alpha = 2$. With $\alpha = 2$, the groundwater flow within twice the borehole radius will converge through the borehole test section, as illustrated in Figures 4-2 and 4-3.

If there is a disturbed zone around the borehole the correction factor α is given by the radial extent and hydraulic conductivity of the disturbed zone. If the drilling has caused a zone with a lower hydraulic conductivity in the vicinity of the borehole than in the fracture zone, e.g. positive skin due to drilling debris and clogging, the correction factor α will decrease. A zone of higher hydraulic conductivity around the borehole will increase α. Rock stress redistribution, when new boundary conditions are created by the drilling of the borehole, may also change the hydraulic conductivity around the borehole and thus affect α. In Figure 4-3, the correction factor, α, is given as a function of K2/K1 at different normalized radial extents of the disturbed zone (r/r_d). If the fracture/fracture zone and groundwater flow is not perpendicular to the borehole axis, this also has to be accounted for. At a 45 degree angle to the borehole axis the value of α will be about 41% larger than in the case of perpendicular flow. This is further discussed in /Gustafsson 2002/ and /Rhén et al. 1991/.

In order to obtain the Darcy velocity in the undisturbed rock the calculated ground water flow, Q_w is divided by A, Equation 4-4.

$$v = Q_w/A \qquad \text{(Equation 4-4)}$$

The hydraulic gradient is then calculated as

$$I = v/K \qquad \text{(Equation 4-5)}$$

where K is the hydraulic conductivity.

4.4.2 The dilution method – evaluation and analysis

The first step of evaluation included studying a graph of the measured concentration versus time data. For further evaluation background concentration, i.e. any tracer concentration in the groundwater before tracer injection, was subtracted from the measured concentrations. Thereafter $\ln(C/C_0)$ was plotted versus time. In most cases that relationship was linear and the proportionality constant was then calculated by performing a linear regression. In the cases where the relationship between $\ln(C/C_0)$ and time was non-linear, a sub-interval was chosen in which the relationship were linear.

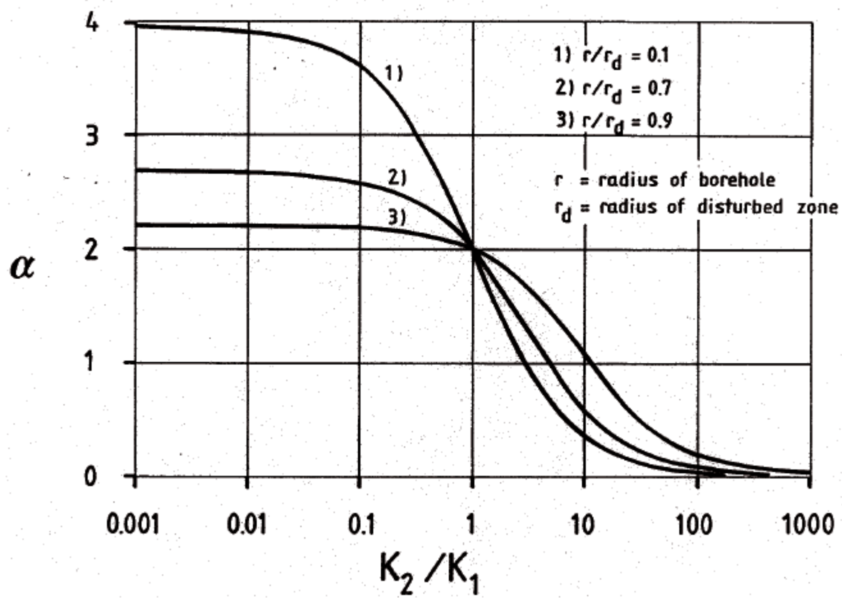

Figure 4-3. *The correction factor, α, as a function of K_2/K_1 at different radial extent (r/r_d) of the disturbed zone (skin zone) around the borehole.*

The value of $\ln(C/C_0)/t$ obtained from the linear regression was then used to calculate Q_w according to Equation (4-1).

The hydraulic gradient, I, was calculated by combining Equations (4-2), (4-4) and (4-5), and choosing $\alpha = 2$. The hydraulic conductivity, K, in Equation (4-5) was obtained from previously performed POSIVA Difference flow measurements (PFL) /Rouhiainen et al. 2005/.

4.4.3 SWIW-test – basic outline

A Single Well Injection Withdrawal (SWIW) test may consist of all or some of the following phases:

1. Filling-up pressure vessel with groundwater from the selected fracture.
2. Injection of water to establish steady state hydraulic conditions (pre-injection).
3. Injection of one or more tracers.
4. Injection of groundwater (chaser fluid) after tracer injection is stopped.
5. Waiting phase.
6. Withdrawal (recovery) phase.

The tracer breakthrough data that is eventually used for evaluation is obtained from the withdrawal phase. The injection of chaser fluid, i.e. groundwater from the pressure vessel, has the effect of pushing the tracer out as a "ring" in the formation surrounding the tested section. This is generally a benefit because when the tracer is pumped back both ascending and descending parts are obtained in the recovery breakthrough curve. During the waiting phase there is no injection or withdrawal of fluid. The purpose of this phase is to increase the time available for time-dependent transport-processes so that these may be more easily evaluated from the resulting breakthrough curve. A schematic example of a resulting breakthrough curve during a SWIW test is shown in Figure 4-4.

The design of a successful SWIW test requires prior determination of injection and withdrawal flow rates, duration of tracer injection, duration of the various injection, waiting and pumping phases, selection of tracers, tracer injection concentrations, etc.

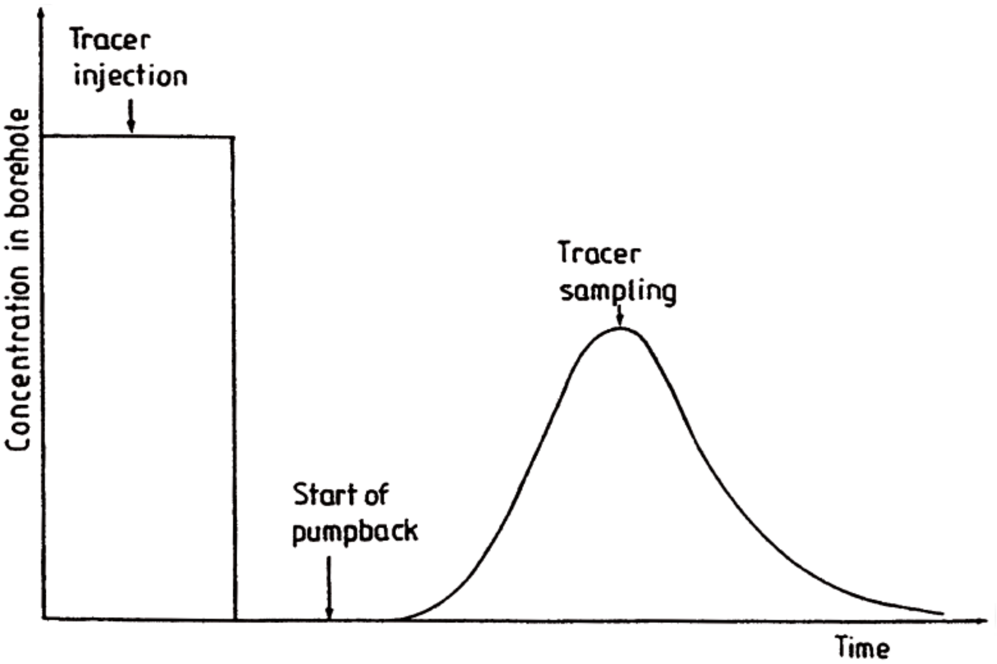

__Figure 4-4.__ Schematic tracer concentration sequence during a SWIW test /Andersson 1995/.

4.4.4 SWIW-test – evaluation and analysis

The model evaluation of the experimental results was carried out assuming homogenous conditions. Model simulations were made using the model code SUTRA /Voss 1984/ and the experiments were simulated without a background hydraulic gradient. It was assumed that flow and transport occurs within a planar fracture zone of some thickness. The volume available for flow was represented by assigning a porosity value to the assumed zone. Modelled transport processes include advection, dispersion and linear equilibrium sorption.

The sequence of the different injection phases were modelled as accurately as possible based on supporting data for flows and tracer injection concentration. Generally, experimental flows and times may vary from one phase to another, and the flow may also vary within phases. The specific experimental sequences are listed in Table 5-2.

In the simulation model, tracer injection was simulated as a function accounting for mixing in the borehole section and sorption (for cesium and rubidium) on the borehole walls. The function assumes a completely mixed borehole section and linear equilibrium surface sorption:

$$C = (C_0 - C_{in})e^{-\left(\frac{Q}{V_{bh}+K_a A_{bh}}\right)t} + C_{in} \qquad \text{(Equation 4-6)}$$

where C is concentration in water leaving the borehole section, and entering the formation (kg/m^3), V_{bh} is the borehole volume including circulation tubes (m^3), A_{bh} is area of borehole walls (m^2), Q is flow rate (m^3/s), C_{in} is concentration in the water entering the borehole section (kg/m^3), C_0 is initial concentration in the borehole section (kg/m^3), K_a is surface sorption coefficient (m) and t is elapsed time (s).

Based on in situ experiments /Andersson et al. 2002/ and laboratory measurements on samples of crystalline rock /Byegård and Tullborg 2005/ the sorption coefficient K_a was assigned a value of 10^{-2} m in all simulations. An example of the tracer injection input function is given in Figure 4-5, showing a 50 minutes long tracer injection phase followed by a chaser phase.

Non-linear regression was used to fit the simulation model to experimental data. The estimation strategy was generally to estimate the dispersivity (a_L) and a retardation factor (R), while setting

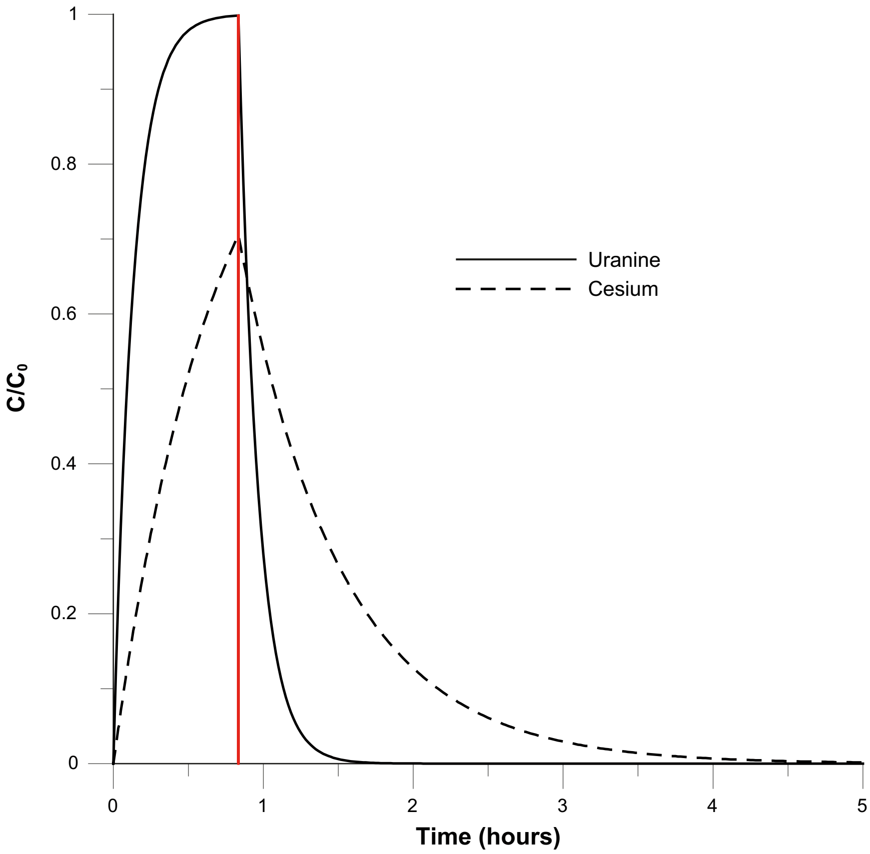

Figure 4-5. *Example of simulated tracer injection functions for a tracer injection (ending at 50 minutes shown by the vertical red line) phase immediately followed by a chaser phase.*

the porosity (i.e. the available volume for flow) to a fixed value. Simultaneous fitting of both tracer breakthrough curves (Uranine and cesium in the example), and calculation of fitting statistics, was carried out using the approach described in /Nordqvist and Gustafsson 2004/. Tracer breakthrough curves for Uranine and rubidium is related and calculated in the same way.

4.5 Nonconformities

Due to technical problems with the Electrical Conductivity device this had to be removed from the dilution probe and replaced by a pipe. As a consequence temperature could not be measured, since the temperature gauge is placed in the Electrical Conductivity device. All groundwater flow measurements were performed with the Optic device.

The nominal borehole diameter is 75.8 mm for KLX03. The nominal method gives borehole diameters that differ from –1.5 to –1.2 mm from the caliper borehole diameter.

Since the groundwater flow is determined from the dilution curve and the calculated water volume in the test section, according to Equation 4-1, impeccable measure of the borehole diameter is of great importance. Because of the recently found uncertainty in the caliper method, the nominal borehole diameter is used for the final calculations of groundwater flow, Darcy velocity and hydraulic gradient presented in this report.

Repeated problems with hoisting and lowering the equipment in the borehole occurred.
At c 160 m borehole length the equipment got stuck. A tractor with a hydraulic lift tool was used to lift the wagon and pull up the equipment. The packer rubber had been stretched and needed to be changed. Although a new rubber was mounted on the packer the problems with hoisting and lowering the equipment in the borehole continued.

Interruptions in the data transfer was another recurring problem. This was caused by potential drops in the electric power supply due to thunderstorms, a broken electric circuit or unexplainable interruptions in communication with the probe. During the SWIW test no data of pressure, circulation flow or fluorescence were transferred from the borehole probe. An electric circuit was exchanged during the first chaser injection which caused an interruption for about 40 minutes in the chaser injection.

The borehole water had a high amount of particles in large portions of the borehole which caused some delay in the measurements. The circulation of the water through a fine-meshed filter needed to go on for several hours in some sections before tracer injections could start.

5 Results

The primary data and original results are stored in the SKB database SICADA, where they are traceable by Activity Plan number. These data shall be used for further interpretation or modelling.

5.1 Dilution measurements

Figure 5-1 exemplifies a typical dilution curve in a single fracture straddled by the test section at 662.2–663.2 m borehole length in borehole KLX03. In the first phase the background value is recorded for about half an hour. In phase two, Uranine tracer is injected in five steps and after mixing a start concentration (C_0) of about 0.7 mg/l above background is achieved. In phase three the dilution is measured for about 60 hours. Thereafter the packers are deflated and the remaining tracer flows out of the test section (not shown in the figure). Figure 5-2 shows the measured pressure during the dilution measurement. Since the pressure gauge is positioned about seven metres from top of test section there is a bias from the pressure in the test section which is not corrected for, as only changes and trends relative to the start value are of great importance for the dilution measurement. Figure 5-3 is a plot of the $\ln(C/C_0)$ versus time data and linear regression best fit to data showing a god fit with correlation $R^2 = 0.9931$. The standard deviation, STDAV, shows the mean divergence of the values from the best fit line and is calculated from

$$\text{STDAV} = \sqrt{\frac{n\sum x^2 - \left(\sum x\right)^2}{n(n-1)}} \qquad \text{(Equation 5-1)}$$

Calculated groundwater flow rate, Darcy velocity and hydraulic gradient are presented in Table 5-1 together with the results from all other dilution measurements carried out in borehole KLX03.

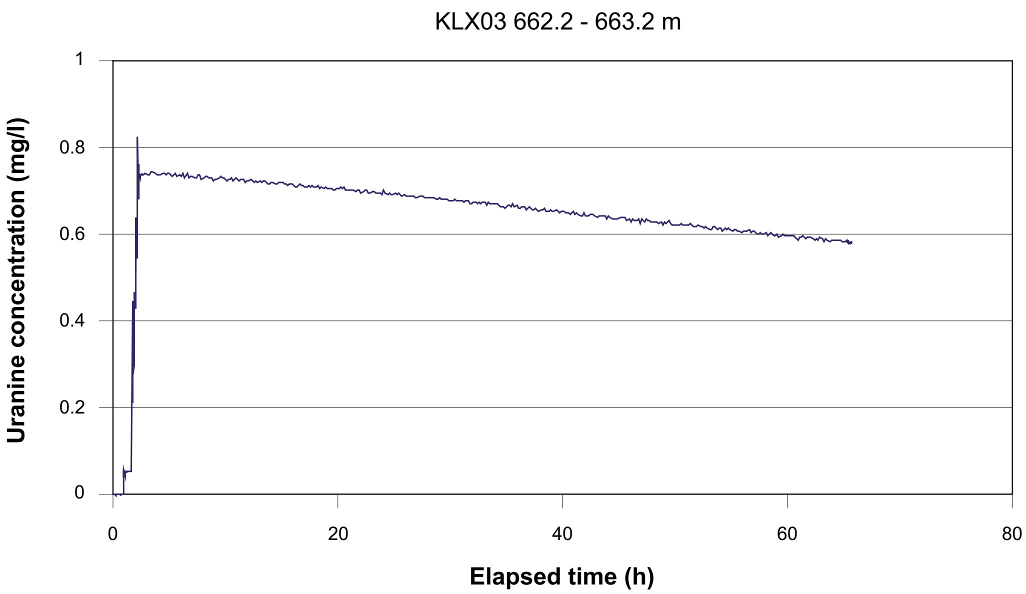

Figure 5-1. Dilution measurement in borehole KLX03, section 662.2–663.2 m.

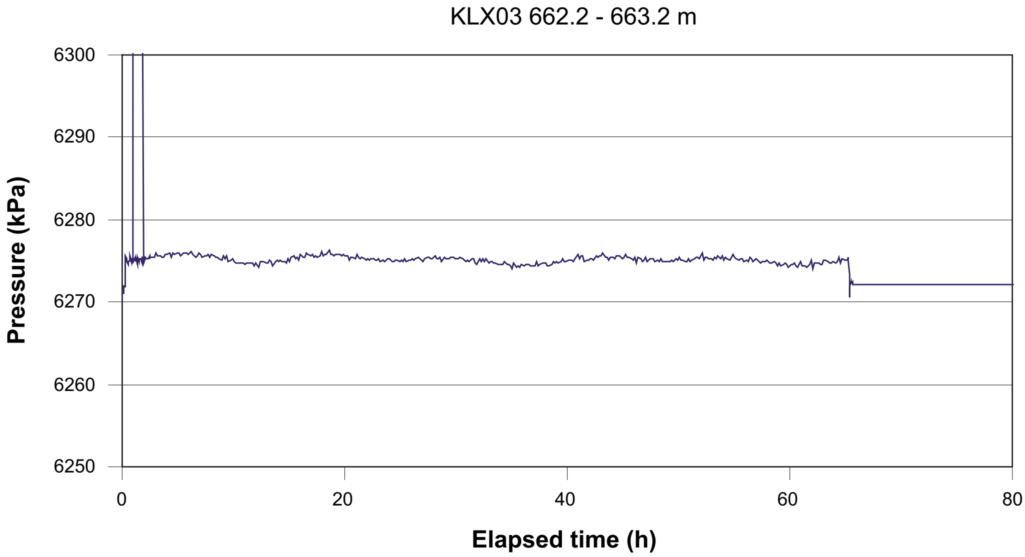

Figure 5-2. Measured pressure during dilution measurement in borehole KLX03, section 662.2–663.2 m.

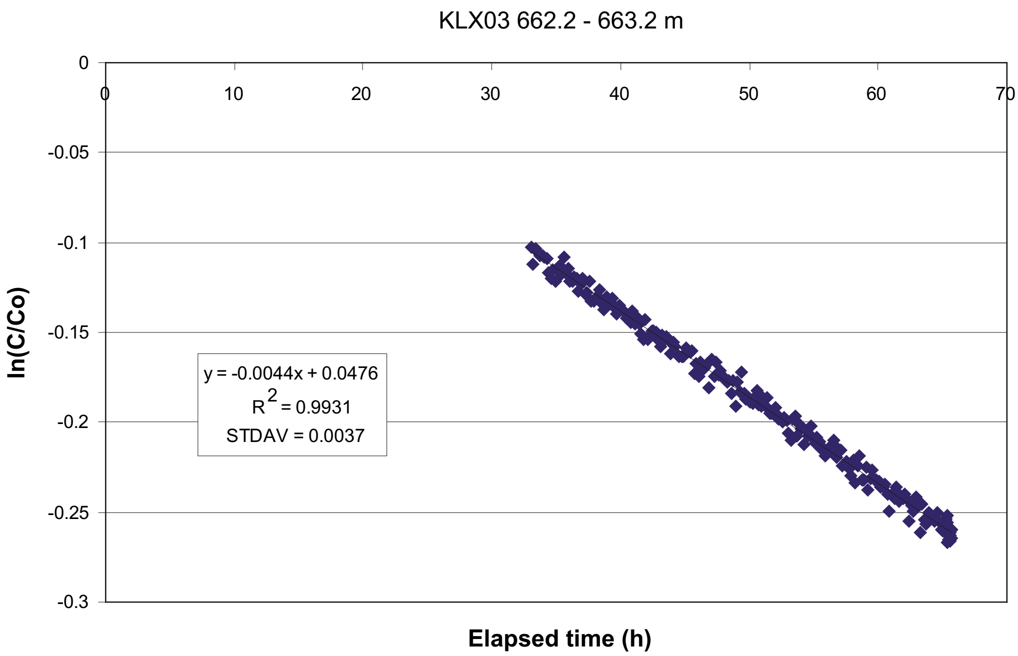

Figure 5-3. Linear regression best fit to data from dilution measurement in borehole KLX03, section 662.2–663.2 m.

The dilution measurements were carried out with the dye tracer Uranine. Uranine normally has a low and constant background concentration and the tracer can be injected and measured in concentrations far above the background value, which gives a large dynamic range and accurate flow determinations.

Details of all dilution measurements and evaluations, with diagrams of dilution versus time and the supporting parameters pressure and circulation flow rate are presented in Appendix B1–B8.

5.1.1 KLX03, section 123.7–124.7 m

This dilution measurement was carried out in a test section with a single flowing fracture. The complete test procedure can be followed in Figure 5-4. Background concentration (0.01 mg/l) is measured for about ten hours while the water is circulated to rinse the dirty borehole water. Thereafter the Uranine tracer is injected in five steps and after mixing it finally reaches a start concentration of 0.75 mg/l above background. Dilution is measured for about 76 hours, the packers are then deflated and the remaining tracer flows out of the test section. Hydraulic pressure shows small diurnal pressure variations due to earth tidal effects (Appendix B1).
The concentration versus time seems to follow a perfect dilution according to theory, but the complete set of the $\ln(C/C_0)$ versus time data could not fit a straight line. For this reason the final evaluation was made on the last part of the dilution measurement, from 68 to 88 hours of elapsed time. The correlation coefficient of the best fit line is $R^2 = 0.8566$ (Figure 5-5), and the groundwater flow rate, calculated from the best fit line, is 0.018 ml/min. Calculated hydraulic gradient is 0.009 and Darcy velocity $2.0 \cdot 10^{-9}$ m/s.

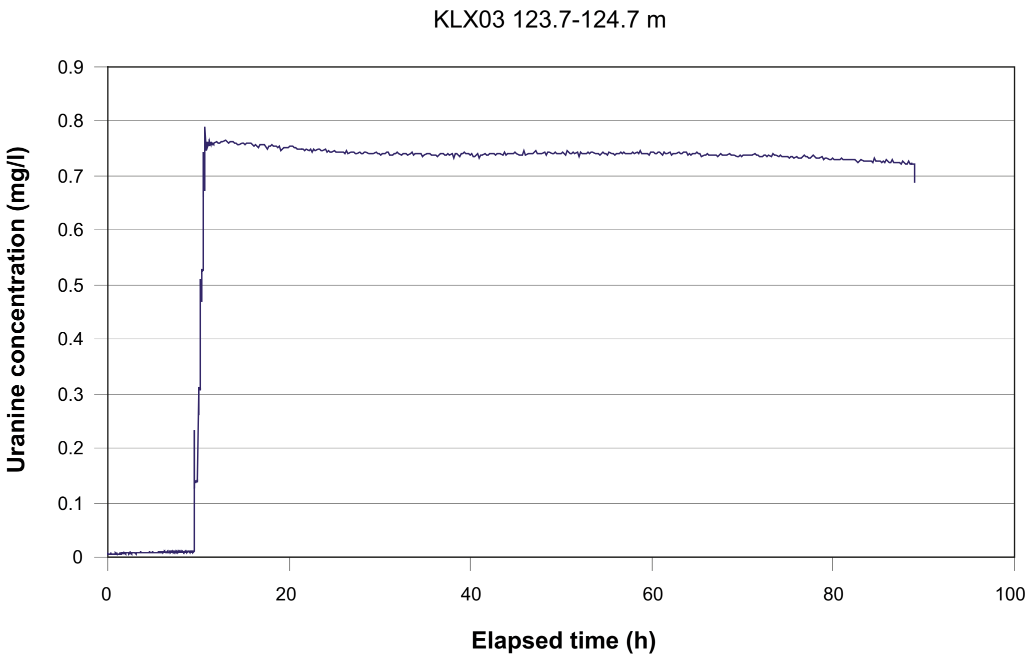

Figure 5-4. *Dilution measurement in borehole KLX03, section 123.7–124.7 m.*

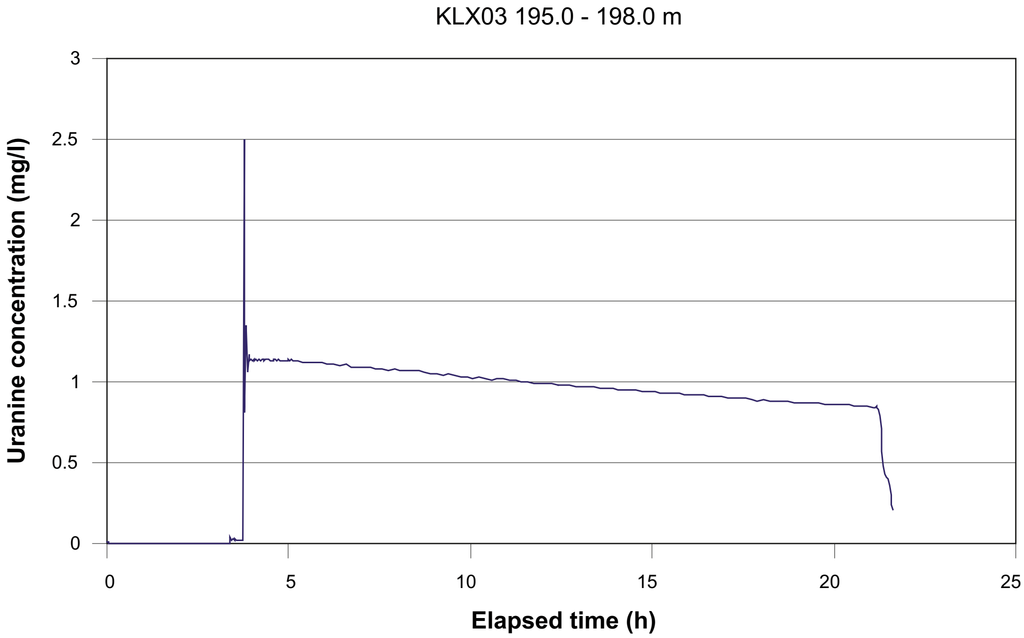

Figure 5-5. *Linear regression best fit to data from dilution measurement in borehole KLX03, section 123.7–124.7 m.*

5.1.2 KLX03, section 195.0–198.0 m

This dilution measurement was carried out in a test section with two-three flowing fractures. The background measurement, tracer injection and dilution can be followed in Figure 5-6. Background concentration (0.02 mg/l) is measured for about three hours. The Uranine tracer is injected in three steps and after mixing it reaches a start concentration of 1.11 mg/l above background. Dilution is measured for about 17 hours, the packers are then deflated and the remaining tracer flows out of the test section. Hydraulic pressure shows a slow decreasing trend during the first five hours of elapsed time (Appendix B2). Groundwater flow is determined from the 6–21 hours part of the dilution measurement. The regression line fits well to the slope of the dilution with a correlation coefficient of $R^2 = 0.9981$ for the best fit line (Figure 5-7). The groundwater flow rate, calculated from the best fit line, is 0.53 ml/min. Calculated hydraulic gradient is 0.005 and Darcy velocity $1.9 \cdot 10^{-8}$ m/s.

5.1.3 KLX03, section 266.2–263.2 m

This dilution measurement was carried out in a single fracture. The background measurement, tracer injection and dilution can be followed in Figure 5-8. Background concentration (0.07 mg/l) is measured for about 11 hours while the water is circulated to rinse the dirty borehole water. The Uranine tracer is injected in four steps and after mixing it reaches a start concentration of 0.44 mg/l above background. Dilution is measured for about 24 hours. Thereafter the packers are deflated, but this and succeeding activities of the dilution measurement were not logged in this case. Hydraulic pressure indicates a very small decreasing trend (Appendix B3). Groundwater flow is determined from the 15–35 hours part of the dilution measurement. The regression line fits well to the slope of the dilution with a correlation coefficient of $R^2 = 0.9933$ for the best fit line (Figure 5-9). The groundwater flow rate, calculated from the best fit line, is 0.18 ml/min. Calculated hydraulic gradient is 0.025 and Darcy velocity $2.0 \cdot 10^{-8}$ m/s.

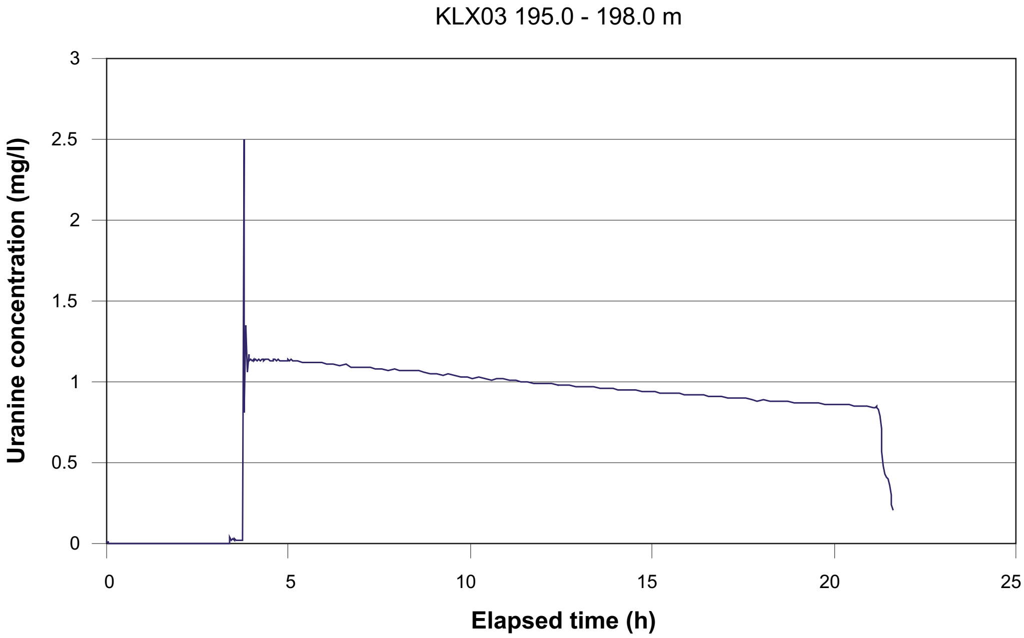

Figure 5-6. *Dilution measurement in borehole KLX03, section 195.0-198.0 m.*

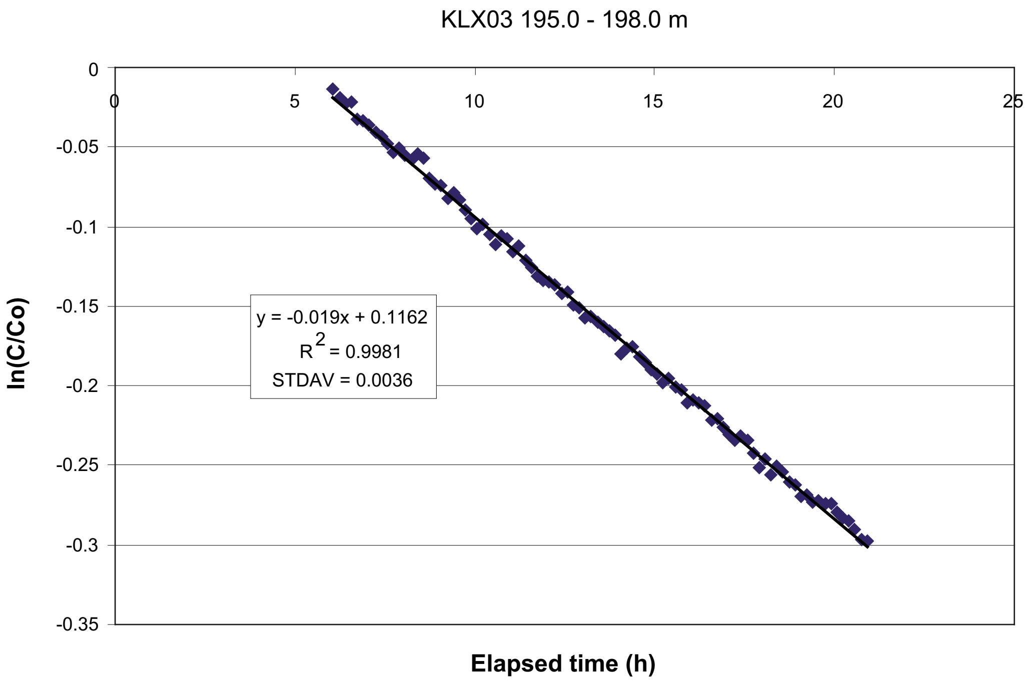

Figure 5-7. *Linear regression best fit to data from dilution measurement in borehole KLX03, section 195.0–198.0 m.*

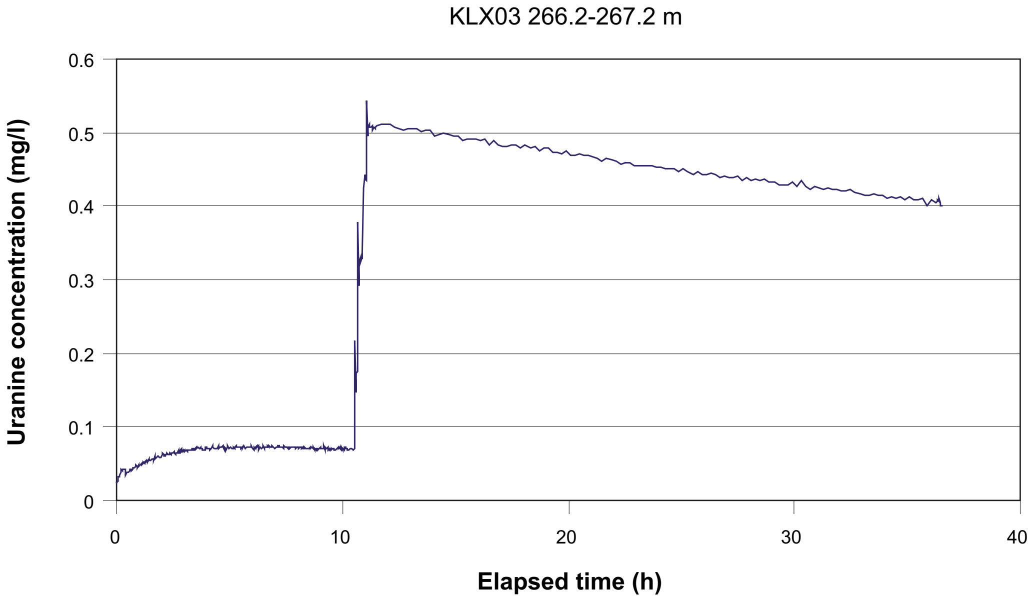

Figure 5-8. *Dilution measurement in borehole KLX03, section 266.2–267.2 m.*

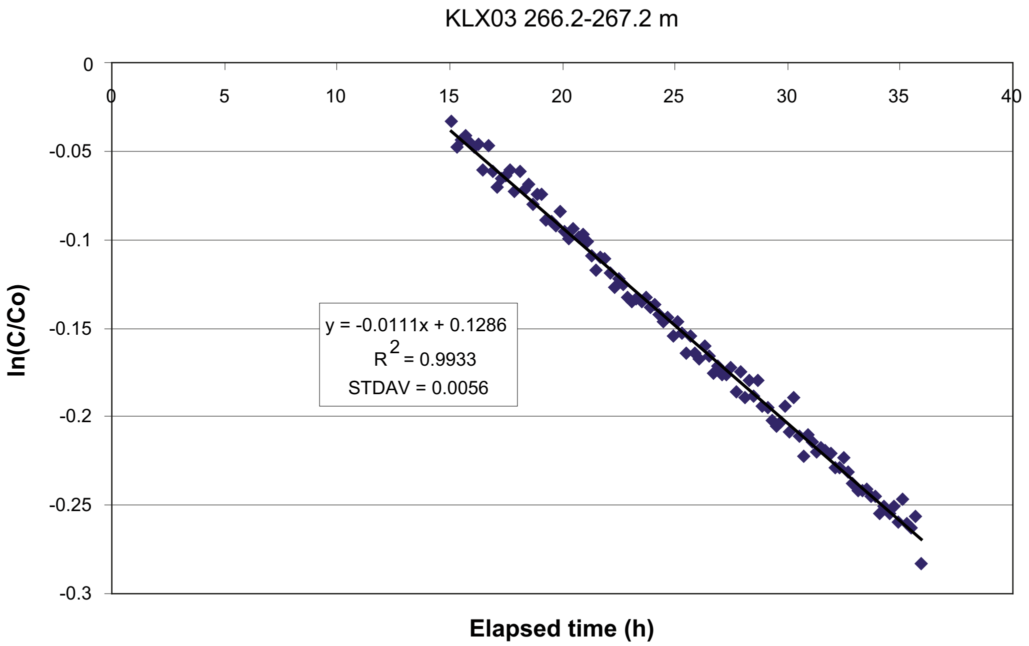

Figure 5-9. *Linear regression best fit to data from dilution measurement in borehole KLX03, section 266.2–267.2 m.*

5.1.4 KLX03, section 409.6–410.6 m

This dilution measurement was carried out in a single fracture. The background measurement, tracer injection and dilution can be followed in Figure 5-10. Background concentration (0.01 mg/l) is measured for about 21 hours while the water is circulated to rinse the dirty borehole water. Thereafter the Uranine tracer is injected in seven steps and after mixing it finally reaches a start concentration of 0.042 mg/l above background. The data transfer of circulation flow is interrupted just before the injection. Dilution is measured for about 14 hours, the packers are then deflated and the remaining tracer flows out of the test section. Hydraulic pressure indicates steady pressure conditions (Appendix B4). Groundwater flow is determined

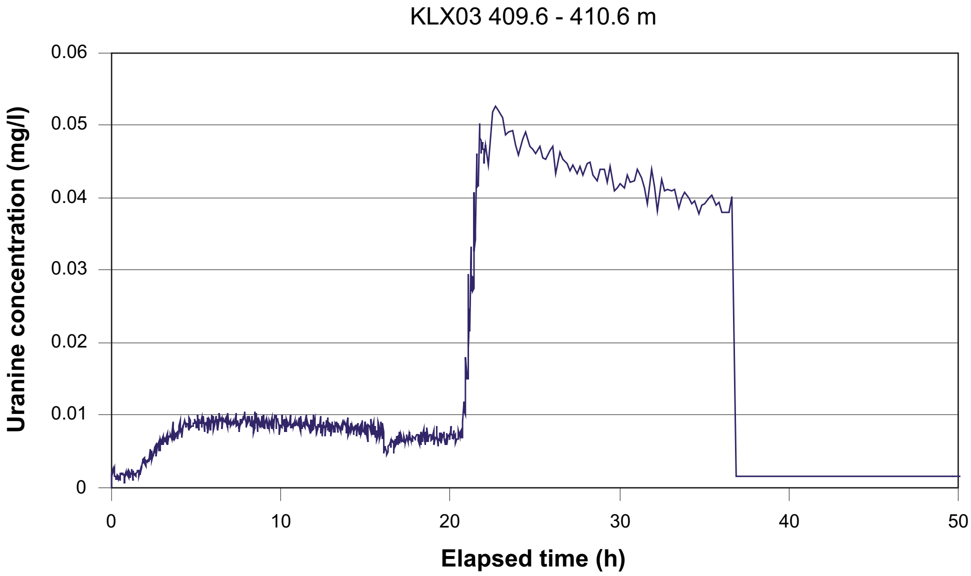

Figure 5-10. *Dilution measurement in borehole KLX03, section 409.6–410.6 m.*

from the 23–36 hours part of the dilution measurement. The regression line shows an acceptable fit to the ln (C/C_0) versus time data with a correlation coefficient of $R^2 = 0.8649$ for the best fit line (Figure 5-11). The groundwater flow rate, calculated from the best fit line, is 0.34 ml/min. Calculated hydraulic gradient is 0.23 and Darcy velocity $3.7 \cdot 10^{-8}$ m/s. The hydraulic gradient is very large and may be caused by local effects where the measured fracture constitutes a hydraulic conductor between other fractures with different hydraulic heads or wrong estimates of the correction factor, α, and/or the hydraulic conductivity of the fracture.

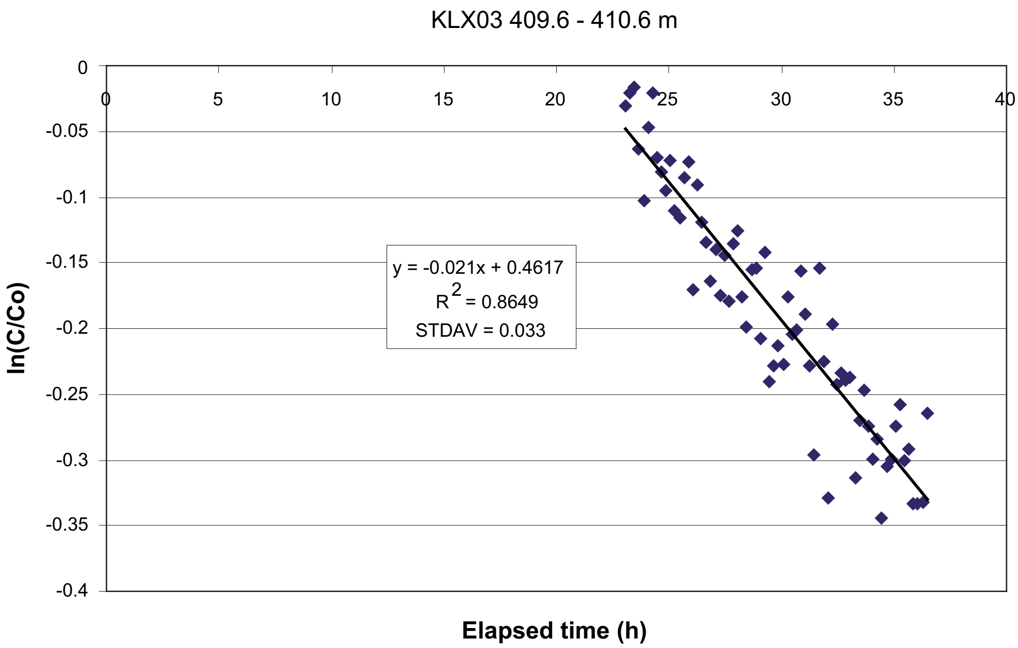

Figure 5-11. *Linear regression best fit to data from dilution measurement in borehole KLX03, section 409.6–410.6 m.*

5.1.5 KLX03, section 662.2–663.2 m

This dilution measurement was carried out in a test section with one-two flowing fractures. The background measurement, tracer injection and dilution can be followed in Figure 5-12. Background concentration (0.05 mg/l) is measured for about one hour. Thereafter the Uranine tracer is injected in five steps and after mixing it finally reaches a start concentration of 0.69 mg/l above background. Dilution is measured for about 61 hours. Thereafter the packers are deflated. A diurnal pressure variation due to earth tidal effects is visible (Appendix B5). The complete set of the ln (C/C_0) versus time data could not fit a straight line, although the correlation coefficient was high (R^2 = 0.9937). For this reason the final evaluation was made on the last part of the dilution measurement, from 33 to 65 hours of elapsed time. The correlation coefficient of the best fit line is R^2 = 0.9931 (Figure 5-13), and the groundwater flow rate, calculated from the best fit line, is 0.070 ml/min. Calculated hydraulic gradient is 0.038 and Darcy velocity $7.7 \cdot 10^{-9}$ m/s.

5.1.6 KLX03, section 740.4–744.4 m

This dilution measurement was carried out in a test section with three-four flowing fractures. The background measurement, tracer injection and dilution can be followed in Figure 5-14. Background concentration is 0.01 mg/l. The Uranine tracer is injected in six steps and after mixing it reaches a start concentration of 0.90 mg/l above background. Dilution is measured for about 18 hours. Thereafter the packers are deflated, but this and succeeding activities of the dilution measurement were not logged in this case. Hydraulic pressure indicates steady pressure conditions (Appendix B6). The complete set of the ln (C/C_0) versus time data could not fit a straight line, although the correlation coefficient was high (R^2 = 0.9942). For this reason the final evaluation was made on the last part of the dilution measurement, from 8 to 19 hours of elapsed time. The correlation coefficient of the best fit line is R^2 = 0.9982 (Figure 5-15), and the groundwater flow rate, calculated from the best fit line, is 4.2 ml/min. Calculated hydraulic gradient is 0.10 and Darcy velocity $1.2 \cdot 10^{-7}$ m/s. The hydraulic gradient is large and may be caused by a hydraulic shortcut or wrong estimates of correction factor, α, and/or the hydraulic conductivity as discussed in Section 5.1.4.

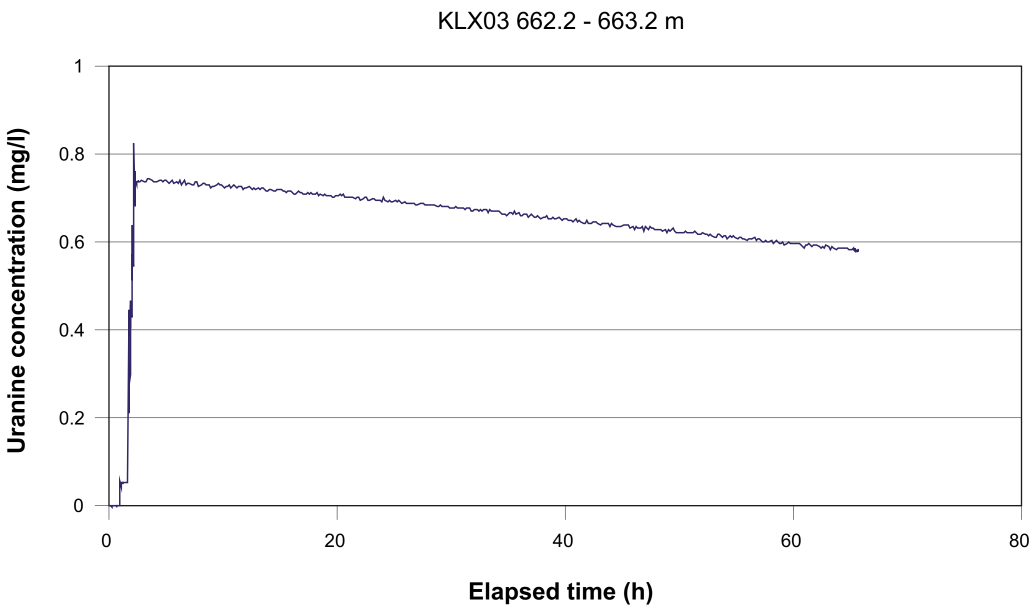

Figure 5-12. Dilution measurement in borehole KLX03, section 662.2–663.2 m.

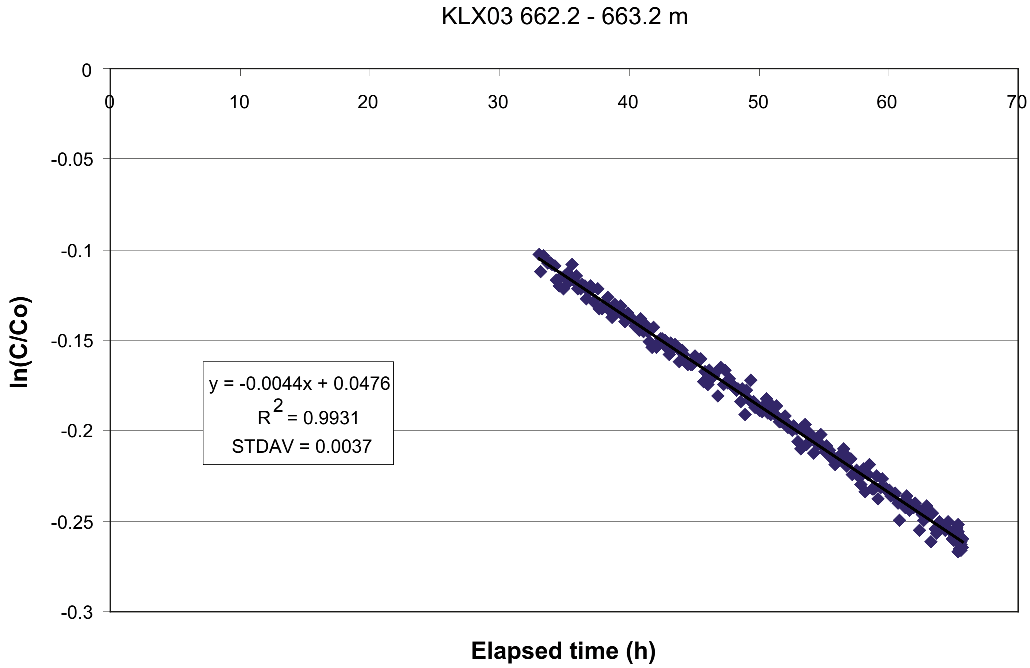

Figure 5-13. *Linear regression best fit to data from dilution measurement in borehole KLX03, section 662.2–663.2 m.*

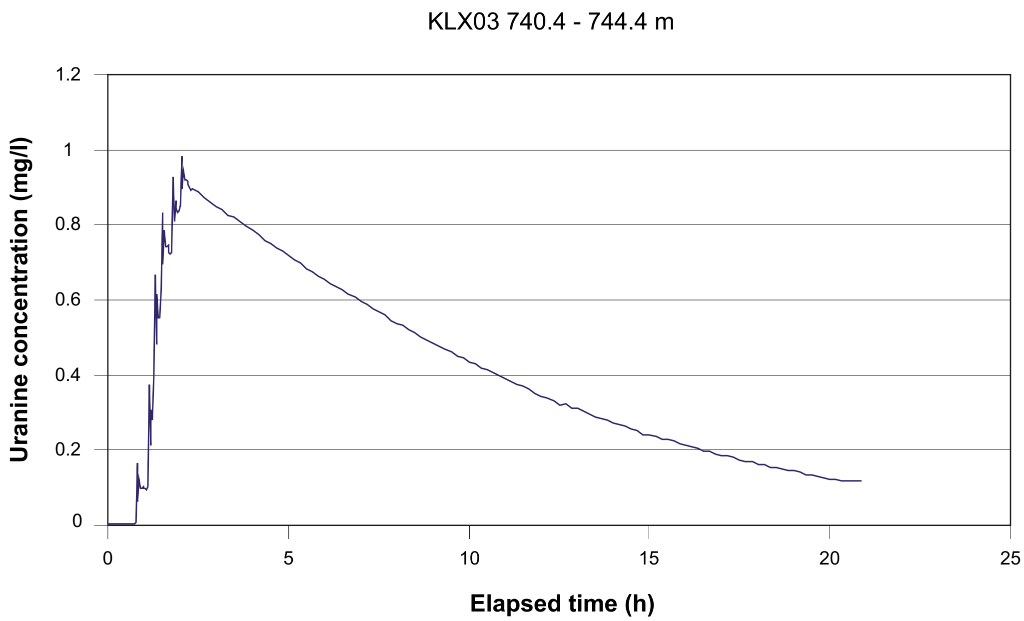

Figure 5-14. *Dilution measurement in borehole KLX03, section 740.4–744.4 m.*

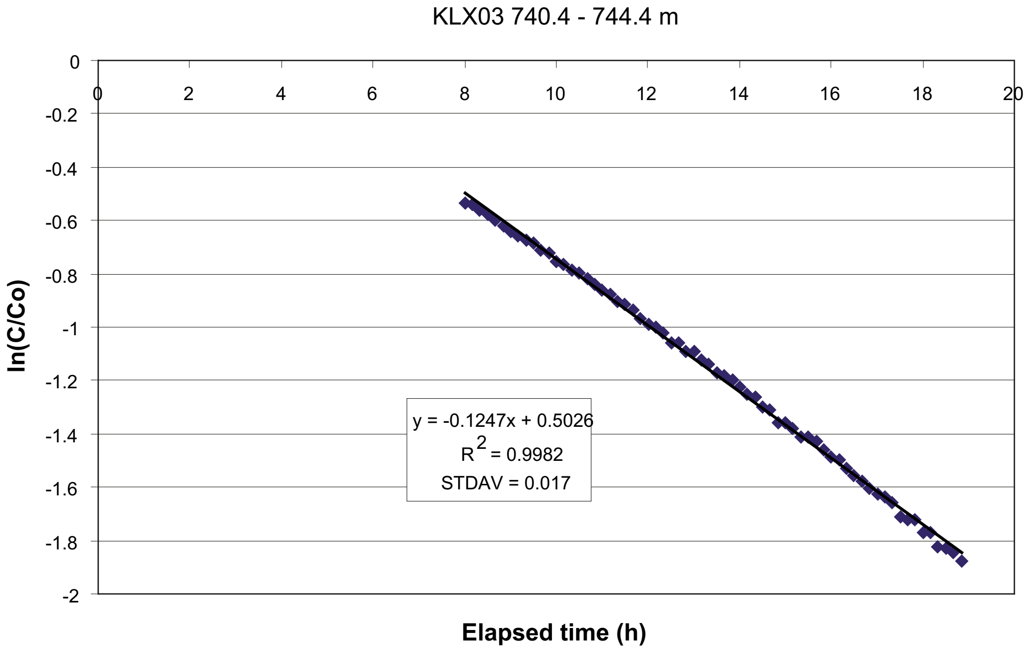

Figure 5-15. *Linear regression best fit to data from dilution measurement in borehole KLX03, section 740.4–744.4 m.*

5.1.7 KLX03, section 769.7–772.7 m

This dilution measurement was carried out in a test section with two-four flowing fractures. The concentration versus time data is presented in Figure 5-16. Background concentration is 0.01 mg/l. The Uranine tracer is injected and after mixing it reaches a start concentration of 1.54 mg/l above background. Dilution is measured for about 91 hours with several interruptions in the data transfer. Thereafter the packers are deflated. Hydraulic pressure shows a slow decreasing trend and small diurnal pressure variations due to earth tidal effects (Appendix B7). The complete set of ln (C/C_0) versus time data, i.e. 10–97 hours of elapsed time, was used for determination of groundwater flow. The regression line shows an acceptable fit to the ln (C/C_0) versus time data with a correlation coefficient of $R^2 = 0.9927$ for the best fit line (Figure 5-17). The groundwater flow rate, calculated from the best fit line, is 0.039 ml/min. Calculated hydraulic gradient is 0.008 and Darcy velocity $1.4 \cdot 10^{-9}$ m/s.

5.1.8 KLX03, section 969.7–970.7 m

This dilution measurement was carried out in a test section with one-two flowing fractures. The concentration versus time data is presented in Figure 5-18. Background concentration is 0.002 mg/l. The Uranine tracer is injected in many small steps and after mixing it reaches a start concentration of 0.87 mg/l above background. Dilution is measured for about 110 hours with several interruptions in the data transfer. Thereafter the packers are deflated. Hydraulic pressure shows no trend (Appendix B8). The complete set of ln (C/C_0) versus time data was used for determination of groundwater flow. The correlation coefficient of the best fit line is $R^2 = 0.9885$ (Figure 5-19). The groundwater flow rate, calculated from the best fit line, is 0.027 ml/min. Calculated hydraulic gradient is 0.007 and Darcy velocity $3.0 \cdot 10^{-9}$ m/s.

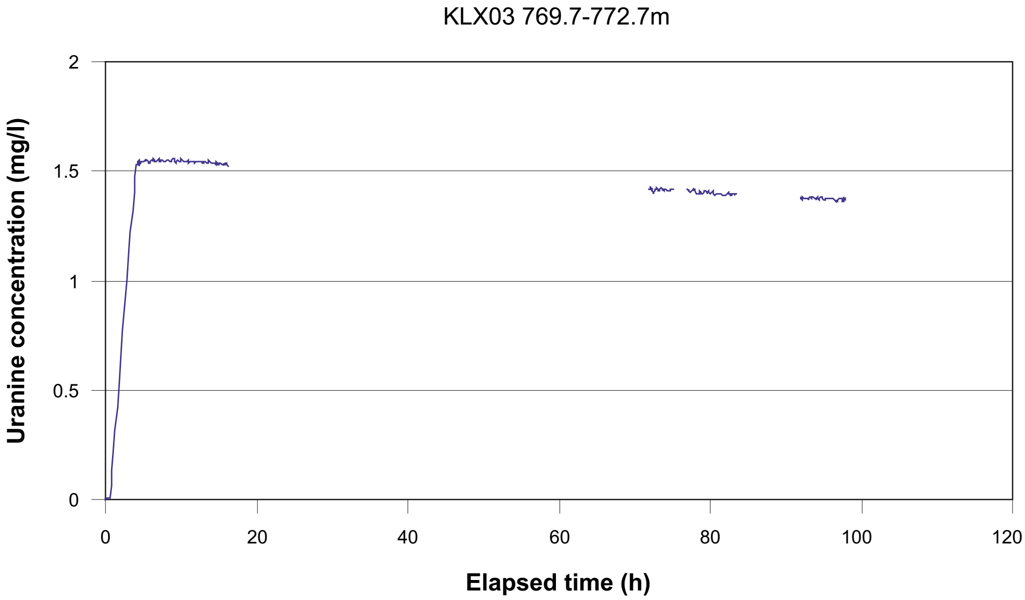

Figure 5-16. *Dilution measurement in borehole KLX03, section 769.7–772.7 m.*

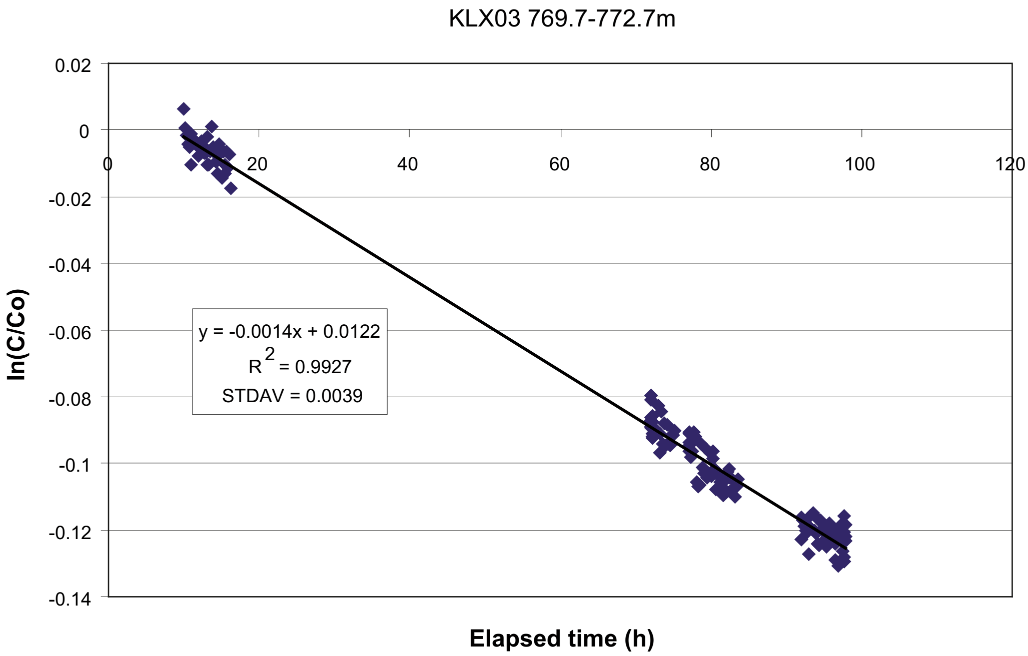

Figure 5-17. *Linear regression best fit to data from dilution measurement in borehole KLX03, section 769.7–772.7 m.*

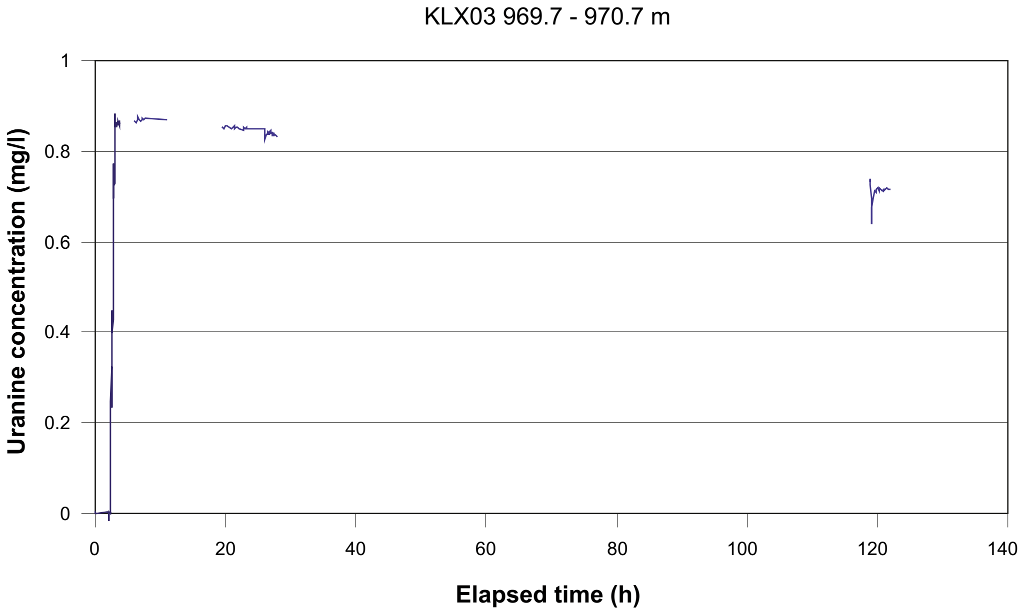

Figure 5-18. *Dilution measurement in borehole KLX03, section 969.7–970.7 m.*

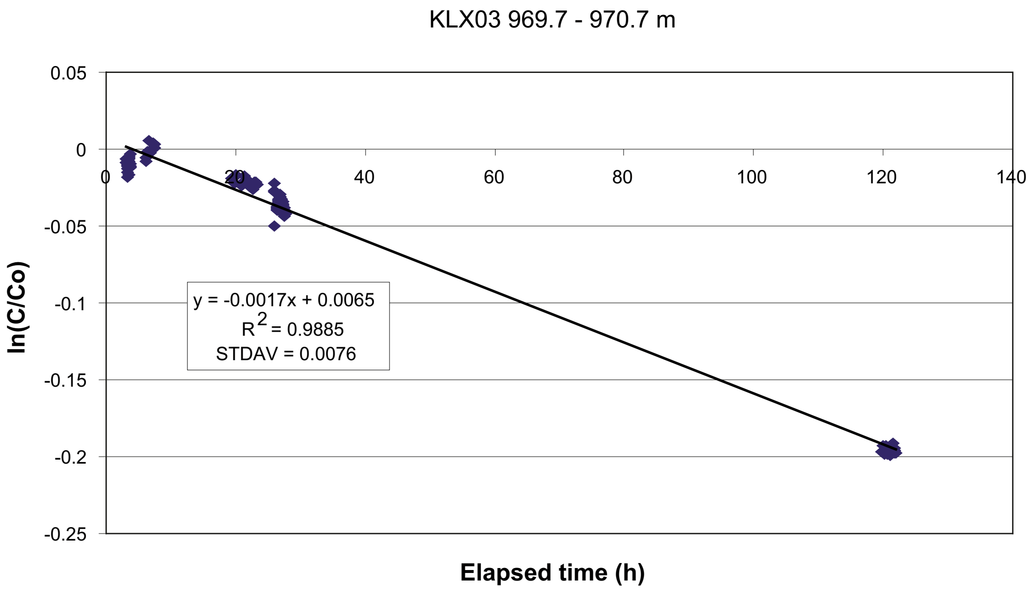

Figure 5-19. *Linear regression best fit to data from dilution measurement in borehole KLX03, section 969.7–970.7 m.*

5.1.9 Summary of dilution results

Calculated groundwater flow rate, Darcy velocity and hydraulic gradient from all dilution measurements carried out in borehole KLX03 are presented in Table 5-1.

The results show that the groundwater flow varies considerably in fractures and fracture zones during natural, i.e. undisturbed conditions, with flow rates from 0.02 to 4.2 ml/min and Darcy velocities from $1.4 \cdot 10^{-9}$ to $1.2 \cdot 10^{-7}$ m/s. The highest flow rates are measured at shallow depth and the flow rates decreases with depth. Exceptions are the single fracture at c 123 m borehole length with low flow rate, and the four metre section straddling a fracture zone at c 740 m borehole length with a number of fractures and high flow rate, Figure 5-20. The Darcy velocity follows the same trend versus depth as the groundwater flow rate, Figure 5-21.

A large portion of the measured fractures/fracture zones are within a small range of transmissivity, however correlation between flow rate and transmissivity is indicated in Figure 5-22, with the highest flow rates at high transmissivity. Exceptions are the section with a single flowing fracture at c 409 m borehole length and at c 740 m borehole length in the four metre section straddling a hydraulically conductive part of a deformation zone, denoted DZ1 in the geological single-hole interpretation of KLX03 /Carlsten et al. 2005/. Hydraulic gradients, calculated according to the Darcy concept, are large in the single fracture section at c 409 m and in the four metre section at c 740 m borehole length. In the other measured fractures/fracture zones the hydraulic gradient is within the expected range. It is not clear if the large gradients are caused by local effects where the measured fracture/fracture zone constitutes a hydraulic conductor between other fractures with different hydraulic heads or due to wrong estimates of the correction factor, α, and/or the hydraulic conductivity of the fracture.

Table 5-1. Groundwater flows, Darcy velocities and hydraulic gradients for all measured sections in borehole KLX03.

Borehole	Test section (m)	Number of flowing fractures*	T (m^2/s)*	Q (ml/min)	Q (m^3/s)	Darcy velocity (m/s)	Hydraulic gradient
KLX03	123.7–124.7	1	2.31E–07	0.018	3.0E–10	2.0E–09	0.009
KLX03	195.0–198.0	2–3	1.25E–05	0.53	8.8E–09	1.9E–08	0.005
KLX03	266.2–267.2	1	7.85E–07	0.18	3.0E–09	2.0E–08	0.025
KLX03	409.6–410.6	1	1.62E–07	0.34	5.7E–09	3.7E–08	0.23
KLX03	662.2–663.2	1–2	2.06E–07	0.070	1.2E–09	7.7E–09	0.038
KLX03	740.4–744.4	3–4	4.48E–06	4.2	7.0E–08	1.2E–07	0.10
KLX03	769.7–772.7	2–4	5.30E–07	0.039	6.5E–10	1.4E–09	0.008
KLX03	969.7–970.7	1–2	4.52E–07	0.027	4.5E–10	3.0E–09	0.007

* From difference flow logging /Rouhiainen et al. 2005/.

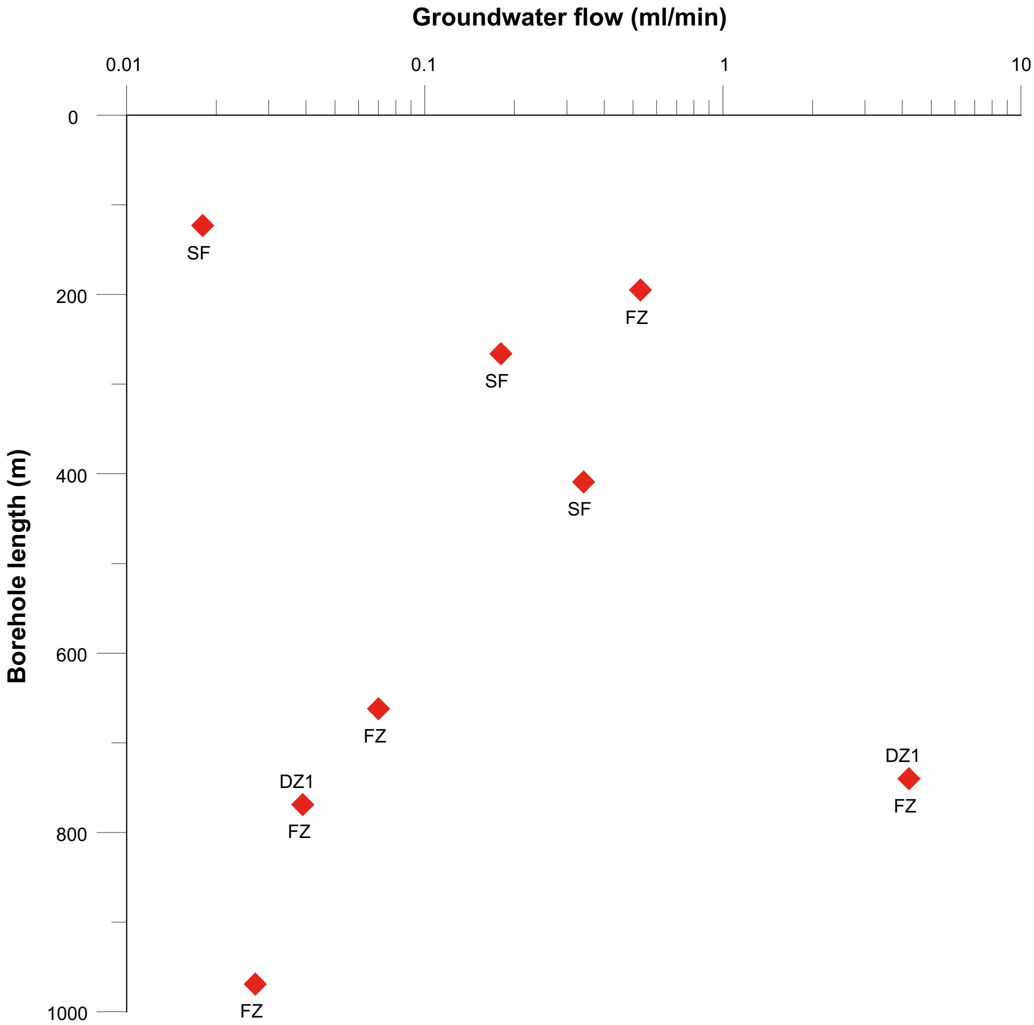

Figure 5-20. *Groundwater flow versus borehole length during undisturbed, i.e. natural hydraulic gradient conditions. Results from dilution measurements in fractures and fracture zones in borehole KLX03. Label DZ1 refer to deformation zone notations in the geological single-hole interpretation of KLX03 /Carlsten et al. 2005/. Labels SF and FZ refer to single fractures and zones with two or more flowing fractures, respectively. SF and FZ are not denoted in /Carlsten et al. 2005/.*

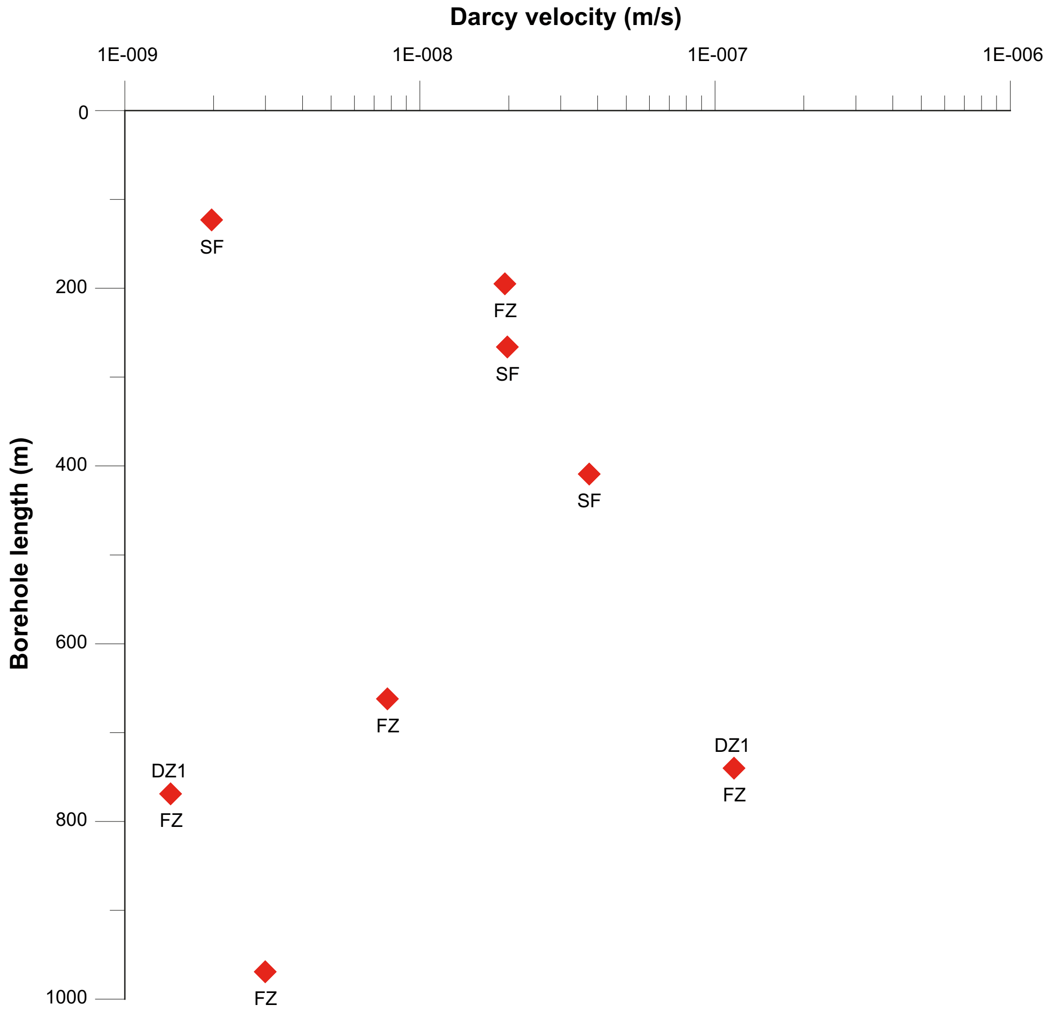

Figure 5-21. *Darcy velocity versus borehole length during undisturbed, i.e. natural hydraulic gradient conditions. Results from dilution measurements in fractures and fracture zones in borehole KLX03. Label DZ1 refer to deformation zone notations in the geological single-hole interpretation of KLX03 /Carlsten et al. 2005/. Labels SF and FZ refer to single fractures and zones with two or more flowing fractures, respectively. SF and FZ are not denoted in /Carlsten et al. 2005/.*

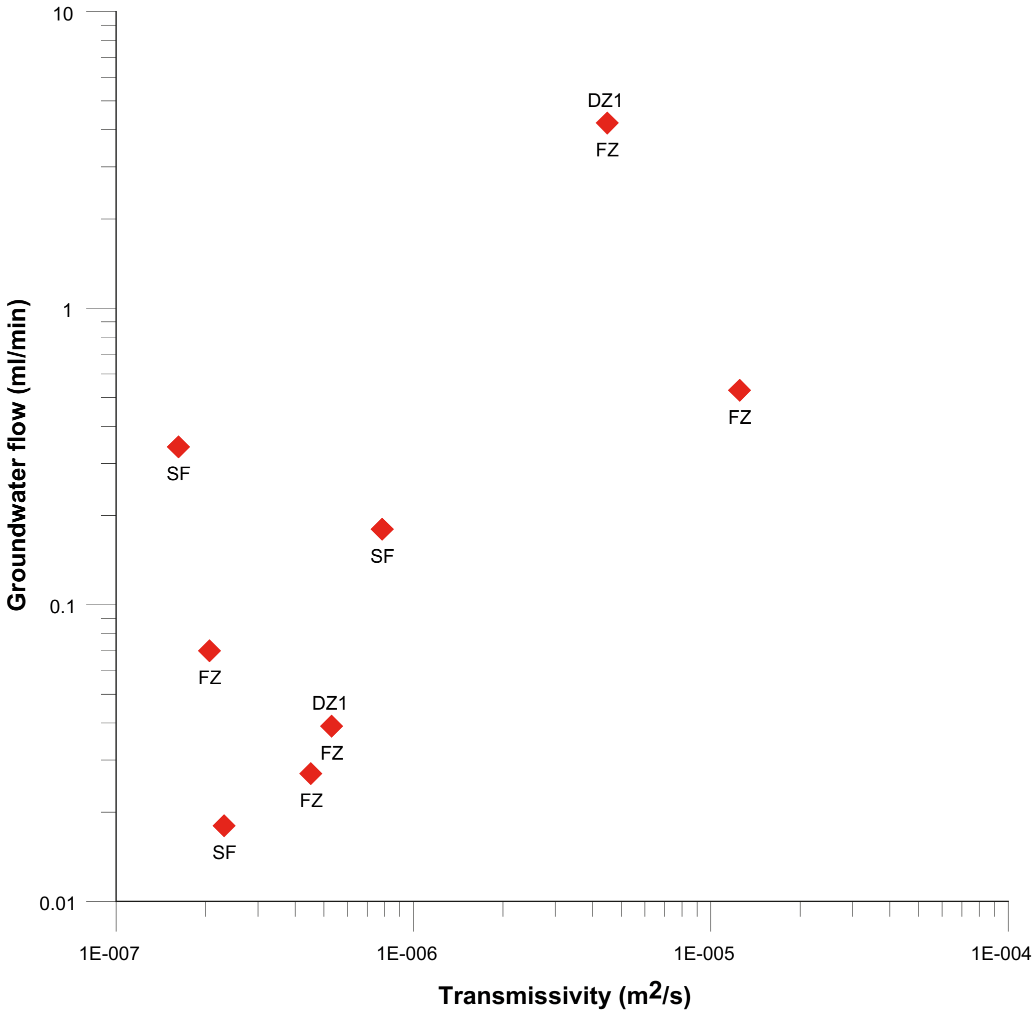

Figure 5-22. *Groundwater flow versus transmissivity during undisturbed, i.e. natural hydraulic gradient conditions. Results from dilution measurements in fractures and fracture zones in borehole KLX03. Label DZ1 refer to deformation zone notations in the geological single-hole interpretation of KLX03 /Carlsten et al. 2005/. Labels SF and FZ refer to single fractures and zones with two or more flowing fractures, respectively. SF and FZ are not denoted in /Carlsten et al. 2005/.*

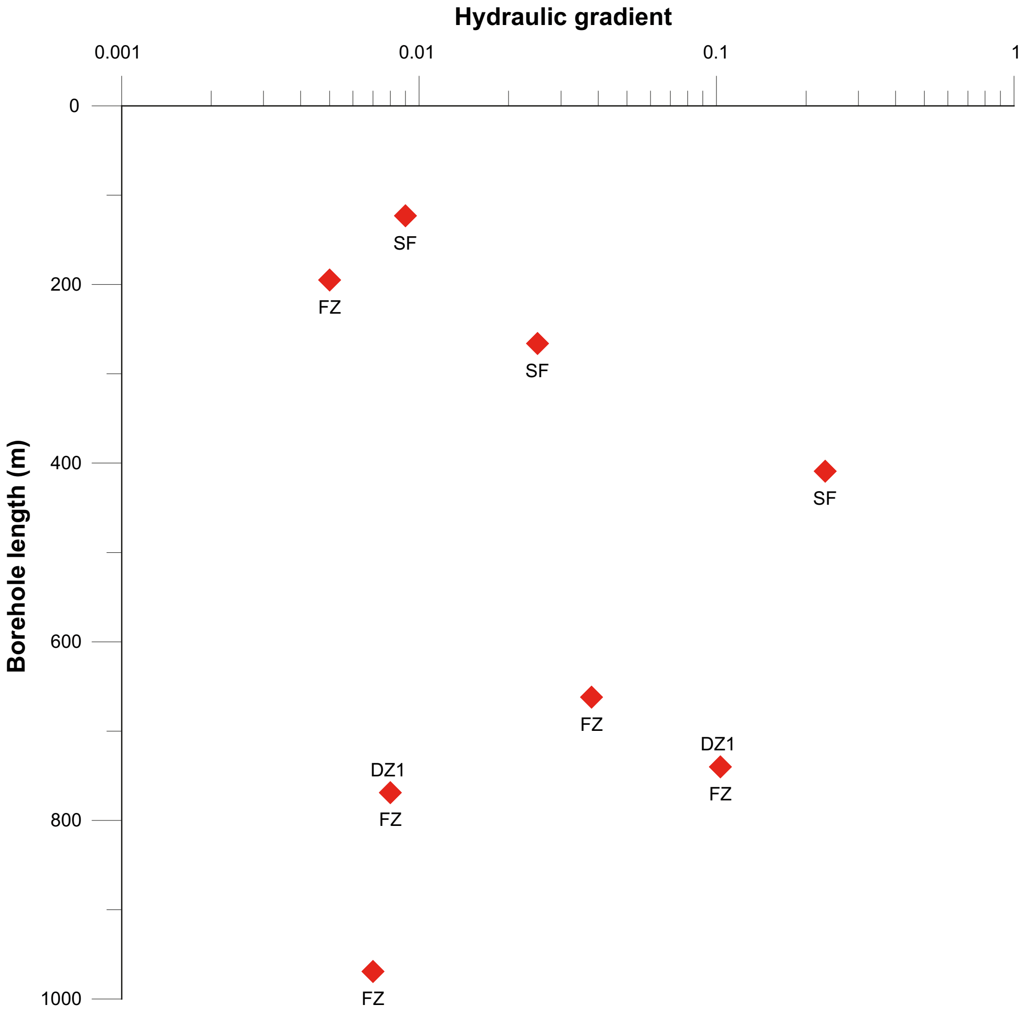

Figure 5-23. *Hydraulic gradient versus borehole length during undisturbed, i.e. natural hydraulic gradient conditions. Results from dilution measurements in fractures and fracture zones in borehole KLX03. Label DZ1 refer to deformation zone notations in the geological single-hole interpretation of KLX03 /Carlsten et al. 2005/. Labels SF and FZ refer to single fractures and zones with two or more flowing fractures, respectively. SF and FZ are not denoted in /Carlsten et al. 2005/.*

5.2 SWIW test

5.2.1 Treatment of experimental data

The experimental data presented in this section have been corrected for background concentrations. Sampling times have been adjusted to account for residence times in injection and sampling tubing. Thus, time zero in all plots refers to when the fluid containing the tracer mixture start to enter the tested borehole section.

5.2.2 Tracer recovery breakthrough in KLX03, 740.4–744.4 m

Durations and flows for the various experimental phases are summarised in Table 5-2. An electric circuit was replaced during the chaser injection. This caused an interruption for about 40 minutes in the chaser injection.

The experimental breakthrough curves from the recovery phase for Uranine, cesium and rubidium, respectively, are shown in Figures 5-24a, 5-24b and 5-24c. The time coordinates are corrected for residence time in the tubing, as described above, and concentrations are normalised through division by the total injected tracer mass.

Normalised breakthrough curves (concentration divided by total injected tracer mass) for the three different tracers are plotted in Figure 5-25. The figure shows that the tracers behave in different ways, presumably caused by different sorption properties. The breakthrough curves appear to approximately conform to what would be expected from a SWIW test using tracers of different sorption properties. The considerable difference between Uranine and the two other curves may also be seen as an indication of a relatively strong sorption effect. The figure indicates similar tracer behaviour as in KFM02A /Gustafsson et al. 2005/ and KSH02 /Gustafsson and Nordqvist 2005/.

The tracer recovery from the recovery phase pumping is rather difficult to estimate from the experimental breakthrough curves, because the tailing parts appear to continue well beyond the last sampling time. Preliminary estimation of recovery from the experimental breakthrough curves at the last sampling time yields values of 89.9%, 51.8% and 43.6% for Uranine, cesium and rubidium, respectively. These estimates are based on the average flow rate during the recovery phase.

Final tracer recovery values, i.e. that would have resulted if pumping had been allowed to continue until tracer background values, are difficult to estimate from the experimental curves. However, plausible visual extrapolations of the curves do not clearly indicate incomplete recovery and that the tracer recovery would be different among the three tracers. Thus, for the subsequent model evaluation, it is assumed that tracer recovery is the same for all of the tracers.

Table 5-2. Durations (hours) and fluid flows (l/h) during various experimental phases for section 740.4–744.4 m. All times have been corrected for tubing residence time such that time zero refers to the time when the tracer mixture starts to enter the tested borehole section.

Phase	Start (h)	Stop (h)	Volume (l)	Average flow (l/h)	Cumulative injected volume (l)
Pre-injection	–2.03	0.00	28.05	13.82	28.05
Tracer injection	0.00	0.85	10.95	12.88	39.00
Chaser injection	0.85	24.25	301.40	12.88	340.40
Interuption period	15.38	16.05	0.00	0.00	
Recovery	24.25	289.71	3,700.70	13.94	

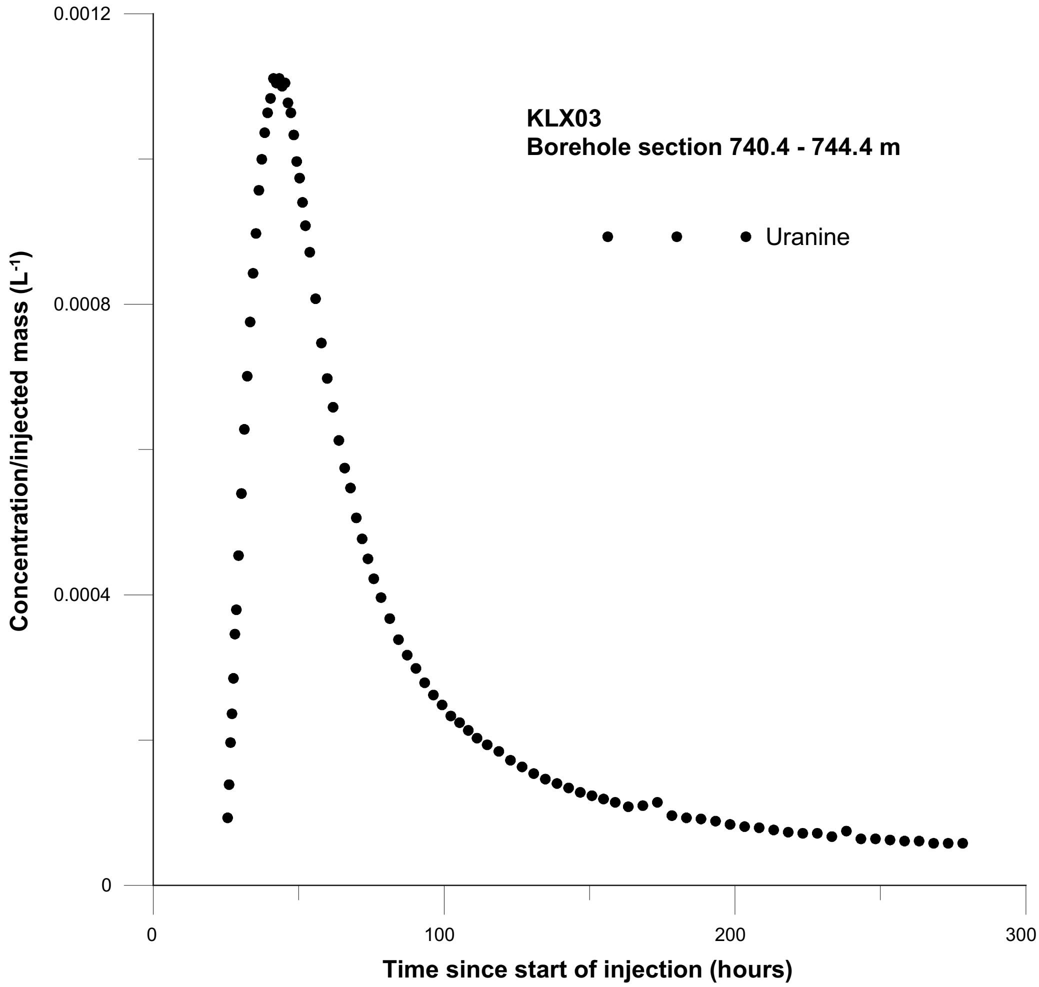

Figure 5-24a. *Withdrawal (recovery) phase breakthrough curve for Uranine in section 740.4–744.4 m in borehole KLX03.*

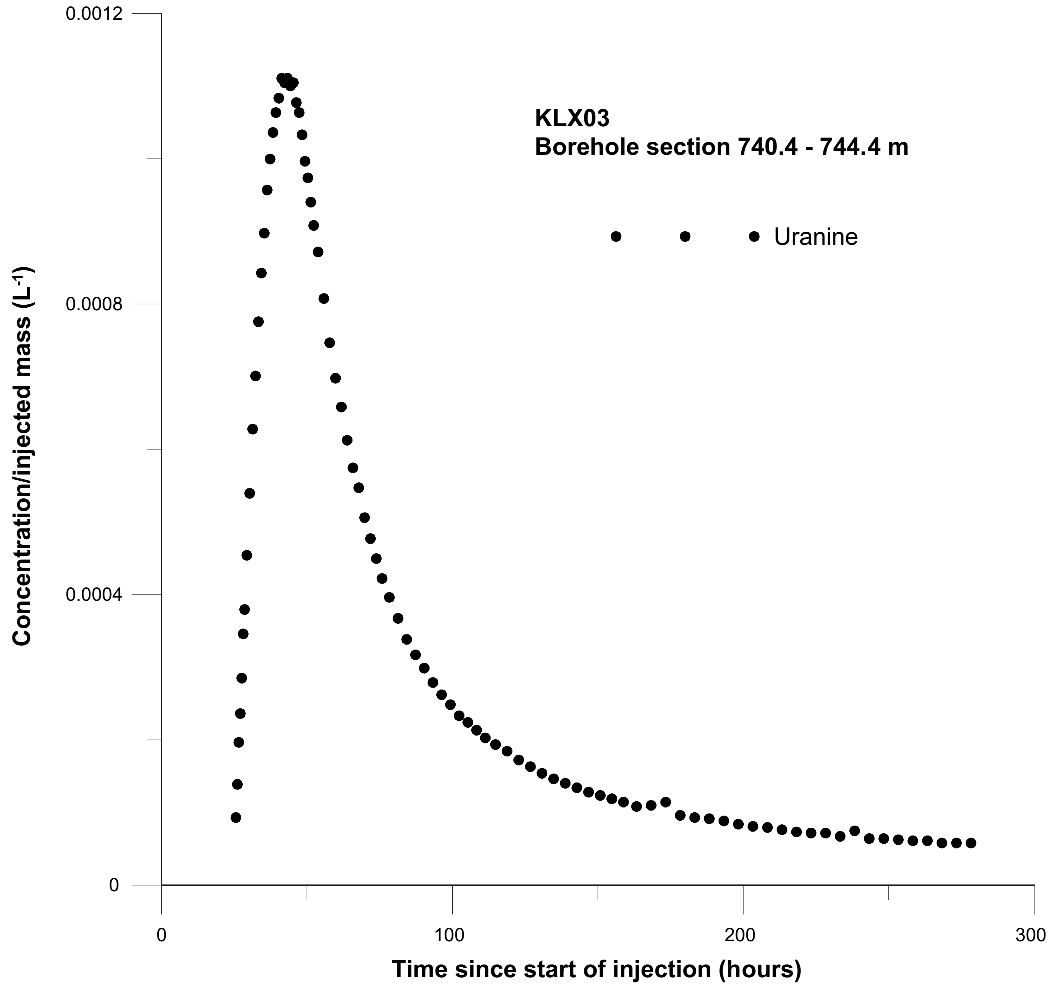

Figure 5-24b. *Recovery phase breakthrough curve for Uranine in section 740.4–744.4 m in borehole KLX03.*

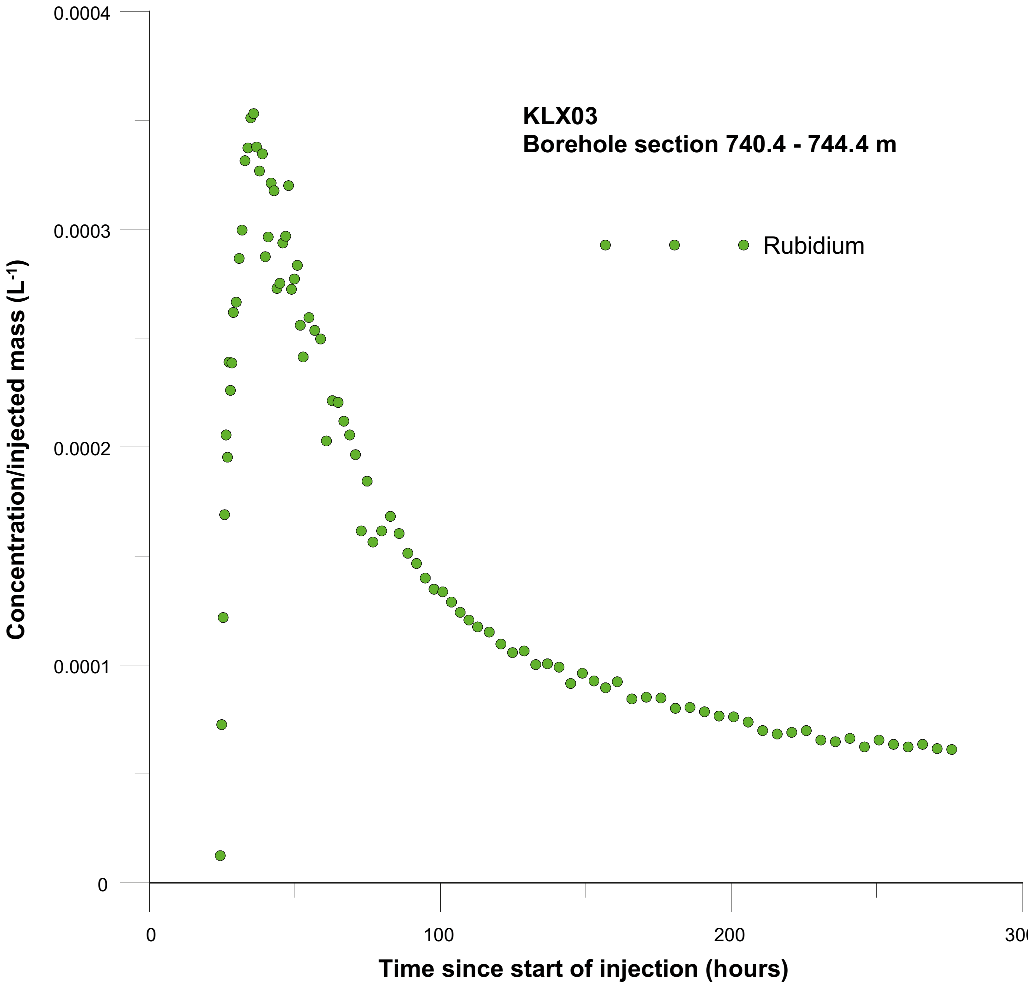

Figure 5-24c. *Recovery phase breakthrough curve for rubidium in section 740.4–744.4 m in borehole KLX03.*

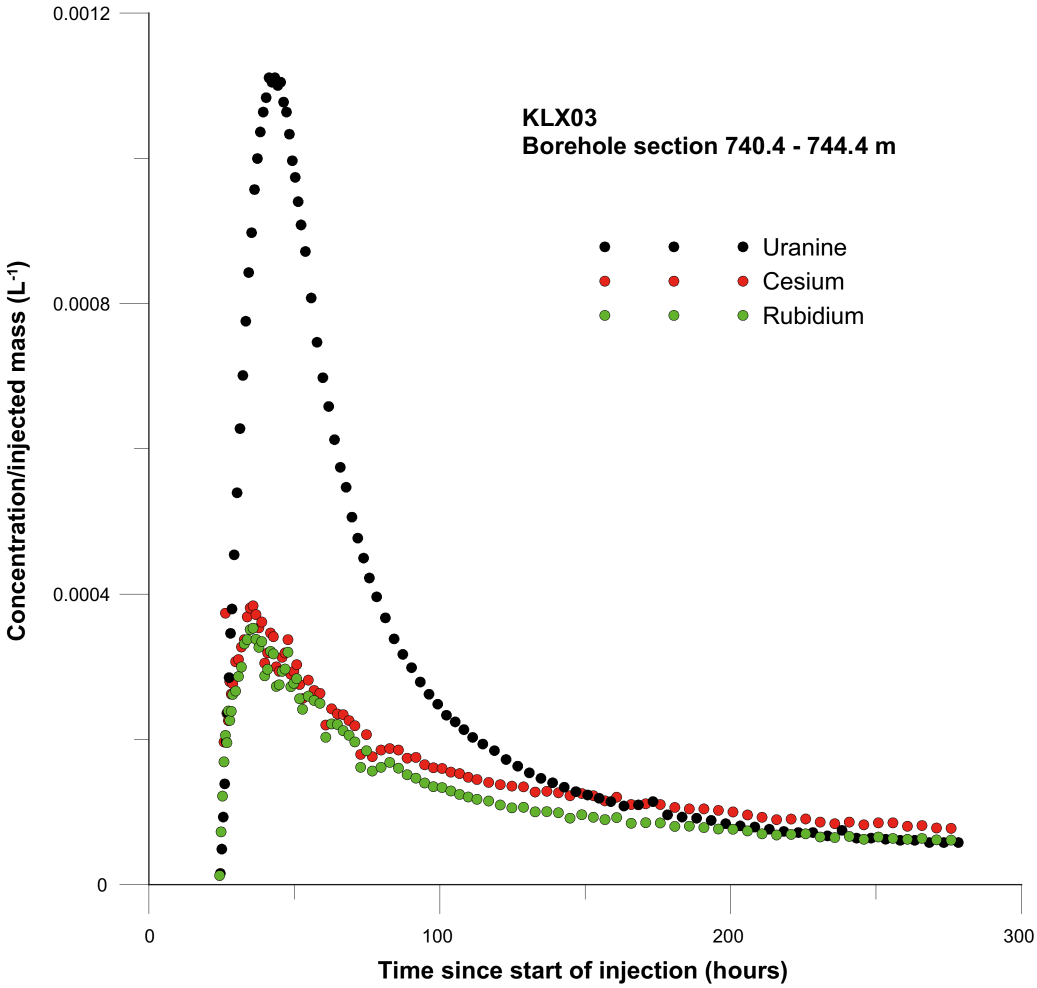

Figure 5-25. *Normalised withdrawal (recovery) phase breakthrough curves for Uranine, cesium and rubidium in section 740.4–744.4 m in borehole KLX03.*

5.2.3 Model evaluation KLX03, 740.4–744.4 m

The model simulations were carried out assuming negligible hydraulic background gradient, i.e. radial flow. The simulated times and flows for the various experimental phases are given in Table 5-2. In the simulation model, the flow zone is approximated by a 0.1 m thick fracture zone.

The experimental evaluation was carried out by simultaneous model fitting of Uranine and a sorbing tracer as outlined in Section 4.4. Thus, separate regression analyses were carried for simultaneous fitting of Uranine/cesium and Uranine/rubidium, respectively.

For a given regression run, estimation parameters were longitudinal dispersivity (a_L) and a linear retardation factor (R), while the porosity is given a fixed value. Regression was carried out for four different values of porosity: 0.005, 0.01, 0.02 and 0.05. For all cases, the fits between model and experimental data are similar. Example of model fits are shown in Figure 5-26a and Figure 5-26b.

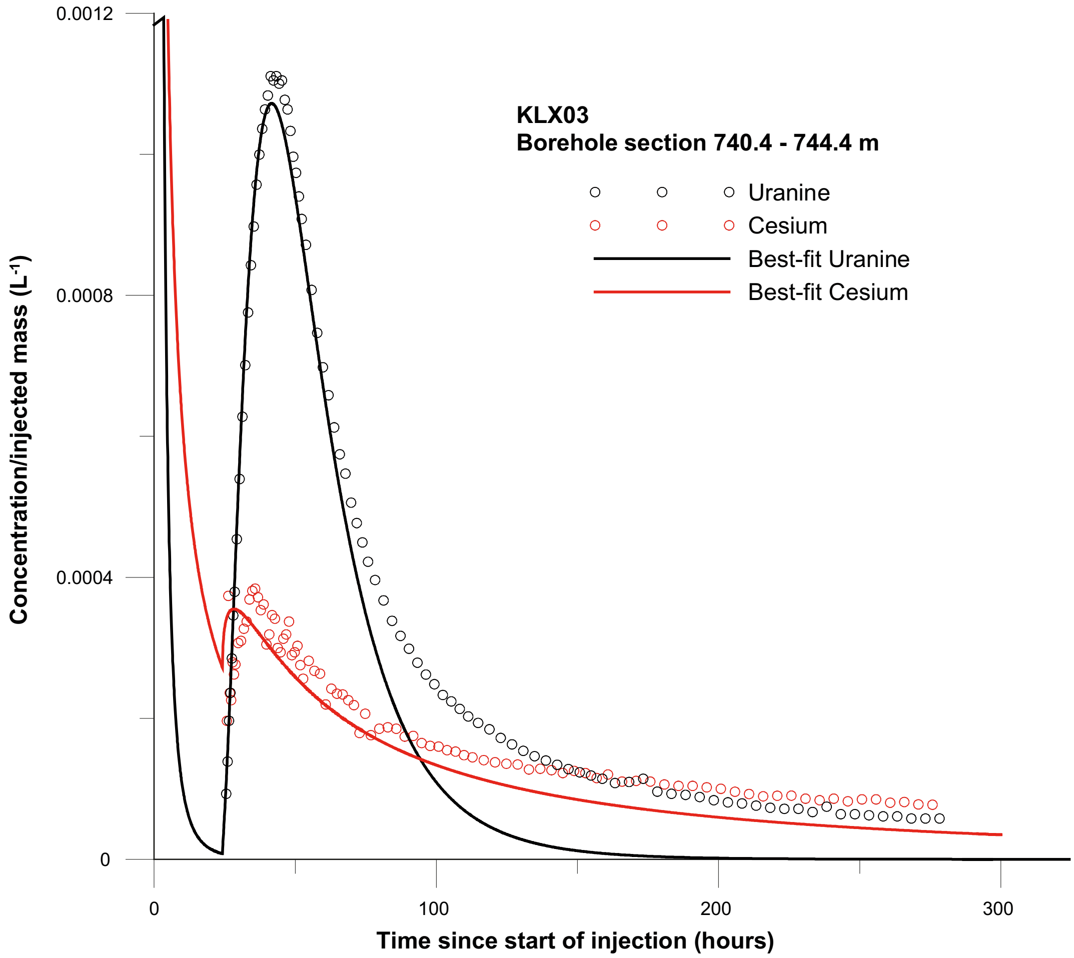

Figure 5-26a. *Example of simultaneous fitting of Uranine and cesium for section 740.4–744.4 m in borehole KLX03.*

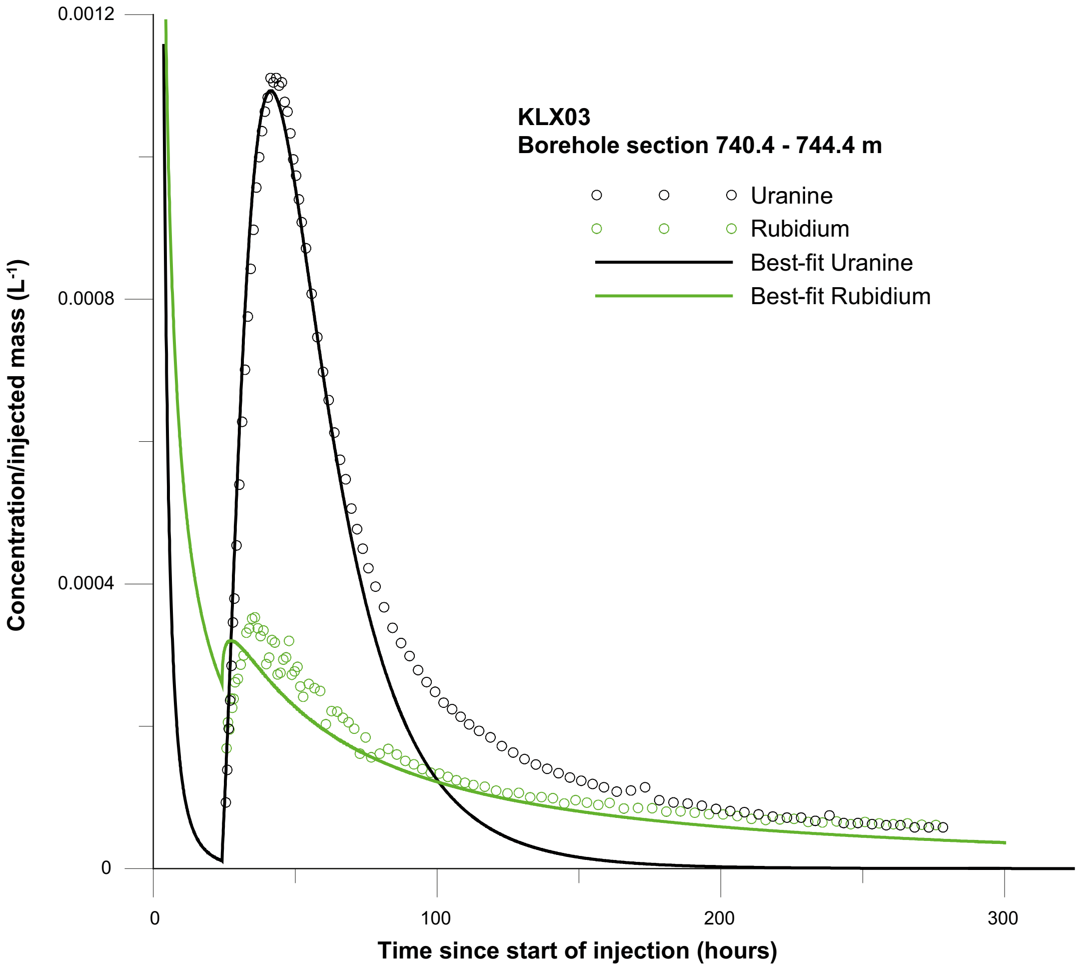

Figure 5-26b. *Example of simultaneous fitting of Uranine and rubidium for section 740.4–744.4 m in borehole KLX03.*

The model fits to the experimental breakthrough curves are generally fairly good, although some discrepancies can be noted. The main discrepancy is observed for the tailing part of the Uranine curve, where the simulated curve levels out to background values faster than the experimental curve. Further, the simulated peaks for cesium and rubidium, respectively, occur somewhat earlier than the observed peaks.

All of the regression runs (Tables 5-3a and 5-3b) resulted in similar values of the retardation coefficient for each sorbing tracer, while the estimated values of the longitudinal dispersivity are strongly dependent on the assumed porosity value. Both of these observations are consistent with prior expectations of the relationships between parameters in a SWIW test /Nordqvist and Gustafsson 2002, 2004/ and /Gustafsson and Nordqvist 2005/.

The estimated values of R for cesium and rubidium indicate strong sorption effects. The value of R for cesium agrees approximately with values from cross-hole tests, obtained using similar transport models (advection-dispersion and linear sorption). For example, /Winberg et al. 2000/ reported a value of R = 69, while a value of R = 140 was reported by /Andersson et al. 1999/. Estimated values of R for rubidium are larger than expected; literature data form the TRUE Block Scale Project /Anderson et al. 2002/ indicate about one magnitude lower values of R for rubidium than for cesium.

Table 5-3a. Results of simultaneous fitting of Uranine and cesium for section 740.4–744.4 m in borehole KLX03. Approximate values of the coefficient of variation (estimation standard error divided by the estimated value) are given within parenthesis.

Porosity (fixed)	a_L (estimated)	R (estimated)
0.005	1.60 (0.1)	240 (0.4)
0.01	1.14 (0.1)	235 (0.4)
0.02	0.81 (0.1)	234 (0.4)
0.05	0.51 (0.1)	232 (0.4)

Table 5-3b. Results of simultaneous fitting of Uranine and rubidium for section 740.4–744.4 m in borehole KLX03. Approximate values of the coefficient of variation (estimation standard error divided by the estimated value) are given within parenthesis.

Porosity (fixed)	a_L (estimated)	R (estimated)
0.005	1.75 (0.1)	392 (0.4)
0.01	1.24 (0.1)	392 (0.4)
0.02	0.87 (0.1)	391 (0.4)
0.05	0.56 (0.1)	389 (0.4)

6 Discussion and conclusions

The dilution measurements were carried out in borehole KLX03 in selected fractures and fracture zones at levels from 123 to 969 m borehole length (elevation –120 to –920 m), where hydraulic transmissivity ranged within T = $1.6 \cdot 10^{-7}$–$1.3 \cdot 10^{-5}$ m^2/s.

The results of the dilution measurements in borehole KLX03 show that the groundwater flow varies considerably in fractures and fracture zones during natural undisturbed conditions, with flow rates from 0.02 to 4.2 ml/min and Darcy velocities from $1.4 \cdot 10^{-9}$ to $1.2 \cdot 10^{-7}$ m/s ($1.2 \cdot 10^{-4}$–$1.0 \cdot 10^{-2}$ m/d). These results are in accordance with dilution measurements carried out in boreholes KSH02 and KLX02 in the Simpevarp and Laxemar areas /Gustafsson and Nordqvist 2005/. In KSH02 and KLX02 hydraulic transmissivity was within T = $1.3 \cdot 10^{-8}$–$7.4 \cdot 10^{-6}$ m^2/s and flow rate ranged from 0.09 to 2.8 ml/min and Darcy velocity from $3.4 \cdot 10^{-9}$ to $1.0 \cdot 10^{-7}$ m/s ($2.9 \cdot 10^{-4}$–$8.6 \cdot 10^{-3}$ m/d). Groundwater flow rates and Darcy velocities calculated from dilution measurements in borehole KLX03 are also within the range that can be expected out of experience from previously preformed dilution measurements under natural gradient conditions at other sites in Swedish crystalline rock /Gustafsson and Andersson 1991, Gustafsson and Morosini 2002/ and /Gustafsson et al. 2005/.

Groundwater flow rate in KLX03 is proportional to hydraulic transmissivity although it should be considered that in fractured rock, during natural hydraulic conditions, the groundwater flow in fractures and fracture zones to a large extent is governed by the direction of the large-scale hydraulic gradient relative to the strike and dip of the conductive fracture zones.

Flow rates and Darcy velocities generally decreases with depth (Table 6-1). However, there are two exceptions from this trend. The single fracture at c 123 m borehole length, with low flow rate, and the four metre section at c 740 m borehole length, which penetrates a conductive part of deformation zone DZ1 having 3–4 flowing fractures and a high flow rate. In fact the highest single flow rate, 4.2 ml/min, and Darcy velocity, $1.2 \cdot 10^{-7}$ m/s, measured in KLX03.

Table 6-1. Intersected zones, rock types, groundwater flows, Darcy velocities and hydraulic gradients for all measured sections in borehole KLX03.

Borehole	Test section (m)	Number of flowing fractures*	Rock types and zones **	T (m^2/s)*	Q (ml/min)	Q (m^3/s)	Darcy velocity (m/s)	Hydraulic gradient
KLX03	123.7–124.3	1	Ävrö granite	2.31E–07	0.018	3.0E–10	2.0E–09	0.009
KLX03	195.0–198.0	2–3	Ävrö granite	1.25E–05	0.53	8.8E–09	1.9E–08	0.005
KLX03	266.2–267.2	1	Ävrö granite	7.85E–07	0.18	3.0E–09	2.0E–08	0.025
KLX03	409.6–410.6	1	Ävrö granite	1.62E–07	0.34	5.7E–09	3.7E–08	0.23
KLX03	662.2–663.2	1–2	Quartz monzo-diorite	2.06E–07	0.070	1.2E–09	7.7E–09	0.038
KLX03	740.4–744.4	3–4	DZ1 fine-grained diorite-gabbro	4.48E–06	4.2	7.0E–08	1.2E–07	0.10
KLX03	769.7–772.7	2–4	DZ1 Quartz monzo-diorite	5.30E–07	0.039	6.5E–10	1.4E–09	0.008
KLX03	969.7–970.7	1–2	Quartz monzo-diorite	4.52E–07	0.027	4.4E–10	3.0E–09	0.007

* From difference flow logging /Rouhiainen et al. 2005/.

** SDM L1.2 /SKB 2006/.

This is also the only section were the rock type is fine-grained diorite-gabbro, the other sections above 600 m are located in Ävrö granite and below 600 m in quartz monzodiorite, cf Table 6-1 and Figure 6-1 /SKB 2006/. Two hydraulically conductive parts of deformation zone DZ1 is breached by KLX03 at c 740 m and c 769 m borehole length respectively /SKB 2006/, Figure 6-1. Hydraulic transmissivity, and also groundwater flow and Darcy velocity is lowest in the deepest section at c 769 m.

Hydraulic gradients are calculated according to the Darcy concept and are within the expected range (0.001–0.05) in the majority of the measured sections. In the single fracture at c 409 m and in the fracture zone in DZ1 at c 740 m borehole length the hydraulic gradient is considered very large. Local effects where the measured fracture constitutes a hydraulic conductor between other fractures with different hydraulic heads or wrong estimates of the correction factor, α, and/or the hydraulic conductivity of the fracture could explain the large hydraulic gradients. In the case of several flowing fractures in the test section also the borehole may act as a hydraulic short circuit between fractures of different hydraulic head and thus enhance flow rate and calculated hydraulic gradient.

The SWIW experiment performed in a conductive part of deformation zone DZ1 at 740.4–744.4 m borehole length resulted in high-quality tracer breakthrough data. Experimental conditions (flows, times, events, etc) are well known and documented, as well as borehole geological conditions with BIPS logging (Appendix C). Together they provide a good basis for possible further evaluation.

The results show relatively smooth breakthrough curves without apparent irregularities or excessive experimental noise in the tested sections. The most significant result is that there is a very clear effect of retardation/sorption of cesium as well as for rubidium.

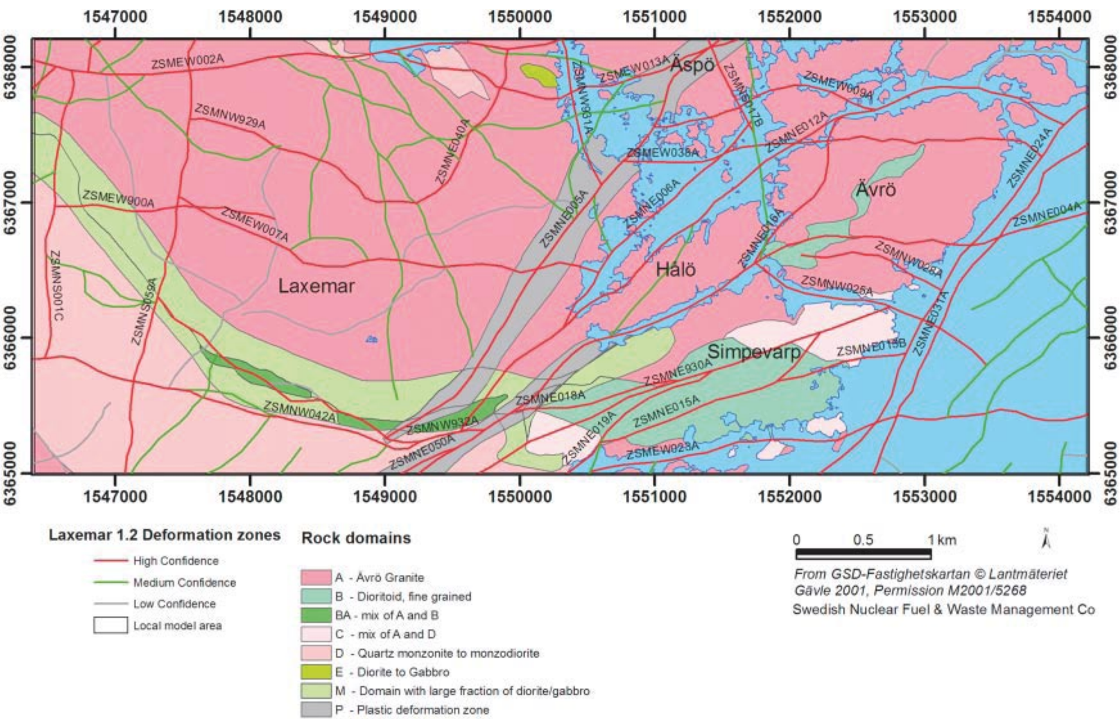

Figure 6-1. *Illustration of rock domains and the base case deformation zone model with high (red), medium, (green) and low (grey) confidence zones within the local model area. (From /SKB 2006/, Figure 3-3). KLX03 is located at coordinates 6366112 north and 1547718 east.*

The model evaluation was made using a radial flow model with advection, dispersion and linear equilibrium sorption as transport processes. It is important that experimental conditions (times, flows, injection concentration, etc) are incorporated accurately in the simulations. Otherwise artefacts of erroneous input may occur in the simulated results. The evaluation carried out may be regarded as a typical preliminary approach for evaluation of a SWIW test where sorbing tracers are used. Background flows were in this case assumed to be insignificant.

The estimated values of the retardation factor for cesium (about 235) and rubidium (about 390) in section 740.4–744.4 m indicates strong sorption. A somewhat un-expected result is that rubidium shows stronger sorption than cesium /Andersson et al. 2002/. Rubidium was introduced as an intermediately sorbing tracer between Uranine and cesium.

It should also be pointed out that the lack of model fit in the tailing parts of the curves (most visible for Uranine) appears to be a consistent feature in the SWIW tests performed so far /Gustafsson and Nordqvist 2005/ and /Gustafsson et al. 2005/. Thus, there seems be some generally occurring process that has not yet been identified, but is currently believed to be an effect of the tested medium and not an experimental artefact. Studies to identify possible causes for the observed discrepancy are ongoing.

7 References

Andersson P, 1995. Compilation of tracer tests in fractured rock. SKB PR 25-95-05, Svensk Kärnbränslehantering AB.

Andersson P, Wass E, Byegård J, Johansson H, Skarnemark G, 1999. Äspö Hard Rock Laboratory. True 1st stage tracer programme. Tracer test with sorbing tracers. Experimental description and preliminary evaluation. SKB IPR-99-15, Svensk Kärnbränslehantering AB.

Andersson P, Byegård J, Winberg A, 2002. Final report of the TRUE Block Scale project. 2. Tracer tests in the block scale. SKB TR-02-14, Svensk Kärnbränslehantering AB.

Byegård J, Tullborg E-L, 2005. Sorption experiments and leaching studies using fault gouge material and rim zone material from the Äspö Hard Rock Laboratory. SKB Technical Report (in prep.).

Carlsten S, Hultgren P, Mattsson H, Stanfors R, Wahlgren C-H, 2005. Oskarshamn site investigation. Geological single-hole interpretation of KLX03, HLX26 and HLX27. SKB P-05-038, Svensk Kärnbränslehantering AB.

Gustafsson E, Andersson P, 1991. Groundwater flow conditions in a low-angle fracture zone at Finnsjön, Sweden. Journal of Hydrology, Vol 126, pp 79–111. Elsvier, Amsterdam.

Gustafsson E, 2002. Bestämning av grundvattenflödet med utspädningsteknik – Modifiering av utrustning och kompletterande mätningar. SKB R-02-31, Svensk Kärnbränslehantering AB (in Swedish).

Gustafsson E, Morosini M, 2002. In-situ groundwater flow measurements as a tool for hardrock site characterisation within the SKB programme. Norges geologiske undersøkelse. Bulletin 439, 33–44.

Gustafsson E, Nordqvist R, 2005. Oskarshamn site investigation. Ground water flow measurements and SWIW-tests in boreholes KLX02 and KSH02. SKB P-05-28, Svensk Kärnbränslehantering AB.

Gustafsson E, Nordqvist R, Thur P, 2005. Forsmark site investigation. Ground water flow measurements and SWIW tests in boreholes KFM01A, KFM02A, KFM03A and KFM03B. SKB P-05-77, Svensk Kärnbränslehantering AB.

Halevy E, Moser H, Zellhofer O, Zuber A, 1967. Borehole dilution techniques – a critical review. In: Isotopes in Hydrology, Proceedings of a Symposium, Vienna 1967, IAEA, Vienna, pp 530–564.

Nordqvist R, Gustafsson E, 2002. Single-well injection-withdrawal tests (SWIW). Literature review and scoping calculations for homogeneous crystalline bedrock conditions. SKB R-02-34, Svensk Kärnbränslehantering AB.

Nordqvist R, Gustafsson E, 2004. Single-well injection-withdrawal tests (SWIW). Investigation of evaluation aspects under heterogeneous crystalline bedrock conditions. SKB R-04-57, Svensk Kärnbränslehantering AB.

Rhén I, Forsmark T, Gustafson G, 1991. Transformation of dilution rates in borehole sections to groundwater flow in the bedrock. Technical note 30. In: Liedholm M. (ed) 1991. SKB-Äspö Hard Rock Laboratory, Conceptual Modeling of Äspö, technical Notes 13–32. General Geological, Hydrogeological and Hydrochemical information. Äspö Hard Rock Laboratory Progress Report PR 25-90-16b.

Rouhiainen P, Pöllänen J, Sokolnicki M, 2005. Oskarshamn site investigation. Difference flow logging of borehole KLX03. Subarea Laxemar. SKB P-05-67, Svensk Kärnbränslehantering AB.

SKB 2001a. Site investigations. Investigation methods and general execution programme. SKB TR-01-29, Svensk Kärnbränslehantering AB.

SKB, 2001b. Platsundersökningar. Undersökningsmetoder och generellt genomförandeprogram. SKB R-01-10, Svensk Kärnbränslehantering AB (in Swedish).

SKB, 2002. Geovetenskapligt program för platsundersökning vid Simpevarp. SKB R-01-44, Svensk Kärnbränslehantering AB (in Swedish).

SKB, 2006. Preliminary safety evaluation for the Laxemar subarea. Based on data and site descriptions after the initial site investigation stage. SKB TR-06-06, Svensk Kärnbränslehantering AB.

Voss C I, 1984. SUTRA – Saturated-Unsaturated Transport. A finite element simulation model for saturated-unsaturated fluid-density-dependent ground-water flow with energy transport or chemically-reactive single-species solute transport. U.S. Geological Survey Water-Resources Investigations Report 84-4369.

Winberg A, Andersson P, Hermansson J, Byegård J, Cvetkovic V, Birgersson L, 2000. Äspö Hard Rock Laboratory. Final report of the first stage of the tracer retention understanding experiment. SKB TR-00-07, Svensk Kärnbränslehantering AB.

Appendix A

Borehole data KLX03

SICADA – Information about KLX03

Title	Value				
	Information about cored borehole KLX03 (2005-11-01).				
Comment:	No comment exists.				
Borhole length (m):	1,000.420				
Reference level:	TOC				
Drilling period(s):	**From date**	**To date**	**Secup (m)**	**Seclow (m)**	**Drilling type**
	2004-05-03	2004-05-03	0.000	100.350	Percussion drilling
	2004-05-28	2004-09-07	100.350	1,000.420	Core drilling
Starting point coordinate:	**Length (m)**	**Northing (m)**	**Easting (m)**	**Elevation**	**Coord system**
	0.000	6366112.593	1547718.925	18.486	RT90-RHB70
Angles:	**Length (m)**	**Bearing**	**Inclination (– =down)**		**Coord system**
	0.000	199.043	–74.931		RT90-RHB70
Borehole diameter:	**Secup (m)**	**Seclow (m)**	**Hole diam (m)**		
	0.100	11.950	0.347		
	11.950	100.350	0.253		
	100.350	101.400	0.086		
	101.400	1,000.420	0.076		
Core diameter:	**Secup (m)**	**Seclow (m)**	**Core diam (m)**		
	100.350	101.400	0.072		
	101.400	500.000	0.050		
	500.000	504.240	0.045		
	504.240	512.700	0.050		
	512.040	514.610	0.045		
	514.610	517.750	0.050		
	517.750	520.650	0.045		
	520.620	528.120	0.050		
	528.120	531.010	0.045		
	531.100	1,000.420	0.050		
Casing diameter:	**Secup (m)**	**Seclow (m)**	**Case in (m)**	**Case out (m)**	
	0.000	100.000	0.200	0.208	
	0.100	11.650	0.311	0.323	
	100.000	100.050	0.170	0.208	
Cone dimensions:	**Secup (m)**	**Seclow (m)**	**Case in (m)**	**Case out (m)**	
	96.750	101.400			

Title	Value	
Grove milling:	**Length(m)**	**Trace detectable**
	110.000	JA
	150.000	JA
	200.000	JA
	250.000	JA
	300.000	JA
	350.000	JA
	399.000	JA
	400.000	JA
	450.000	JA
	500.000	JA
	550.000	JA
	600.000	JA
	650.000	JA
	700.000	JA
	750.000	JA
	800.000	JA
	850.000	JA
	900.000	JA
	950.000	JA

Dilution measurement KLX03 123.7–124.7 m

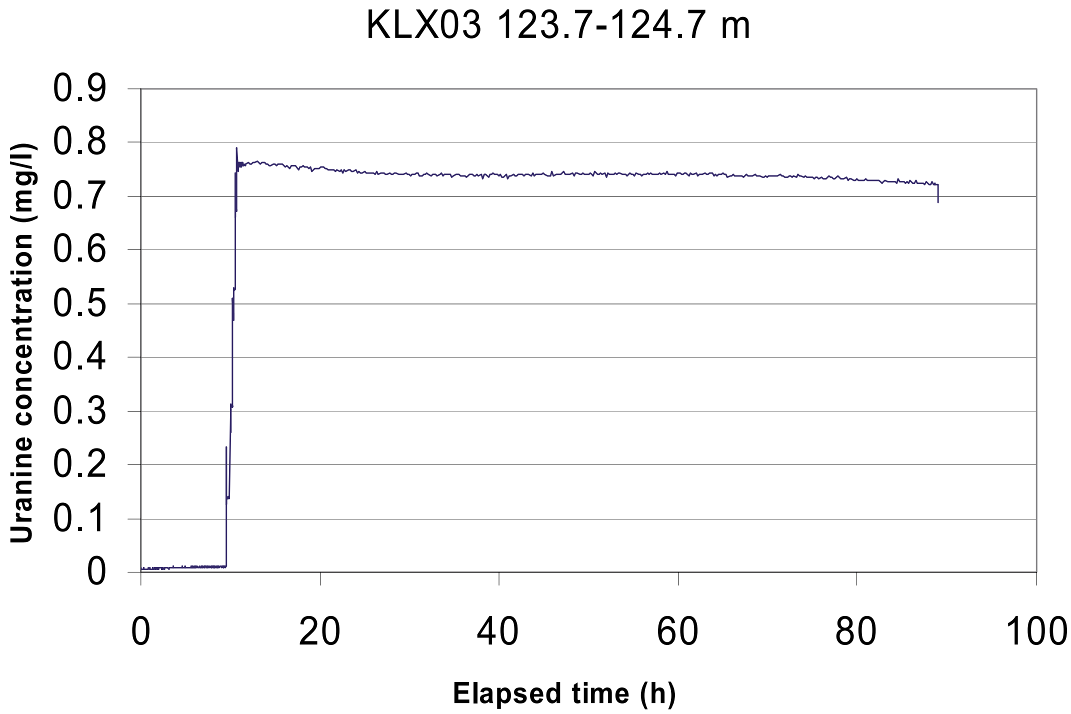

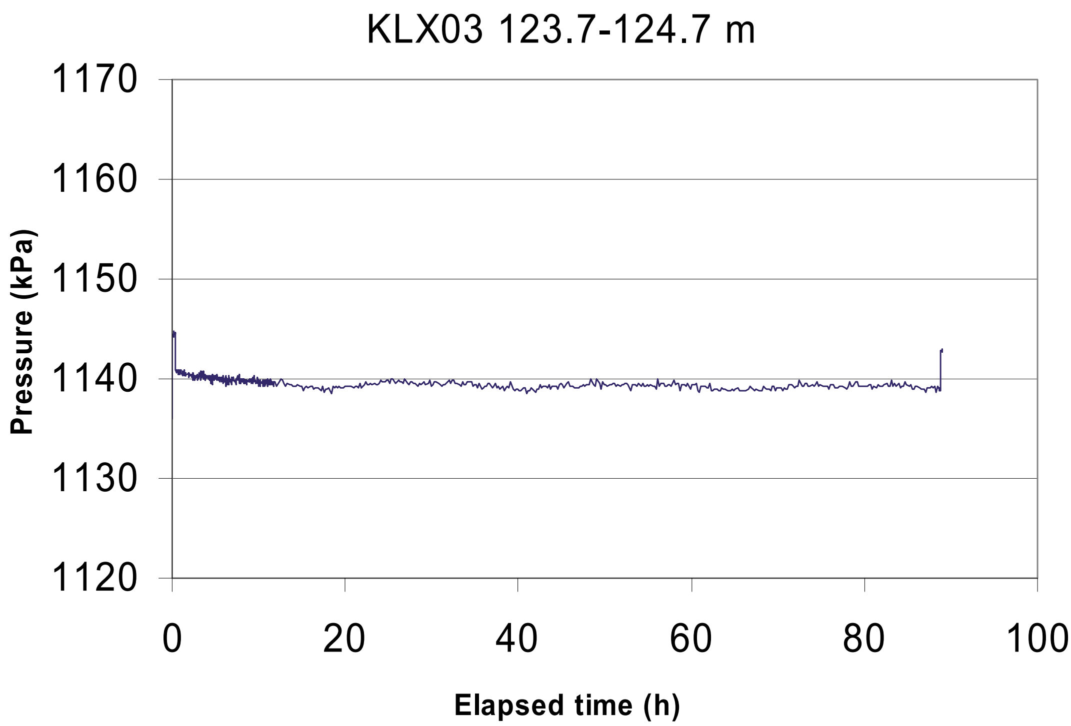

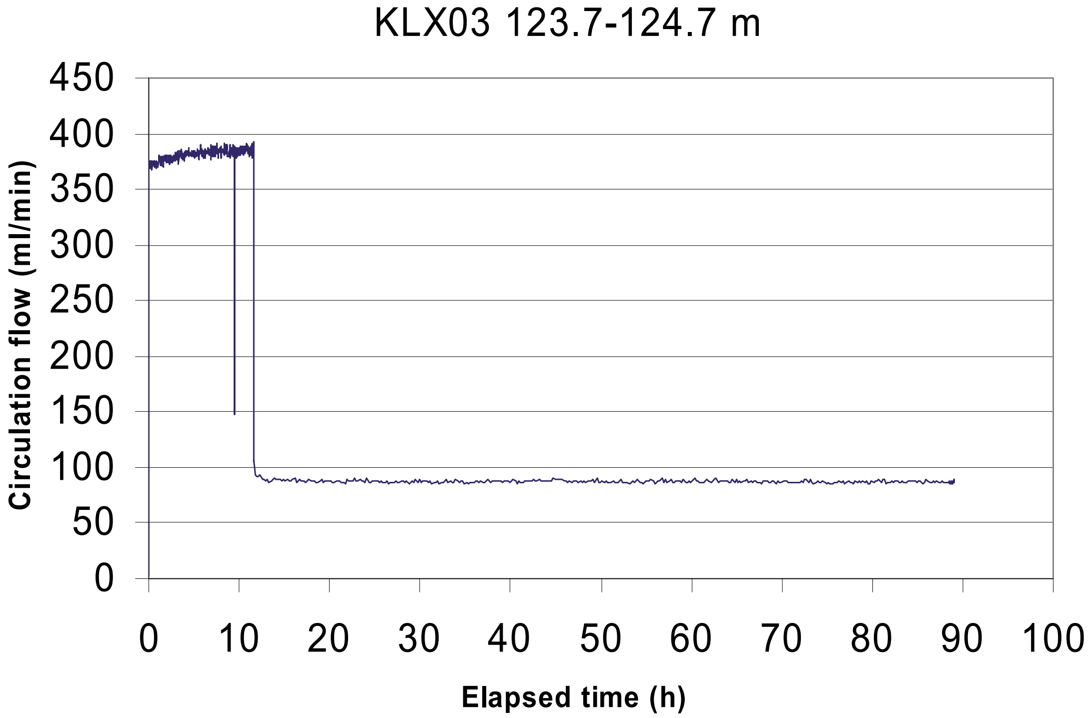

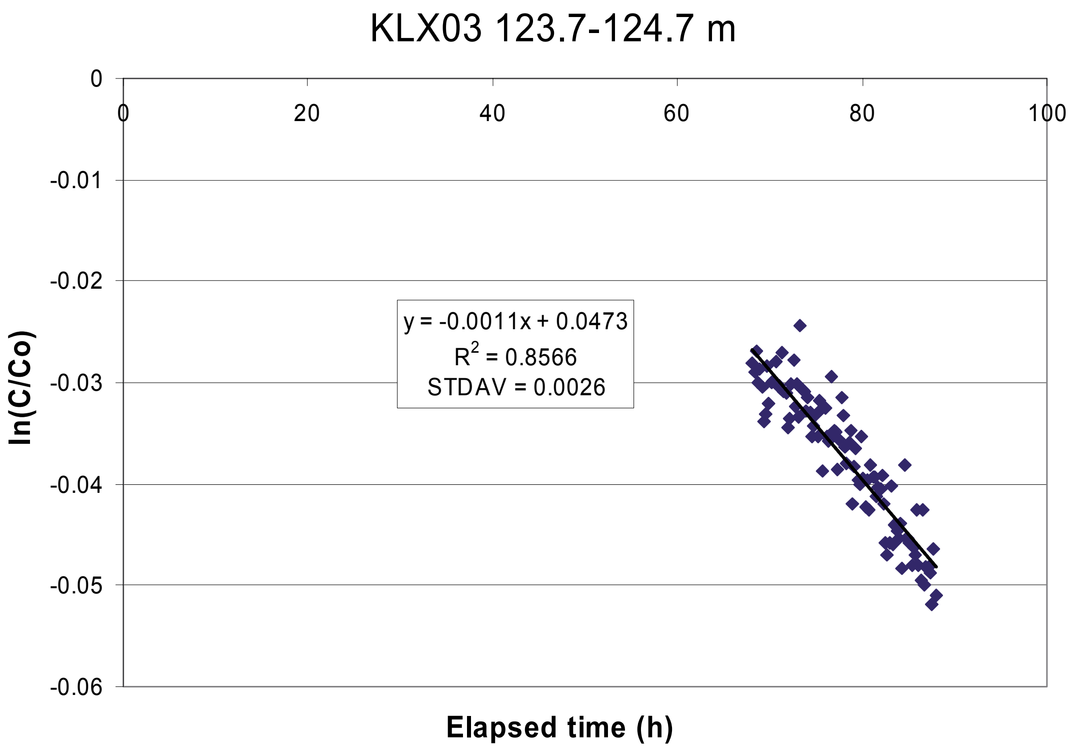

Part of dilution curve (h)	V (ml)	ln(C/Co)/t	Q (ml/h)	Q (ml/min)	Q (m3/s)	R2-value
68-88	975	-0.0011	1.07	0.018	2.98E-10	0.8566

Part of dilution curve (h)	K (m/s)	Q (m3/s)	A (m2)	v(m/s)	I
68-88	2.31E-07	2.98E-10	0.1516	1.97E-09	0.009

Dilution measurement KLX03 195.0–198.0 m

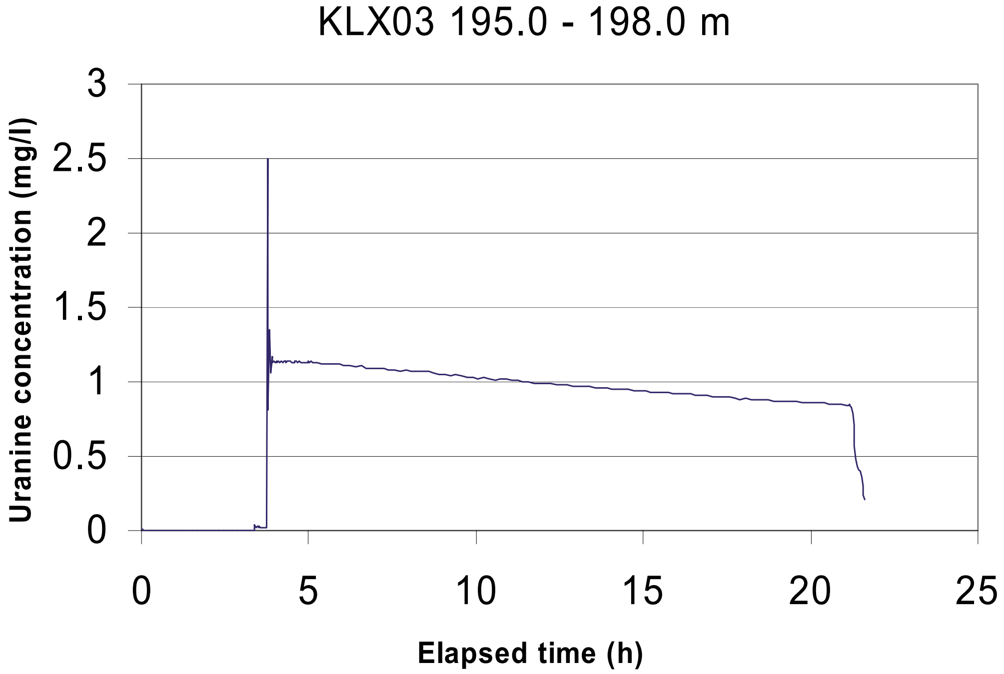

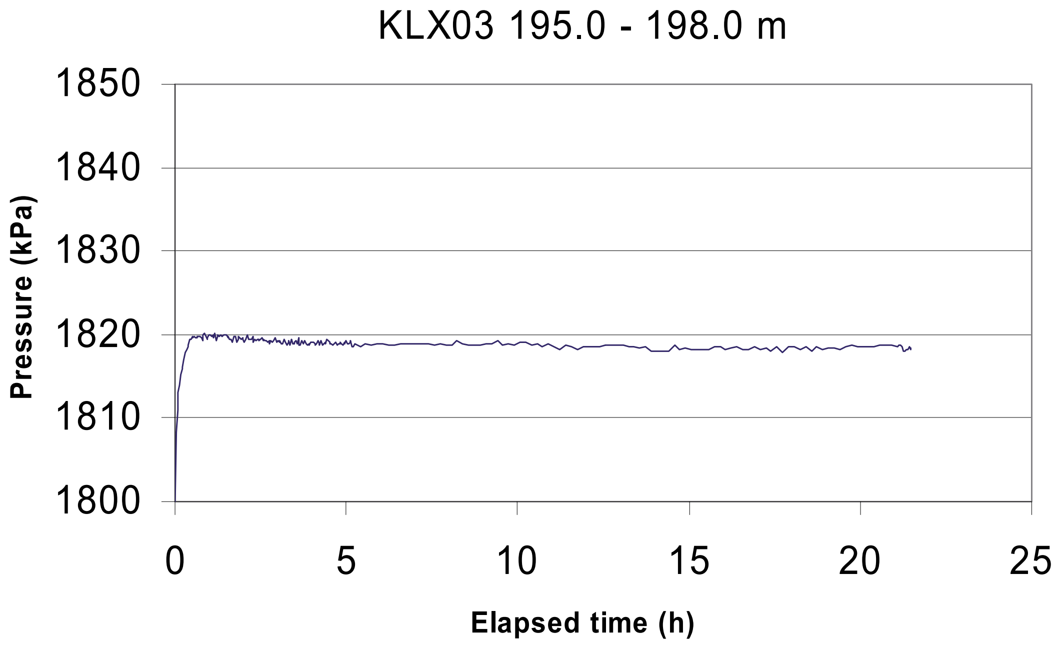

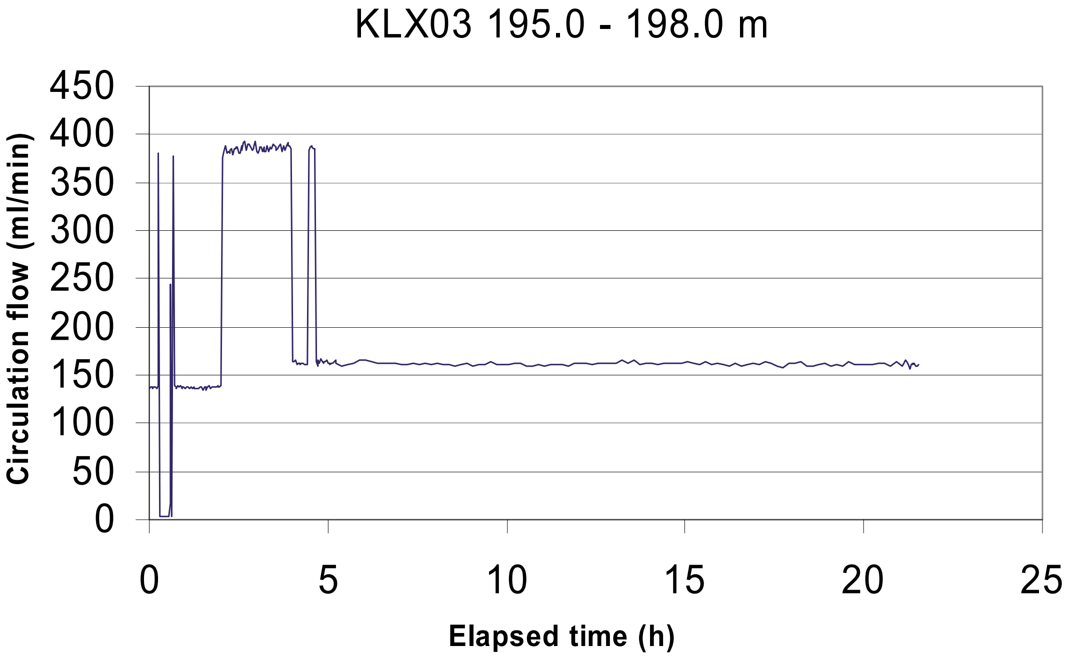

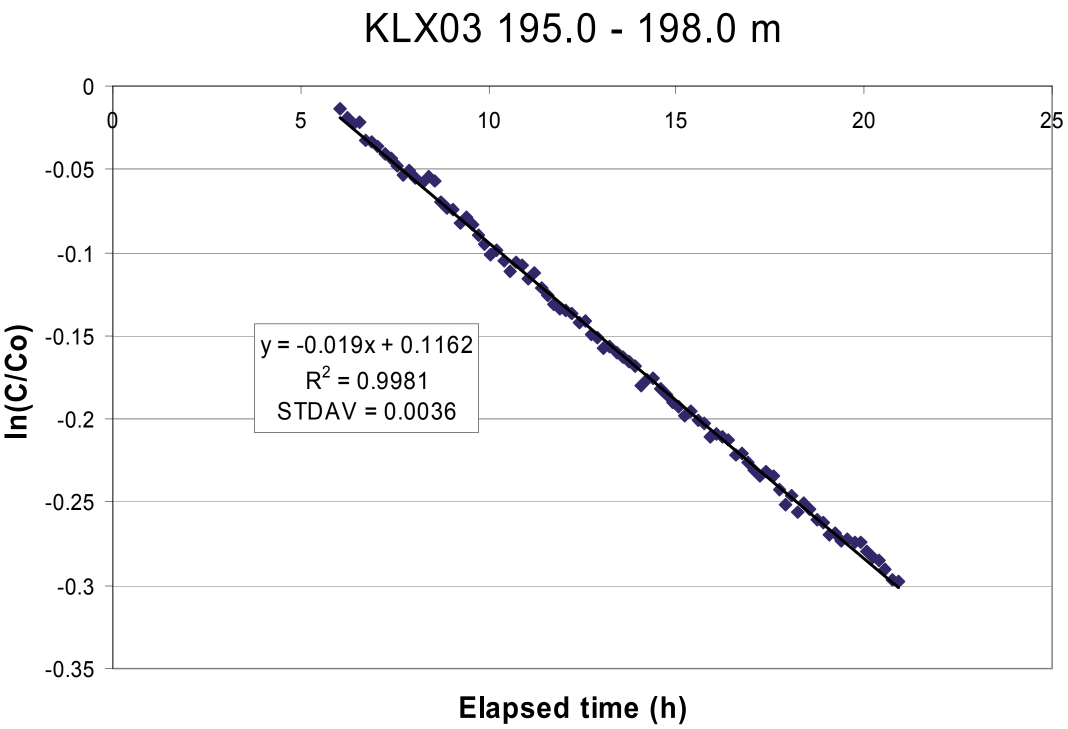

Part of dilution curve (h)	V (ml)	ln(C/Co)/t	Q (ml/h)	Q (ml/min)	Q (m3/s)	R2-value
6 ~ 21	1672	-0.019	31.768	0.529	8.82E-09	0.9981

Part of dilution curve (h)	K (m/s)	Q (m3/s)	A (m2)	v(m/s)	I
6 ~ 21	4.16E-06	8.82E-09	0.4548	1.94E-08	0.005

Dilution measurement KLX03 266.2–267.2 m

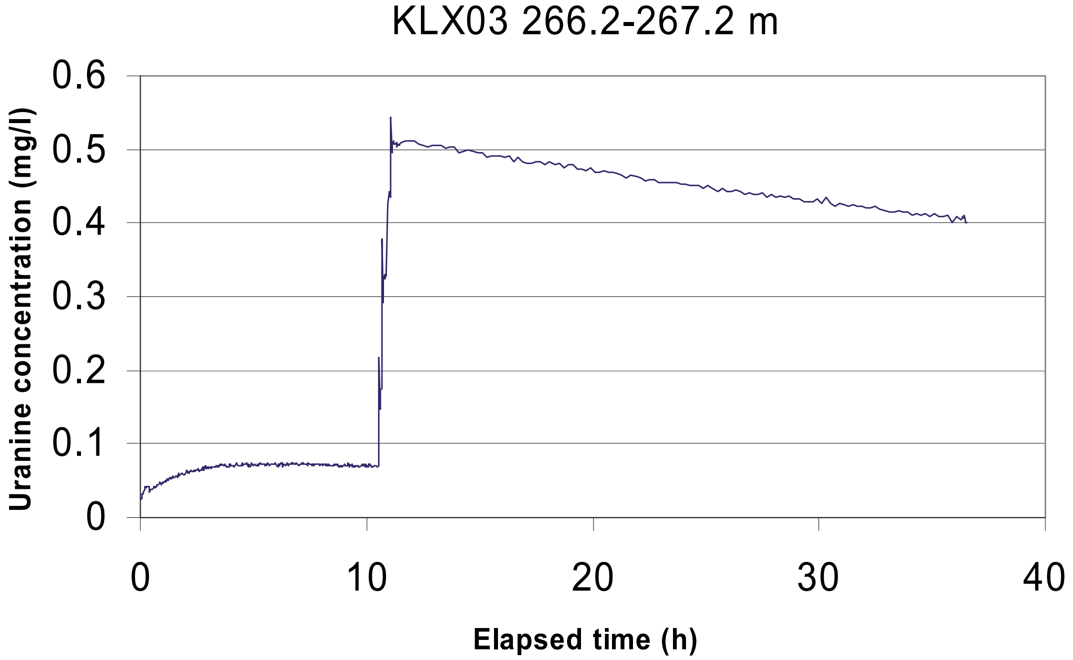

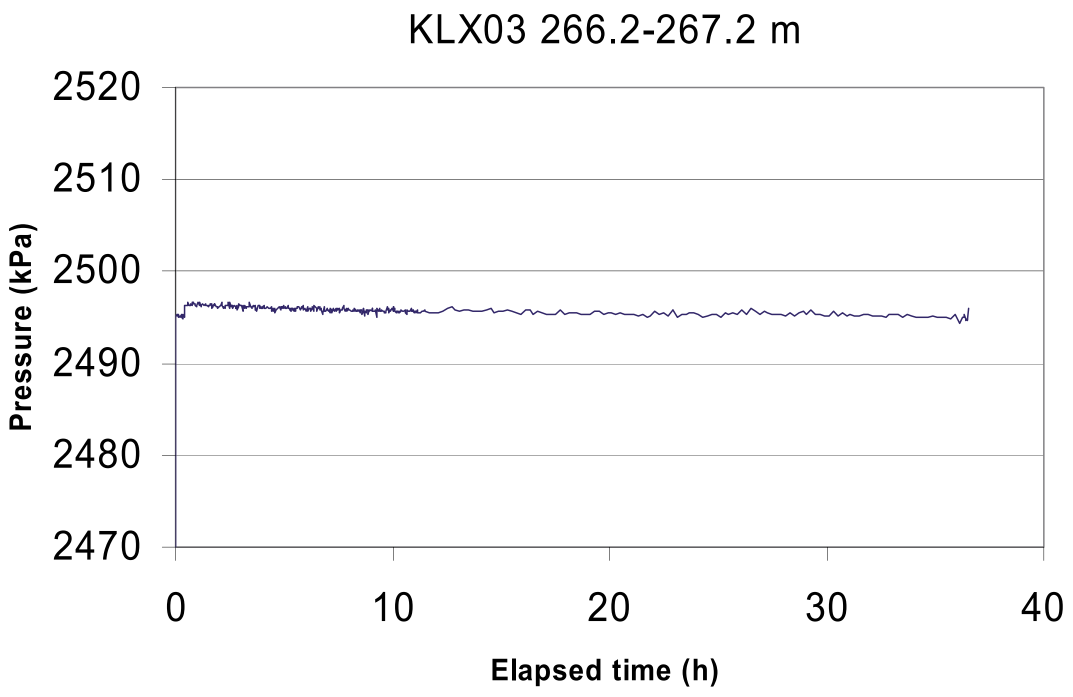

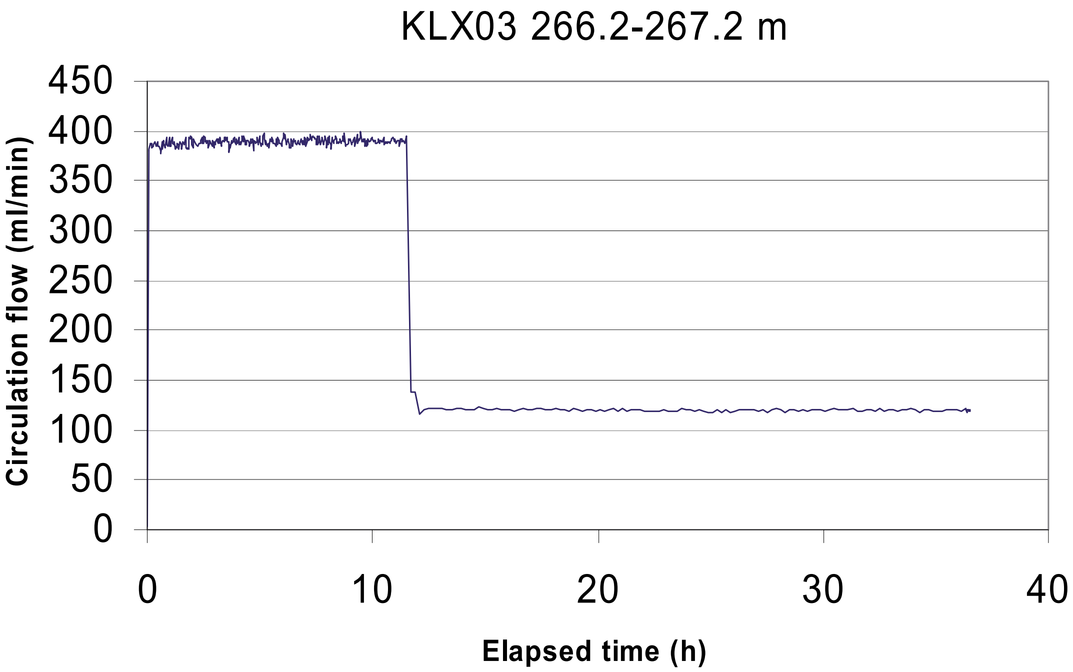

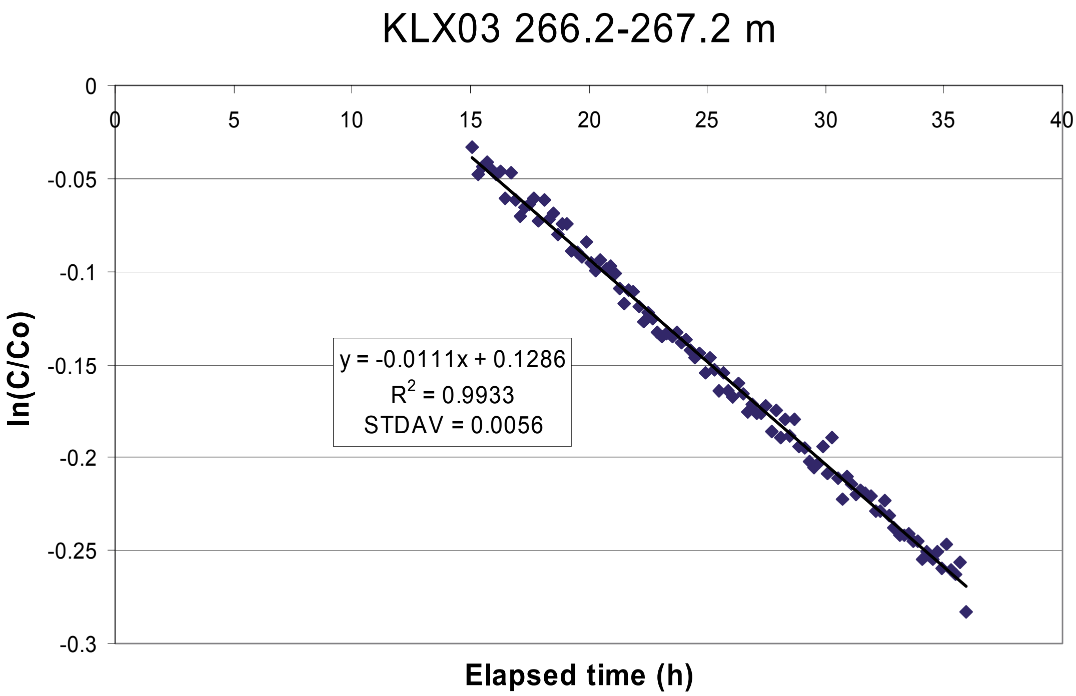

Part of dilution curve (h)	V (ml)	ln(C/Co)/t	Q (ml/h)	Q (ml/min)	Q (m3/s)	R2-value
15-35	975	-0.0111	10.82	0.180	3.01E-09	0.9933

Part of dilution curve (h)	K (m/s)	Q (m3/s)	A (m2)	v(m/s)	I
15-35	7.85E-07	3.01E-09	0.1516	1.98E-08	0.025

Dilution measurement KLX03 409.6–410.6 m

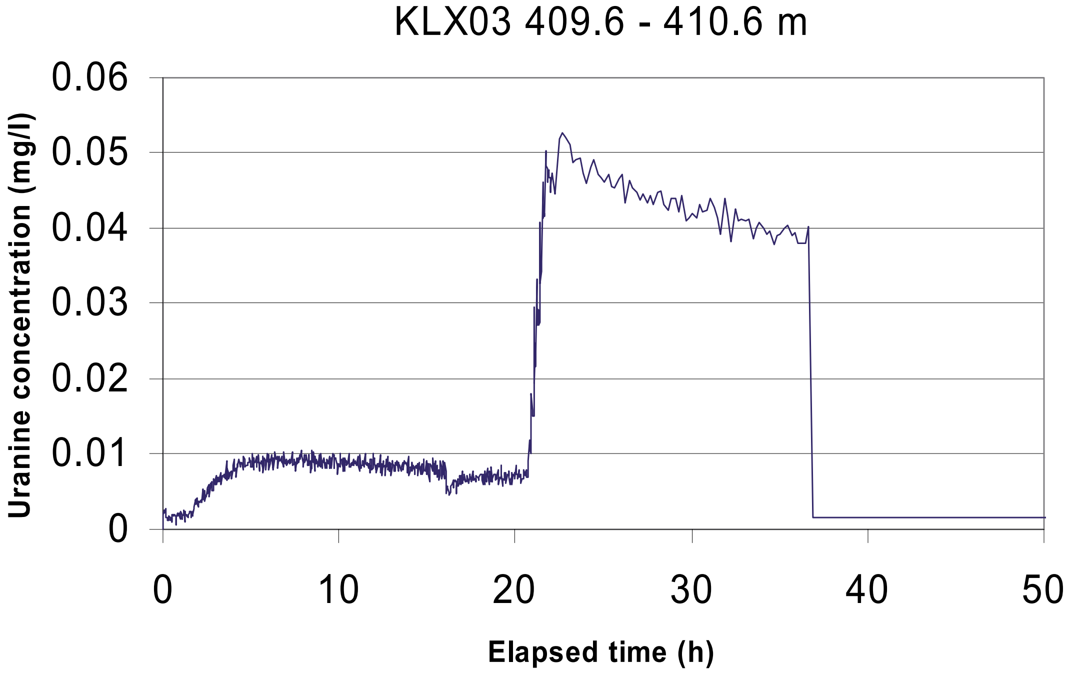

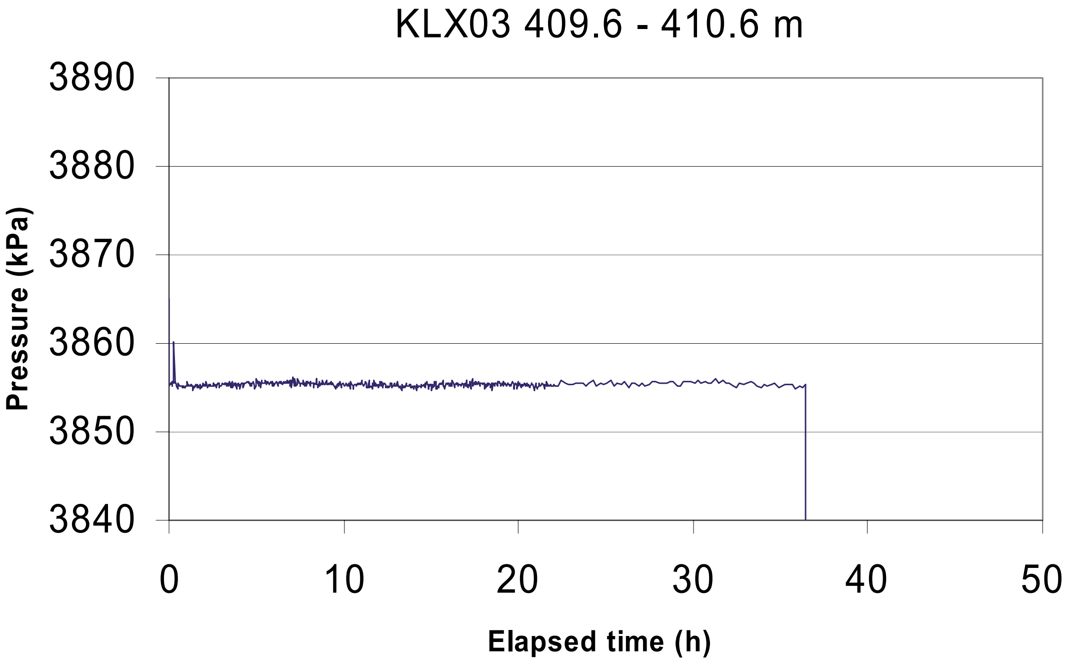

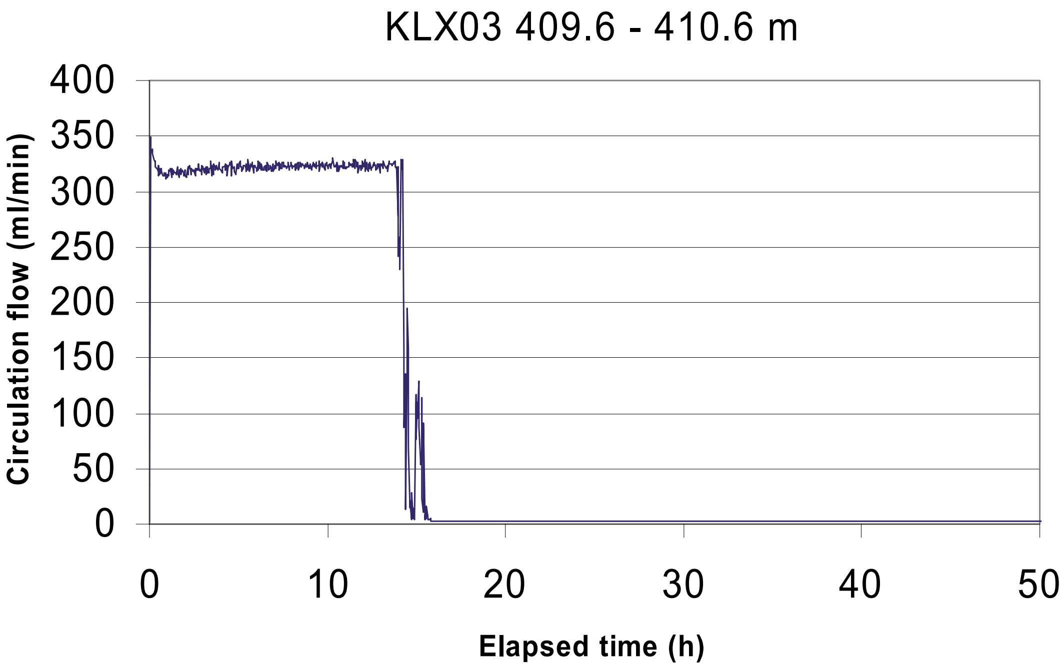

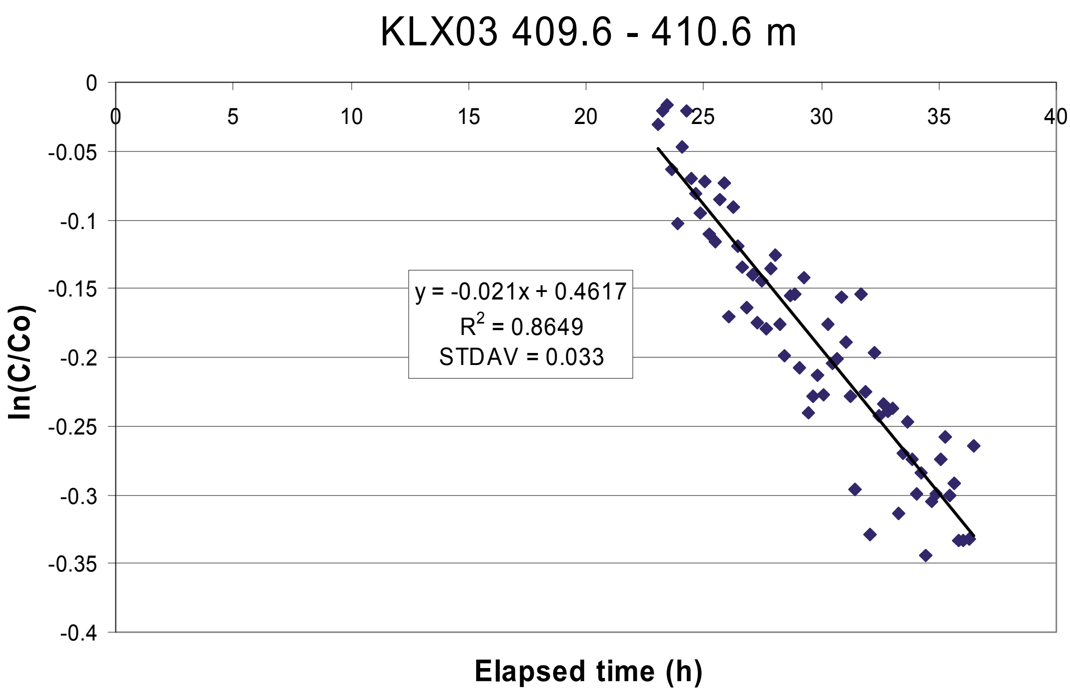

Part of dilution curve (h)	V (ml)	ln(C/Co)/t	Q (ml/h)	Q (ml/min)	Q (m3/s)	R2-value
23-36	975	-0.0210	20.48	0.341	5.69E-09	0.8649

Part of dilution curve (h)	K (m/s)	Q (m3/s)	A (m2)	v(m/s)	I
23-36	1.62E-07	5.69E-09	0.1516	3.75E-08	0.232

Dilution measurement KLX03 662.2–663.2 m

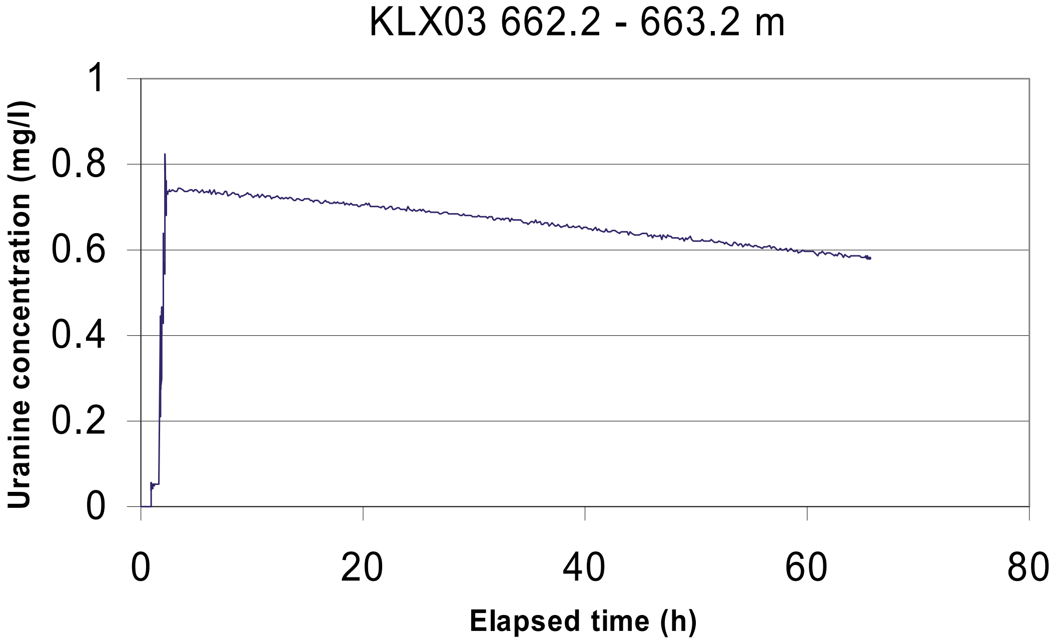

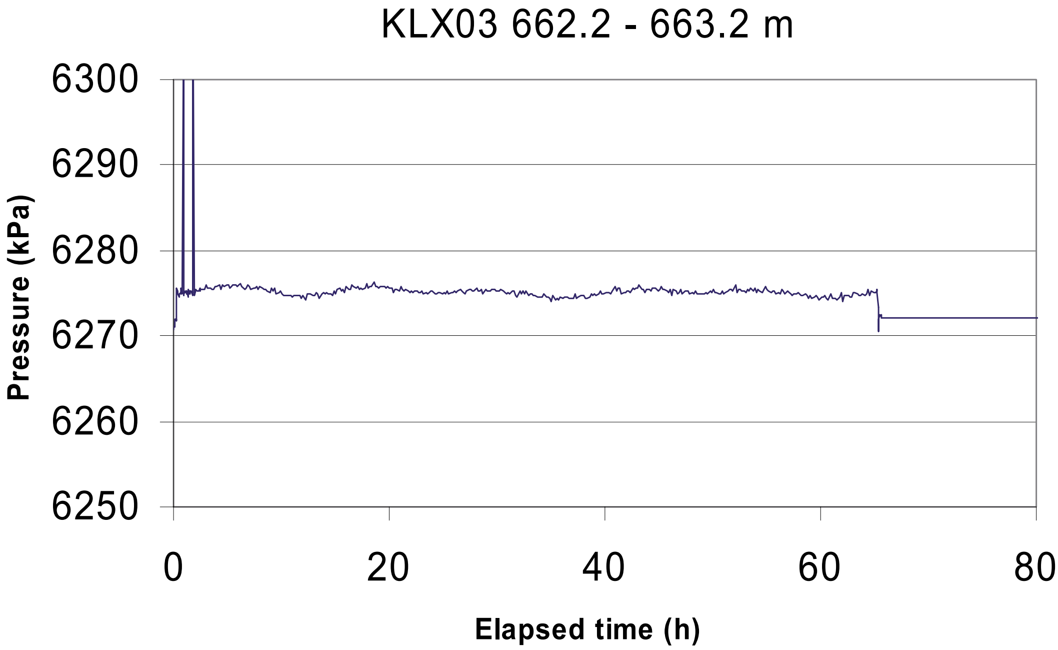

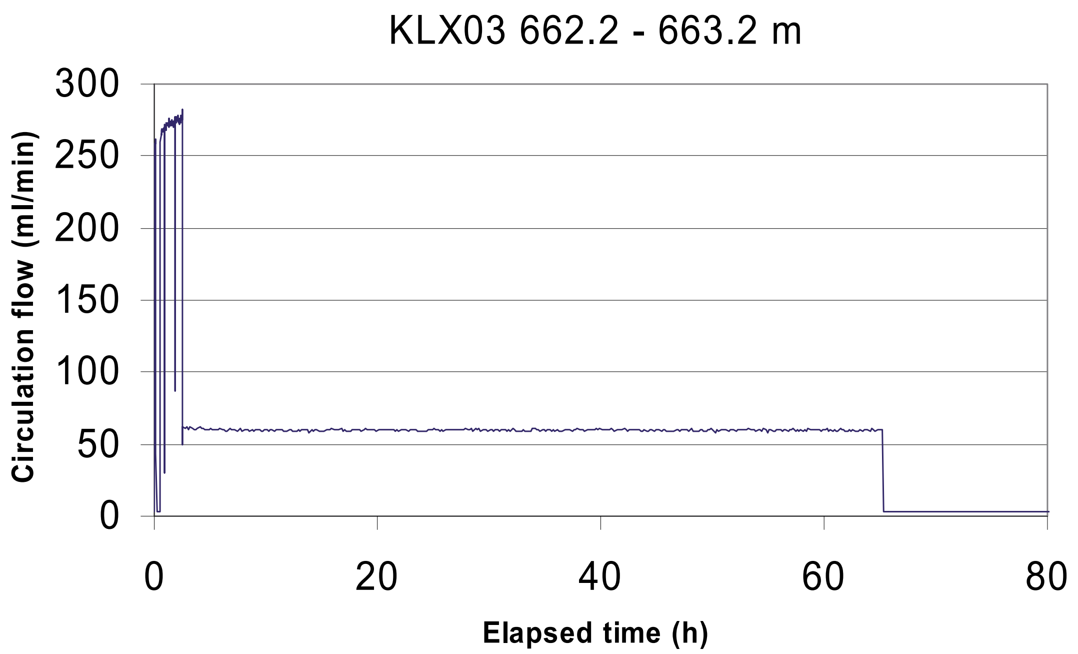

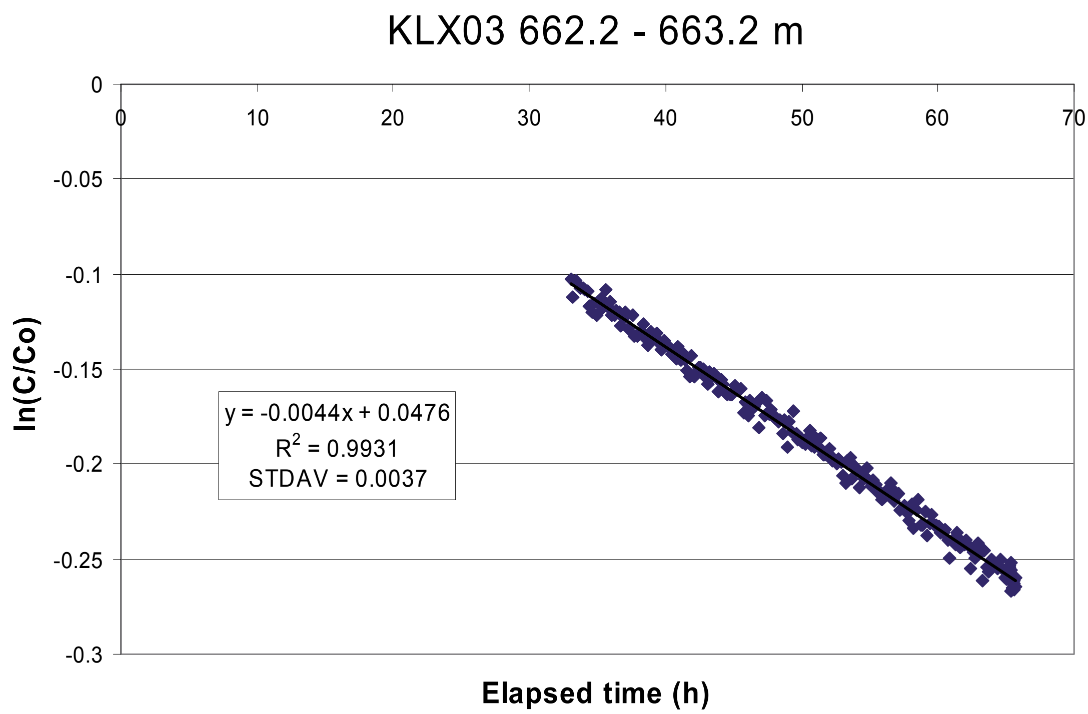

Part of dilution curve (h)	V (ml)	ln(C/Co)/t	Q (ml/h)	Q (ml/min)	Q (m3/s)	R2-value
33-65	961	-0.0044	4.23	0.070	1.17E-09	0.9931

Part of dilution curve (h)	K (m/s)	Q (m3/s)	A (m2)	v(m/s)	I
33-65	2.06E-07	1.17E-09	0.1516	7.75E-09	0.038

Dilution measurement KLX03 740.4–744.4 m

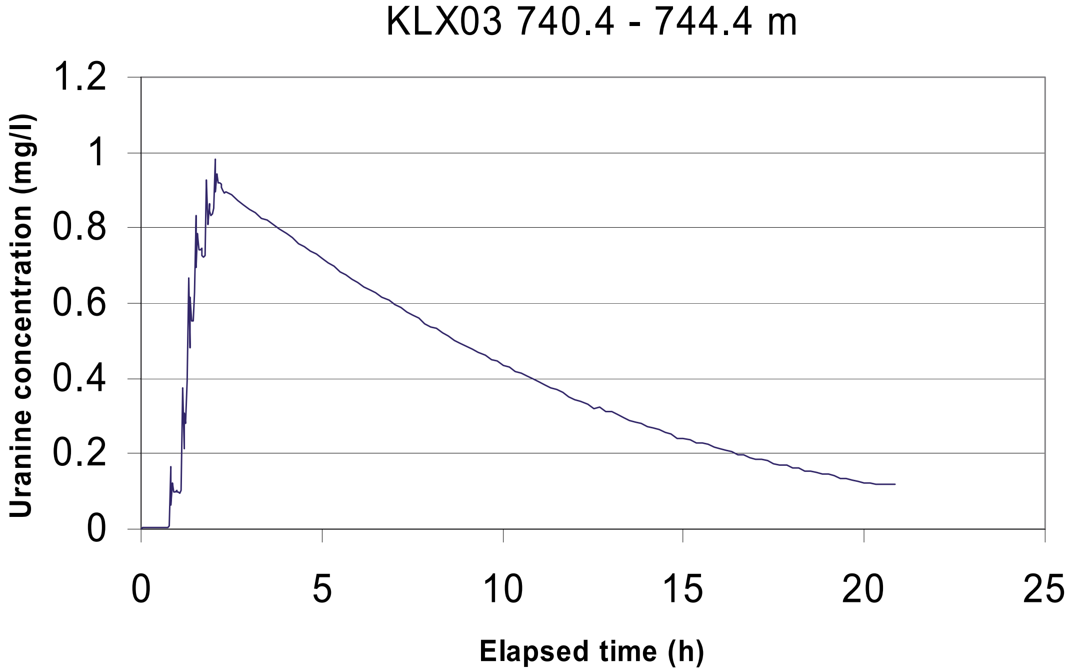

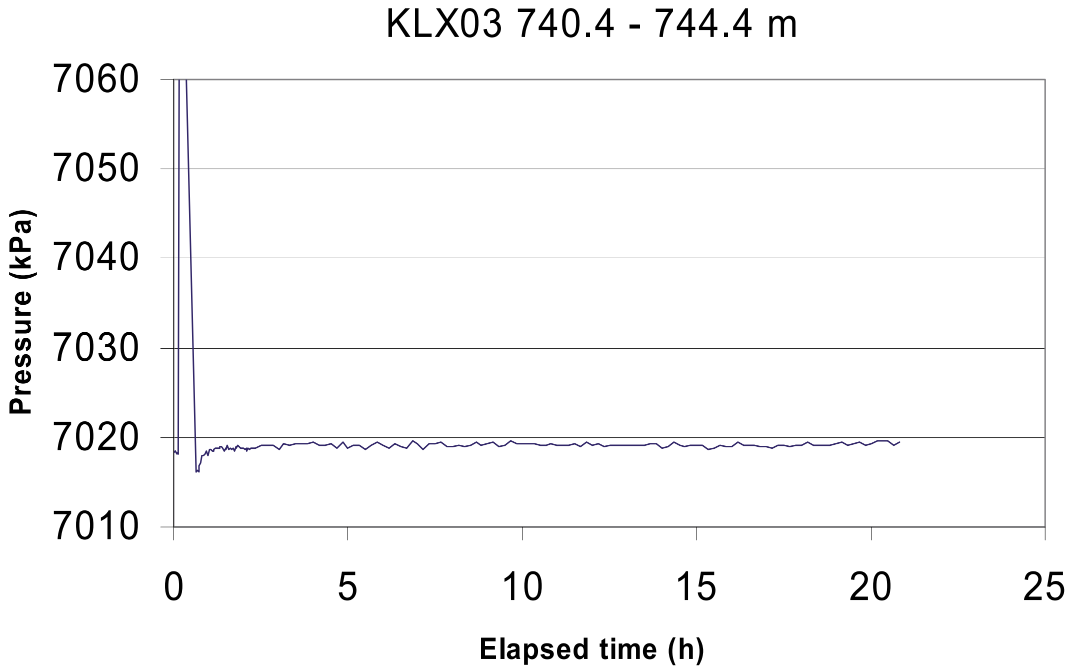

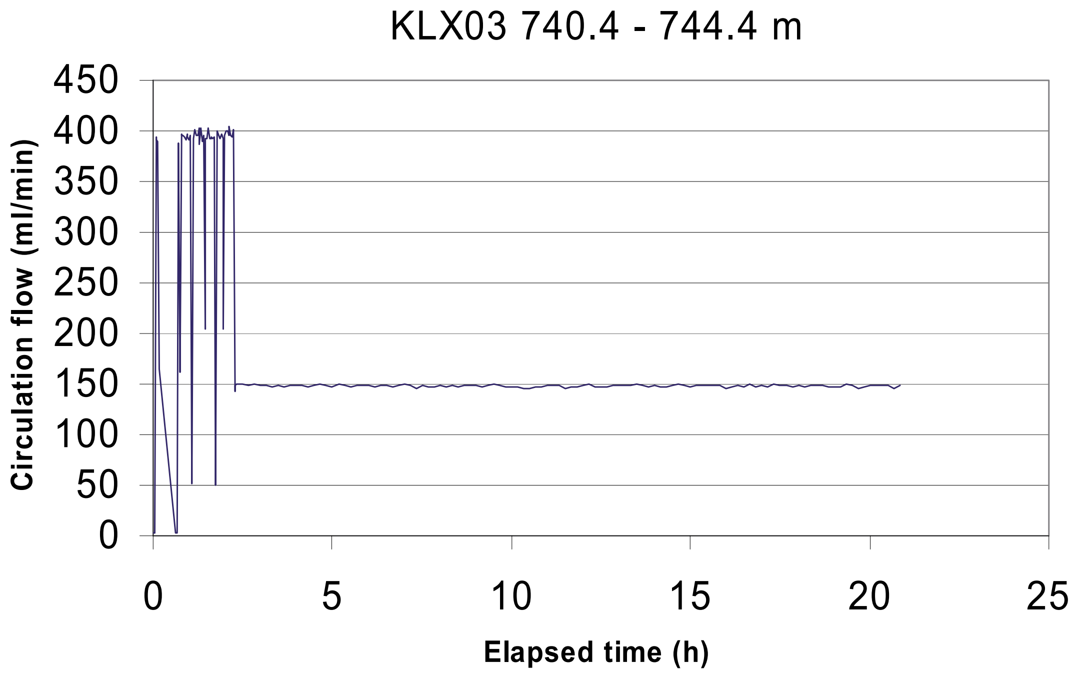

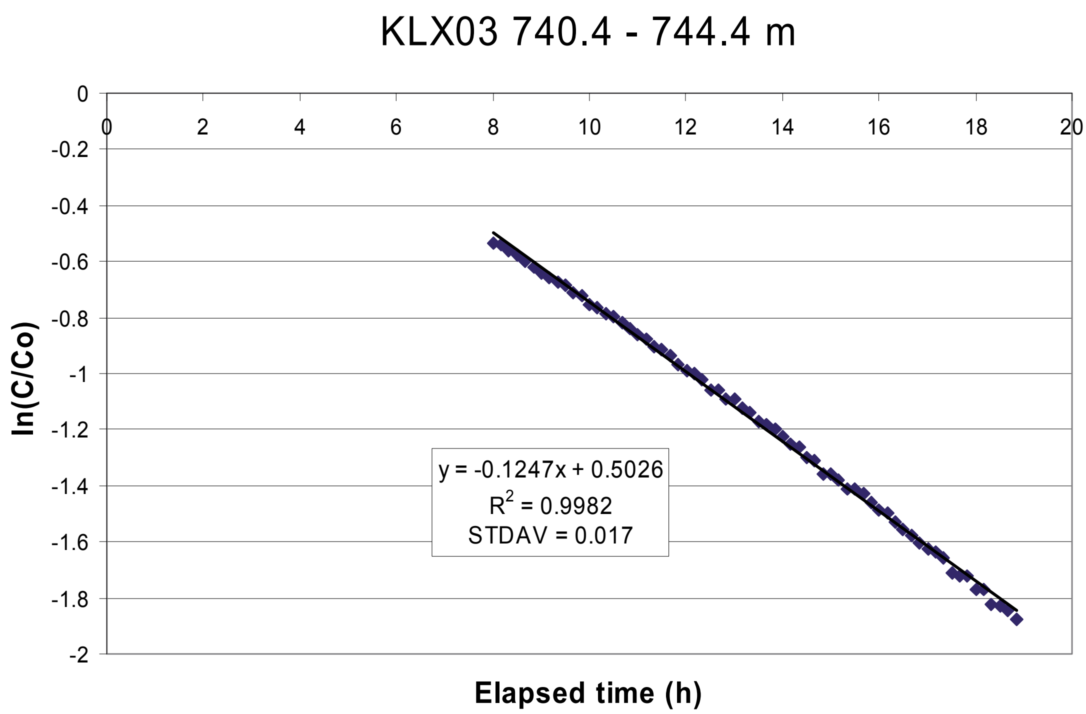

Part of dilution curve (h)	V (ml)	ln(C/Co)/t	Q (ml/h)	Q (ml/min)	Q (m3/s)	R2-value
8 ~19	2027	-0.1247	252.767	4.213	7.02E-08	0.9982

Part of dilution curve (h)	K (m/s)	Q (m3/s)	A (m2)	v(m/s)	I
8 ~19	1.12E-06	7.02E-08	0.6064	1.16E-07	0.103

Dilution measurement KLX03 769.7–772.7 m

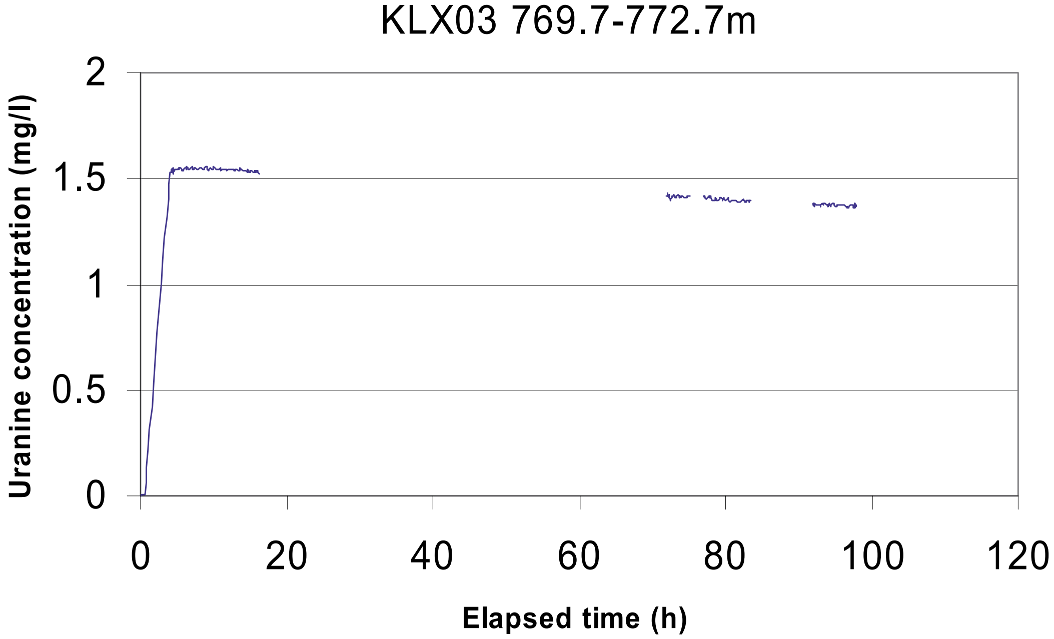

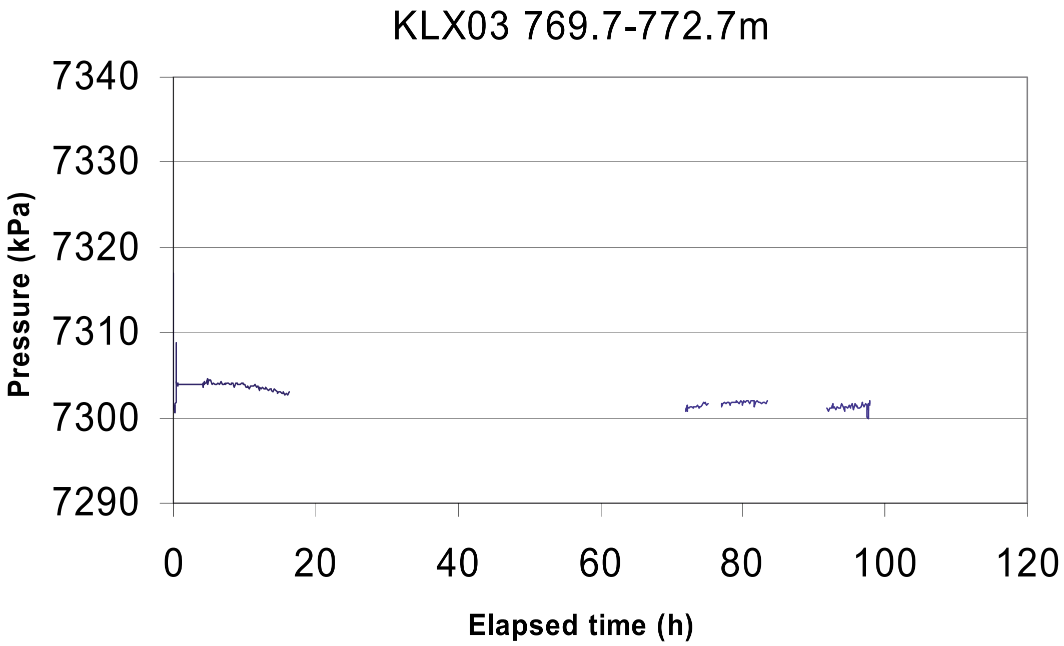

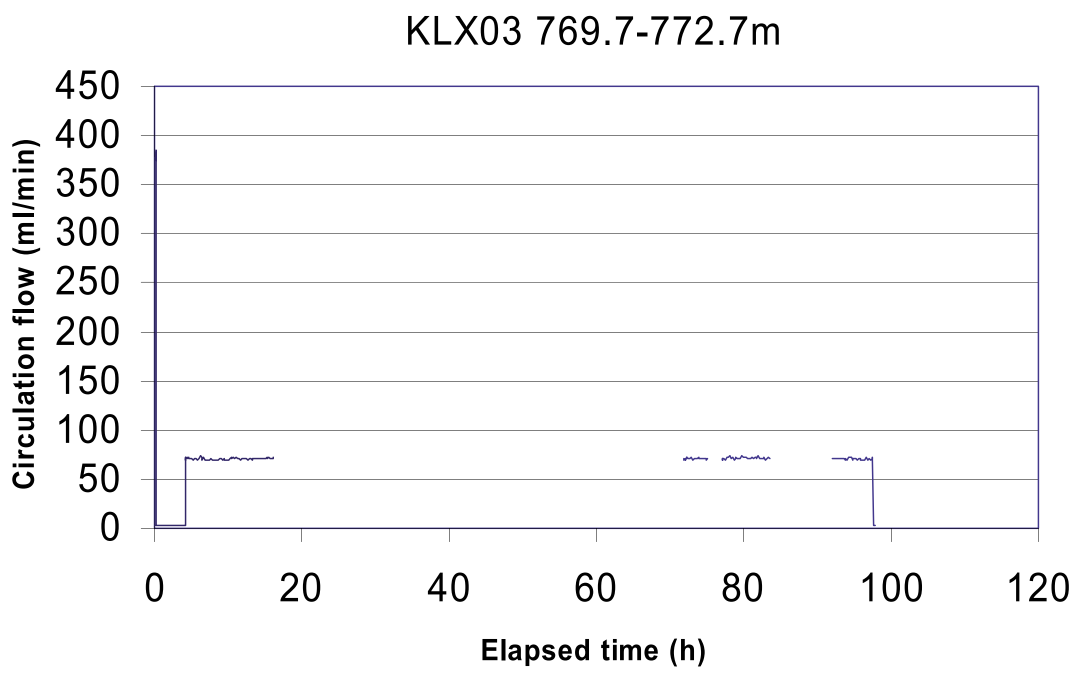

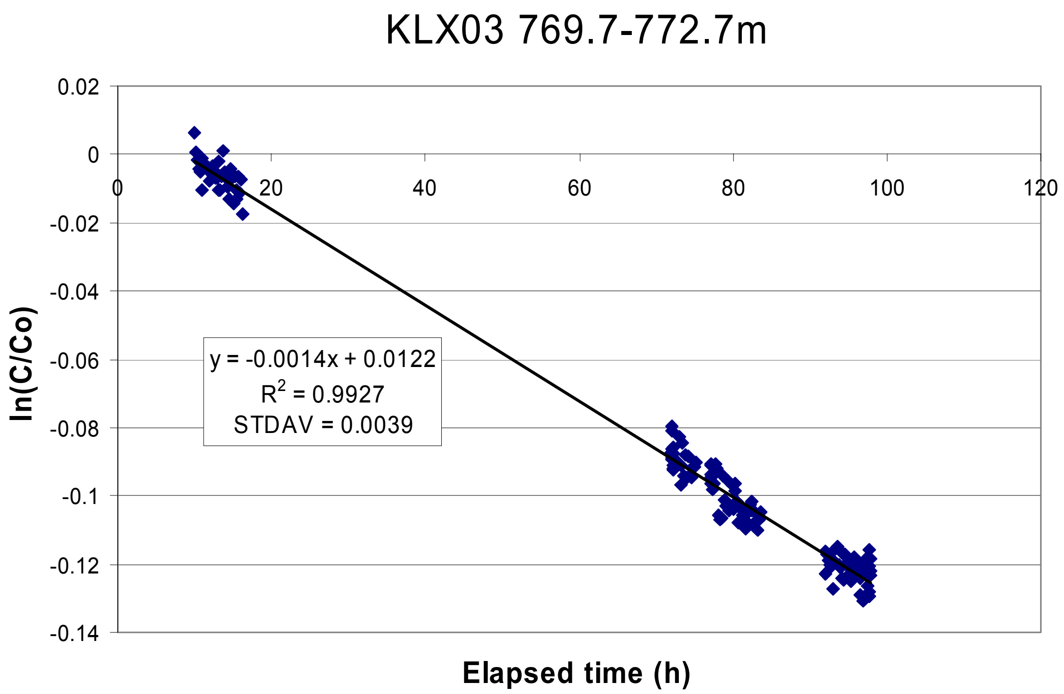

Part of dilution curve (h)	V (ml)	ln(C/Co)/t	Q (ml/h)	Q (ml/min)	Q (m3/s)	R2-value
10-97	1672	-0.0014	2.34	0.039	6.50E-10	0.9927

Part of dilution curve (h)	K (m/s)	Q (m3/s)	A (m2)	v(m/s)	I
10-97	1.77E-07	6.50E-10	0.4548	1.43E-09	0.008

Dilution measurement KLX03 969.7–970.7 m

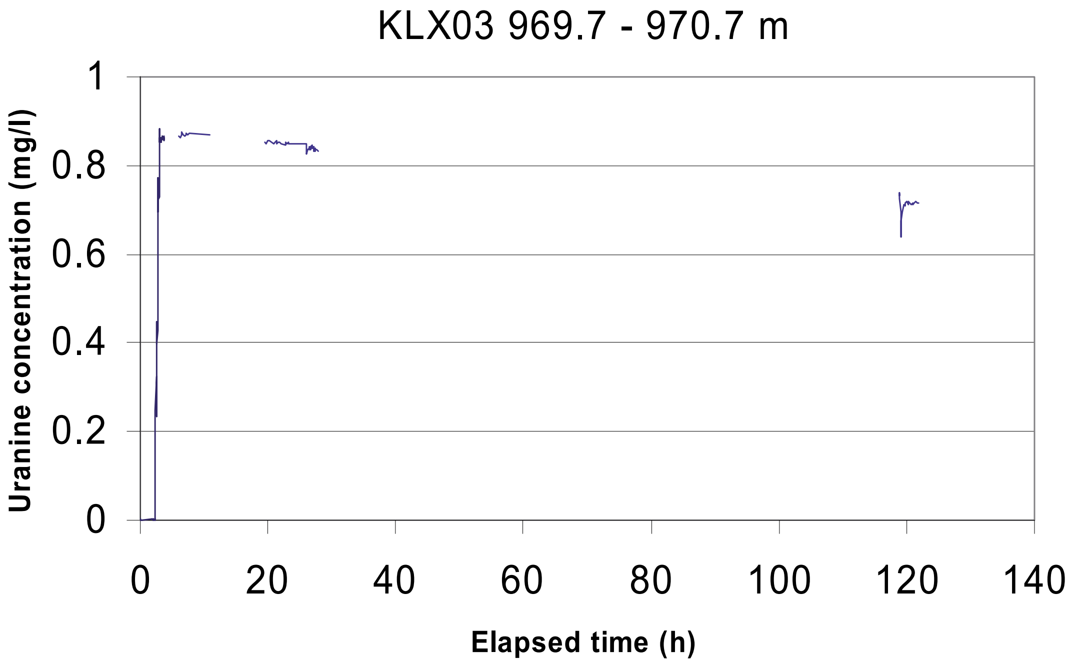

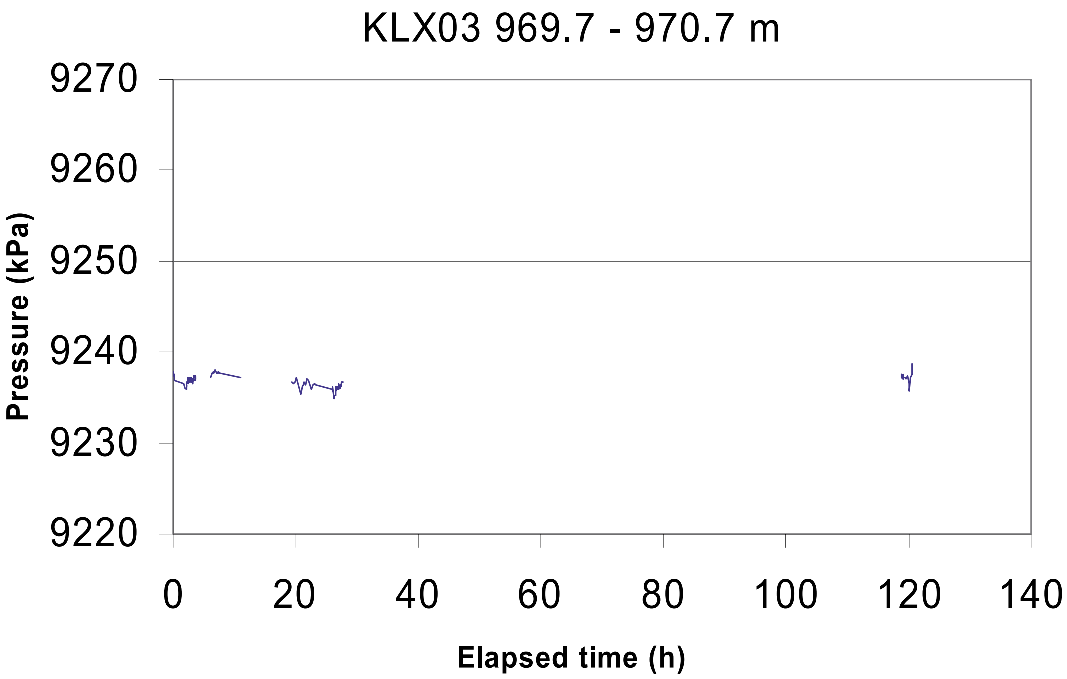

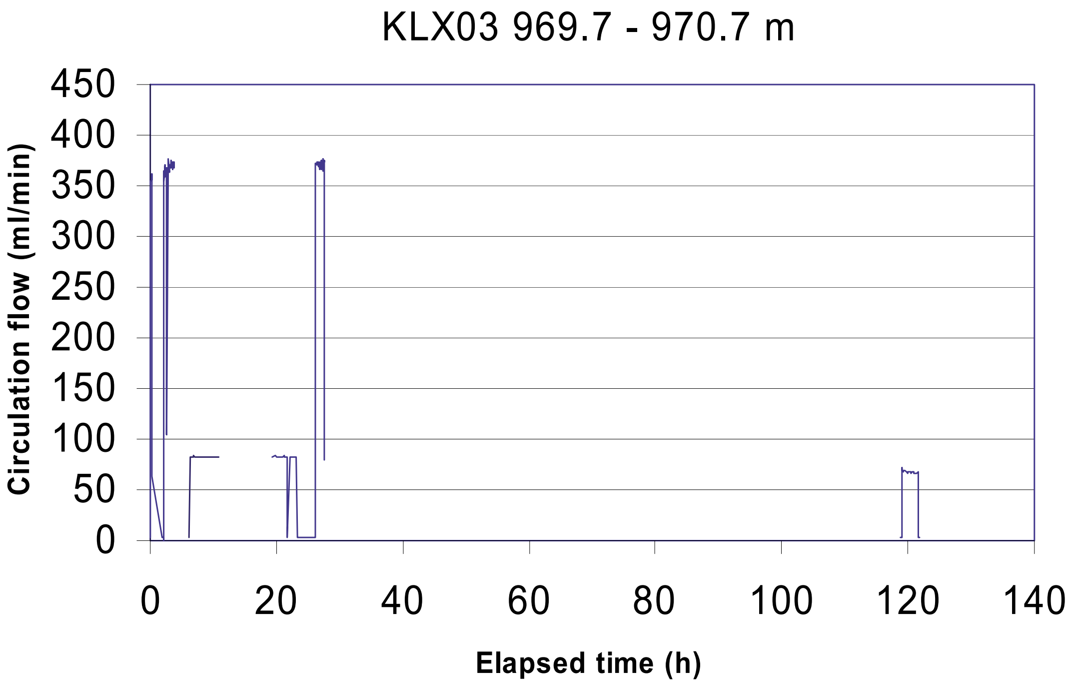

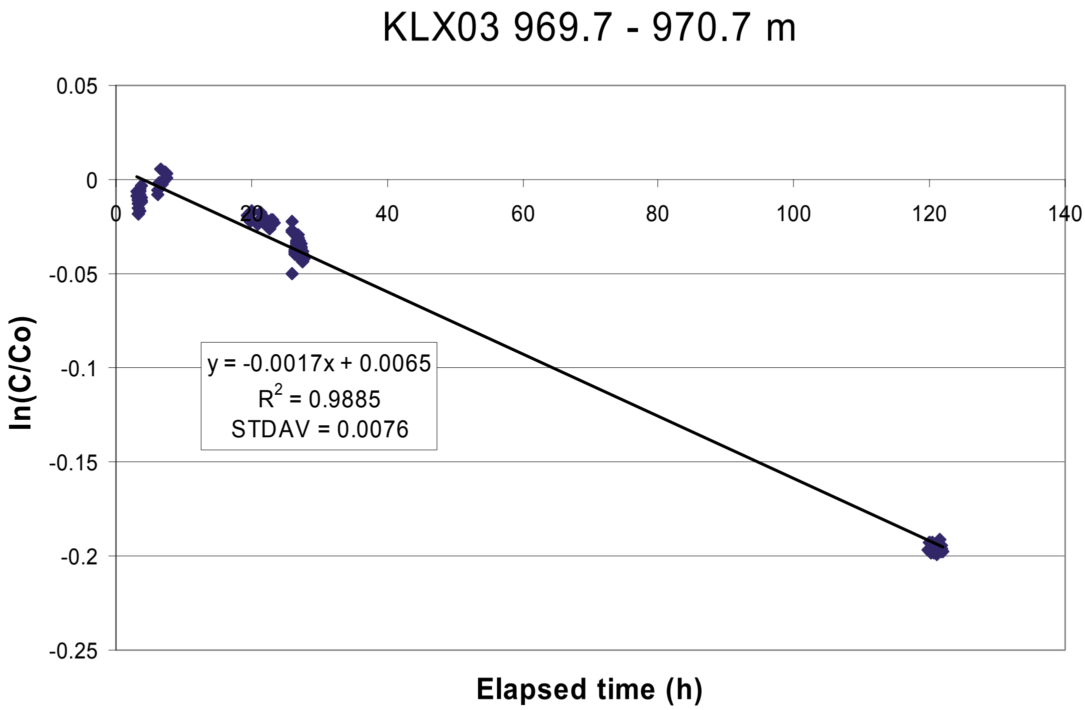

Part of dilution curve (h)	V (ml)	ln(C/Co)/t	Q (ml/h)	Q (ml/min)	Q (m3/s)	R2-value
3-121	961	-0.0017	1.63	0.027	4.54E-10	0.9885

Part of dilution curve (h)	K (m/s)	Q (m3/s)	A (m2)	v(m/s)	I
3-121	4.52E-07	4.54E-10	0.1516	2.99E-09	0.007

BIPS logging in KLX03 735.001–745.001 m

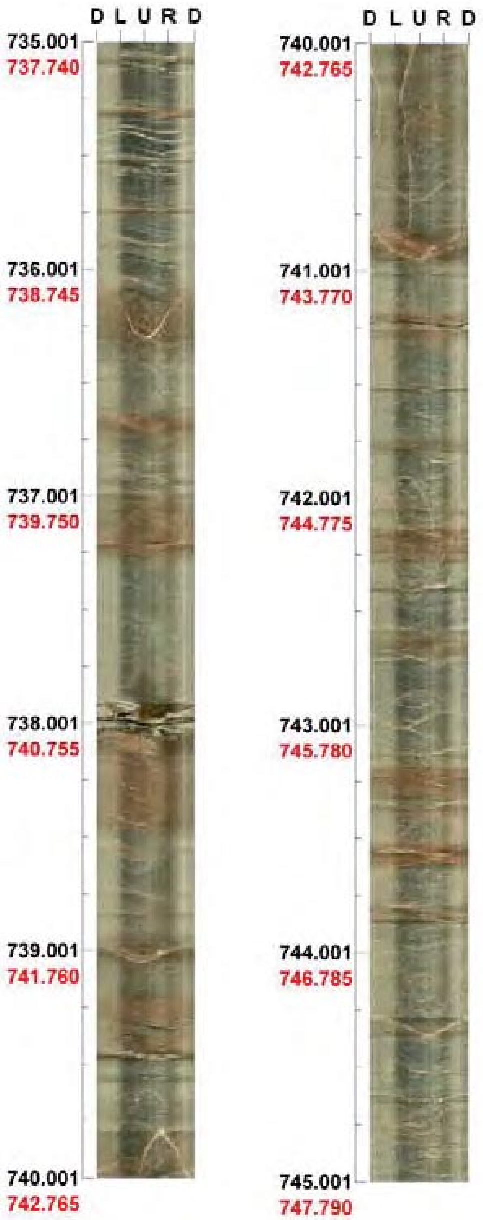

Black number = Record depth
Red number = Adjust depth

Azimuth: 199
Scale: 1/25
Inclination: -75
Aspect ratio: 175%